



LIBRARY Michigan State University

This is to certify that the

thesis entitled
A METHOD FOR LOCATING HIP JOINT
CENTER AND CALCULATING THREE-DIMENSIONAL QUASISTATIC HIP JOINT MOMENTS AND POWER DURING GAIT.

presented by

DAVID MATTHEW MARCHINDA

has been accepted towards fulfillment of the requirements for

MS degree in Mechanics

Major professor

Date 27 August 1993

PLACE IN RETURN BOX to remove this checkout from your record. TO AVOID FINES return on or before date due.

DATE DUE	DATE DUE	DATE DUE

MSU is An Affirmative Action/Equal Opportunity Institution ctchedetedus.pm3-p.1

A METHOD FOR LOCATING HIP JOINT CENTER AND CALCULATING THREE-DIMENSIONAL QUASI-STATIC HIP JOINT MOMENTS AND POWER DURING GAIT

Ву

David Matthew Marchinda

A THESIS

Submitted to Michigan State University in partial fulfillment of the requirements for the degree of

MASTER OF SCIENCE

Department of Material Science and Mechanics

ABSTRACT

A METHOD FOR LOCATING HIP JOINT CENTER AND CALCULATING THREE-DIMENSIONAL QUASI-STATIC HIP JOINT MOMENTS AND POWER DURING GAIT

By

David Matthew Marchinda

The purpose of this thesis was to calculate the three-dimensional moments at the hip joint due to external forces applied to the lower limb during ambulation. In order to accurately compute the moments at the hip, the precise location of hip joint center (HJC) had to be defined. An anatomical study of adult human cadaveric pelves was initiated to investigate the correlation between HJC and pelvic geometry. Pearson product-moment correlations revealed that HJC could be accurately located relative to the anterior superior iliac spline (ASIS) 14% of pelvic width medial, 34% of pelvic depth posterior, and 80% of pelvic height inferior. With the location of HJC defined, the quasi-static hip joint moments were calculated during the stance phase of gait. Power in the plane of progression and actual power at the hip joint were also defined and calculated during the stance phase of gait.

In loving memory of my brother, Anthony. Semper Fidelis.

ACKNOWLEDGMENTS

To Dr. Robert Soutas-Little, my sincere thanks for your guidance, for having faith in me (especially when I did not), for your knowledge, and for our friendship.

To my committee members, Dr. Robert Soutas-Little, Dr. Charlie DeCamp, and Dr. Tom Pence, thank you for your insights and comments on my thesis.

To Dr. Geoffrey Seidel, thank you for including me in your research, and for introducing me to the human body.

To Patricia Soutas-Little, LeAnn Slicer, and Bob Wells, thank you for all the "little things" that provided me with the tools to complete my research.

To Brooks Shoes for their generous funding of my research.

A special THANKS to my fellow graduate students: Gordie Alderink, Terry Bemis, Cheng Cao, Yasin Dhaher, Kathy Hillmer, Brock Horsley, Kim Lovasik, Jim Patton, and Tammy Reid. Wow, what memories!

To all the other workers and friends at BEL: Jennifer, Adam, Mark, Neha, and Shawn. Thanks for your support.

To all my friends who have "been there" for me over these years of study. Thanks for everything!

Most importantly, to my family, Mom, Dad, Ken, and Anna Maria, thank you for your love, support, and kindness. I could not have done it without you!

TABLE OF CONTENTS

LIST OF TABLES	Page vii
LIST OF FIGURES	vii
CHAPTERS	
I. INTRODUCTION	1
II. SURVEY OF LITERATURE	7
A. Hip Joint Center	7
B. The kinetics of biomechanics	11
1. The basic kinetic equations	12
2. The history of kinetic analysis	15
III. METHODS OF DATA COLLECTION	27
A. Hip Joint Center Location	27
B. Kinematic and kinetic data collection	32
1. Equipment	32
2. Walking data collection	34
IV. ANALYTICAL METHODOLOGY	42
A. Hip Joint Center	42
B. Moments and Power	44
1. Force plate calculations	44
2. Kinematic analysis	47
3. Combining motion and force data	53
4. Solution of moments at the hip expressed in	55
lab coordinates	55
5. Joint coordinate system and angle calculations	57

6. Transformation of moments from lab space to joint	
coordinate space	58
7. Power	60
V. RESULTS AND DISCUSSION	64
A. Hip Joint Center	64
B. Moments and power at the hip during stance	73
VI. CONCLUSIONS	96
LIST OF REFERENCES	98

LIST OF TABLES

TABLE		AGE
1	Comparison of maximum moments (Ramakrishnan, 1990)	24
2	Sample force plate data for walking	35
3	Sample motion data	39
4	Comparison of female and male pelvic measurements	66
5	Mean pelvic measurements and interrater reliability (IRR) coefficients	66
6	Pearson product-moment correlations of HJC related to pelvic geometry	67
7	Errors of HJC-x location estimation	70
8	Comparison of maximum moments (N-m/kg)	82

LIST OF FIGURES

FIGURE		PAGE
1	Anatomy of femur and pelvis	4
2	Hip motion definitions	5
3	Newton-Euler schematic	14
4	Quasi-static schematic	14
5	Bresler and Frankel's free body diagram of the lower limb	16
6	Joint moment results (Bresler and Frankel, 1950)	17
7	Contribution of reactions for flex/ext moment	17
8	Hip resultant moments (kN-m) (Crowninshield et al., 1978)	18
9	Boccardi's flexion/extension and abduction/adduction hip moments due to ground reaction effects alone	19
10	Projection of GRF up the body (Wells, 1981)	20
11	Net joint moments, N-m (Wells, 1981)	20
12	Flexion/extension moments (Winter, 1980)	22
13	Moments in joint coordinate system (Cappozzo, 1984)	22
14	Hip moments of walking normalized to % body weight limb length (Ramakrishnan, 1990)	23

15	Frontal and sagittal plane hip moments and power (Ounpuu et al. 1991)	25
16	Medial/lateral view of pelvic measurements	29
17	Frontal view of pelvic measurements	31
18	Calibration set-up with lab space (ls) and force plate space (fps) coordinate systems	33
19	Targeting scheme	36
20	Vertical ground reaction force (F _Z) of three trials	38
21	EV3D stick figure of standing subject	40
22	EV3D stick figure of walking subject	41
23	Pelvic geometry of frontal plane	43
24	Equivalent force system of force plate	46
25	Local segment coordinate systems	48
26	Position vector in lab space	49
27	Joint coordinate system	57
28	Scatter plots of HJC vs. pelvic measurements	69
29	Splined HJC-z	73
30	Hip angles during gait - subject 1	<i>7</i> 5
31	Hip angles during gait - subject 2	7 6
32	Forces in lab space - subject 1	<i>7</i> 7
33	Forces in lab space - subject 2	7 7

34	Applied quasi-static hip moments - subject 1	<i>7</i> 9
35	Applied quasi-static hip moments - subject 2	80
36	Stick figure depicting forces and moment arms in the sagittal plane - subject 1	83
37	Inertial and gravitational terms in moments (Boccardi, 1981)	84
38	Applied hip moments with and without gravity terms - subject 1	85
39	Applied hip moments with and without gravity terms - subject 2	86
4 0	Flexion/extension moments at hjc and greater trocanter (gt)	88
41	Hip angular velocity during stance - subject 1	90
42	Hip angular velocity during stance - subject 2	91
43	Hip power during stance phase - subject 1	92
44	Hip power during stance phase - subject 2	93

I. INTRODUCTION

Biomechanics can be defined as the science of the application of the laws of mechanics to biological systems. In this research, the laws of classical statics and dynamics are applied to the human body to study movement, particularly locomotion. This is commonly referred to as gait analysis. Gait analysis is performed on humans to achieve an objective description of the motion and forces associated with locomotion and to use these objective results to aid in the correction of dysfunctional gait patterns of people with neuromuscular abnormalities. These "abnormalities" can be caused, but are not limited to, cerebral palsy, spina bifida, arthritis, traumatic brain injury, Charcot-Marie Tooth disease, congenital and surgical amputations, traumatic musculo-skeletal injury, and Parkinson's disease. It is the goal of gait analysis to obtain an objective assessment of a subject's gait pattern in order to better define what surgical procedures, physical rehabilitation, and/or orthotic devices could improve the subject's gait and quality of life. The primary locomotive pattern of humans is, of course, walking.

Walking has been described as a series of nearly missed catastrophes. During this motion the body is literally in a cyclic pattern of falling and catching itself. Although the process of walking appears very basic since it is done so often and without conscious thought, its intricacies

are actually quite complicated. This act of walking involves the interactions of the brain, the spinal column, nerves, muscles, ligaments, tendons, bones, and joints. A person's stride is measured as the distance between two successive initial contacts of the same foot with the ground or floor. The gait cycle is divided into two phases — stance and swing. Stance occurs when the foot is in contact with the ground and swing occurs when the foot is airborne. Stance is divided into three phases: initial foot contact, when the foot first comes in contact with the ground; midstance, when the foot is firmly planted on the ground, and toe off, when the foot is leaving or pushing off from the ground. At normal walking speed, stance occurs approximately for 60-62% of the gait cycle and swing for 38-40% of the gait cycle.

Gait analysis or evaluation includes three major components — kinematics, kinetics, and electromyography. In biomechanical definitions, kinematics describe the motions of body limbs and joints. This includes angular ranges of motion, angular velocities and accelerations, and translational components. Kinetics describe the forces, moments of forces, and powers associated with movement of the limbs and joints. Electromyography (EMG) is the measurement of muscle activity. EMG is performed by using fine wire or surface electrodes. When a muscle contracts in response to impulses, depolarization occurs. This gives rise to action potentials that are picked up by surface electrodes placed on the skin near the muscle's motor point. In order to understand the procedures involved and the results obtained by the kinematic and kinetic analysis, a general knowledge of anatomical terms is needed.

Descriptions of the human body reference a standard anatomical position. This position is defined as standing erect with feet together,

looking straight forward, with arms at the sides of the body, and palms forward. From this position, the body is divided into three planes. The frontal or coronal plane divides the body into front and back segments. The transverse or horizontal plane divides the body into upper and lower segments. The sagittal plane divides the body into right and left segments. This plane is also called the plane of progression, since it is in this plane that most forward motion occurs during gait. In describing the positions of objects on the body or body segments in relationship to each other, various descriptive names are used. Medial is towards the midline (the line from head to floor, in the middle of the body) and lateral is towards the sides. Superior describes the upper positions, closer to the head and inferior describes the lower positions, closer to the feet. Anterior describes the position closer to the front and posterior describes the position closer to the back. Proximal describes an object as being towards something; whereas, distal describes an object as being away from something.

The hip is the major place of support between the upper body and the lower limbs. The hip musculature is also responsible for the most positive work (in comparison to the knee and ankle joints) during walking (Ounpuu et al. 1991). Therefore, describing the function, movements, forces, and moments at the hip are vital to obtaining an accurate description of gait. The hip joints are the joints connecting the pelvis with the femurs (Figure 1). The hip joint is a ball and socket joint, formed by the articulation of the femoral head (extended by the femoral neck) with the acetabulum (Johnston, 1973). The acetabulum is the hemi-spherical socket of the joint imbedded in the pelvis. The center of the hip joint is difficult to accurately measure since its location is deep within the upper thigh. It is medial, anterior, and superior to the greater trochanter of the

femur, a distance that is subject specific. It is crucial to accurately define hip joint center (HJC) in order to define the moment arms, and hence, the moments at this joint.

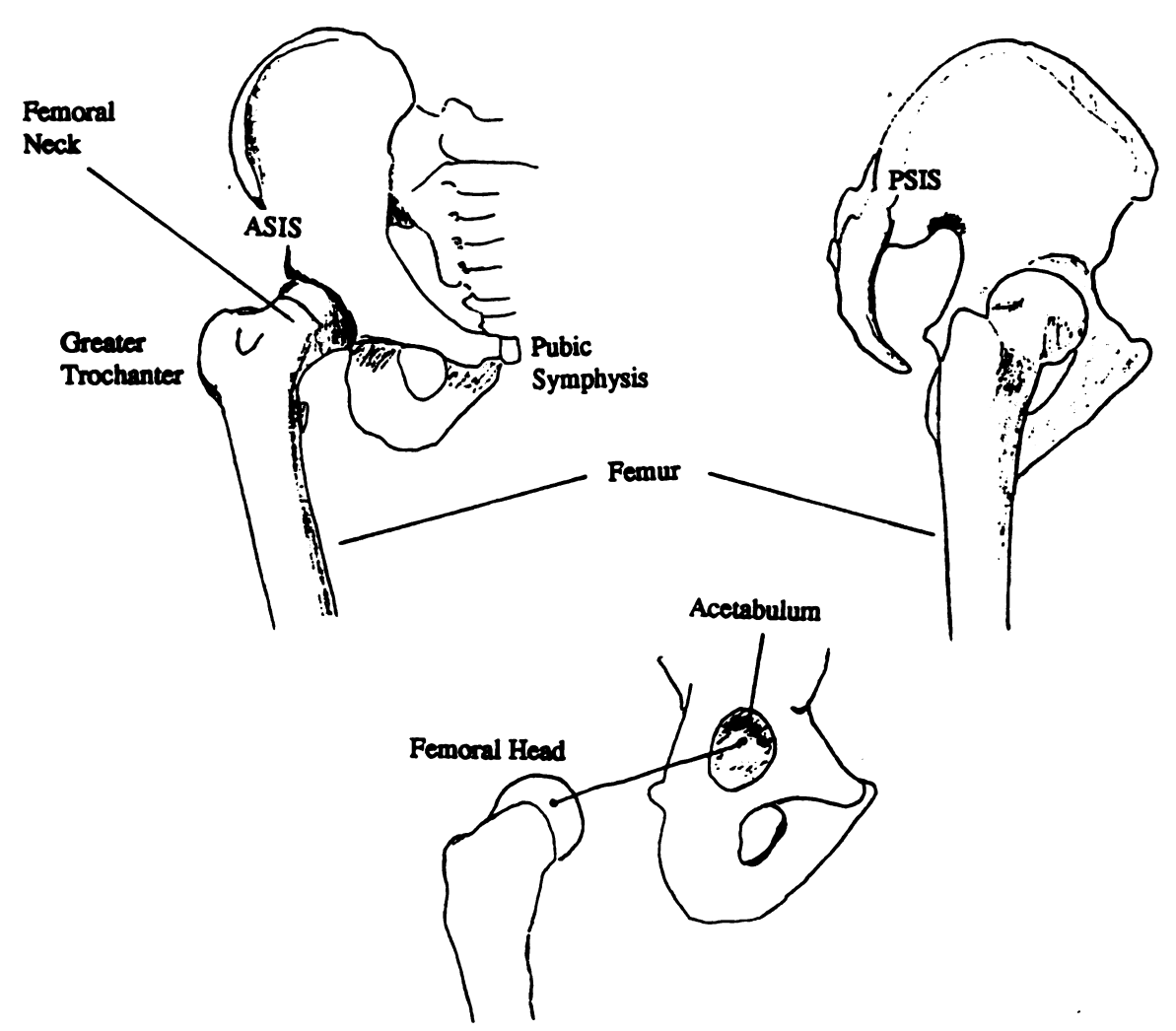


Figure 1. Anatomy of the femur and pelvis

Most of the muscles responsible for movement at the hip have origins on the pelvis and insertions on the femur. The motion at the hip is described by three angles: flexion/extension (sagittal plane motion); abduction/adduction(frontal plane motion); and external/internal rotation (transverse plane motion) (Figure 2). Each of the muscles across the joint are responsible for one or more of these motions. The flexor group

includes the iliopsoas, rectus femoris, sartorius, and tensor fasciae latae. The extensors include the gluteus maximus, biceps femoris, semimembranosus, and semitendinous. The gluteus medius and minimus abduct the hip and the adductor magnus, brevis, and longus adduct the hip. The rotators include the piriformis, obturator internus and externus, and the gemellus superior and inferior. Hip joint moments are described by the motions they induce. Hence, the flexion/extension moment is the moment about the axis of flexion/extension. This axis rests in the frontal plane and is perpendicular to the sagittal plane. The abduction/adduction moment axis rests in the sagittal plane and is perpendicular to the frontal plane. The external/internal rotation moment axis rests in the sagittal plane and is perpendicular to the transverse plane.

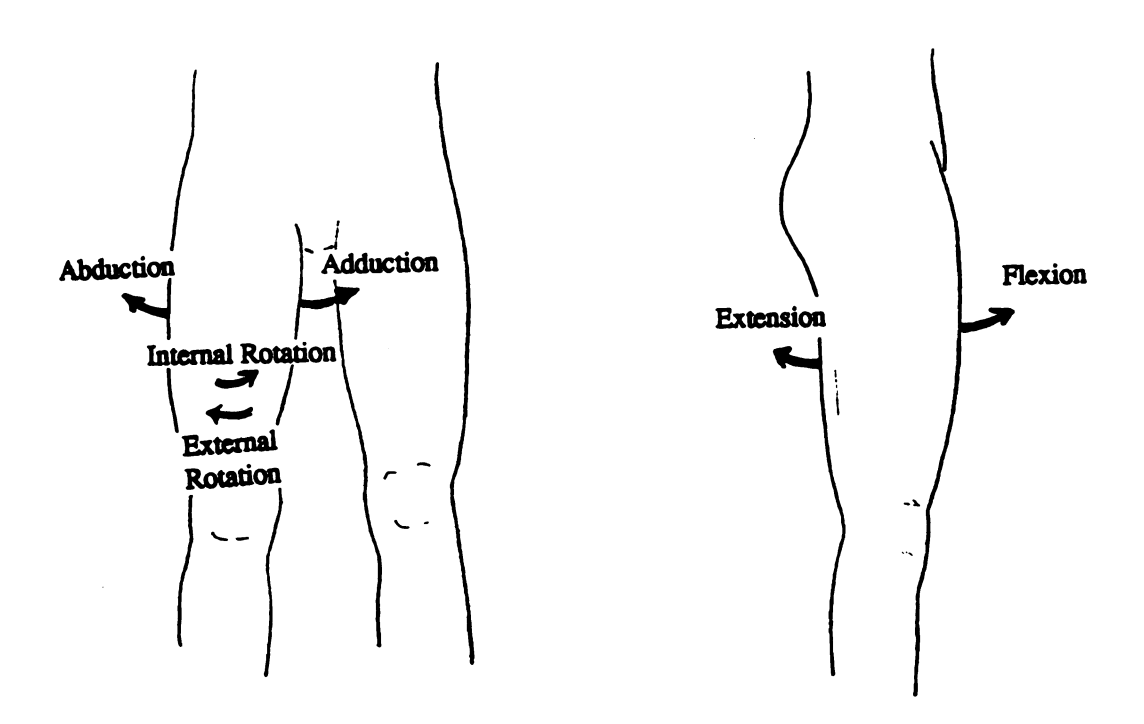


Figure 2. Hip motion definitions

In studying the different pathologies (the functional changes due to diseases or inflictions) of a gait analysis subject, it is important to separate the direct results of the primary abnormality from the secondary compensatory results associated with the problem. Kinematics describe the movement of a body, such as, the range of angular motion and the angular velocities. Kinetics help to differentiate between the primary and secondary results of deformities since it describes the driving mechanisms of motion. The joint moments, in particular, indicate which muscle groups are active in order to produce a desired motion. Joint power defines the rate of energy absorption or generation which further enables a clearer description of the gait evaluation. The objective of this study was to accurately define a three-dimensional hip joint center on a subject specific basis and to compute three-dimensional hip joint moments and power during the stance phase of gait. It is believed that these parameters will provide tools for an accurate gait analysis of research subjects and patients.

II. SURVEY OF LITERATURE

The literature survey is presented in two sections. The first section explains why the precise location of hip joint center for biomechanical studies is needed and how this location has been determined by previous investigators. The second section explains the methods of calculating the moments at the hip joint during the stance phase of gait and the history behind these methods.

A. Hip Joint Center

Hip center location is important in defining the kinematics and kinetics of the hip during gait. Small errors in locating HJC result in large errors in moment computation. Crowninshield et al. (1977) conducted an investigation on the effect of HJC location on the peak total muscle force (TMF) and peak joint contact forces (JCF) occurring during gait. Lateral displacement of HJC 2 cm resulted in 20% greater TMF and 15% greater JCF while a medial displacement of 2 cm reduced TMF by 35% and JCF by 25%. Superior displacement of HJC 2 cm resulted in 15% greater TMF and 10% greater JCF, while an inferior displacement of 2 cm reduced TMF 20% and JCF 15%. Posterior displacement of HJC 1 cm resulted in 20% greater JCF in early phase of gait. If HJC was displaced 2 cm laterally and 2 cm superiorly the abductor force increased to three times normal.

Delp et al. (1993) also studied the effects of HJC location on

the moment generating capacity of the muscles. They concluded that a 2 cm displacement of the hip center superiorly effected abduction muscle force up to 44%, the flexion force 27%, abduction moment up to 49%, and the flexion moment 22%. A 2 cm inferior displacement of HJC effected the abduction force by 20% and the abduction moment by 26% while also increasing the flexion force and moment. They found that anterior-posterior displacement of HJC by 2 cm effected the flexion/extension muscle force up to 16% and the flexion/extension moment capacity up to 36%, while a medial-lateral displacement of HJC by 2 cm affected the adduction muscle force by 20% and moment capacity by 40%.

Many studies using different techniques have been conducted to predict the three dimensional hip joint center (HJC). Some investigators have used radiographs of subjects to locate HJC (Crowninshield et al., 1978; Bell et al. 1989,1990). This procedure's accuracy depends on the ability to measure the hip center in three dimensions from two dimensional pictures. Magnification errors and alignments must be taken into account and the use of radiation on patients makes this an invasive technique. Ellis et al., 1979, obtained the center of rotation of hip joint center in two dimensions by the use of Moiré fringes.

Other investigators have proposed the use of intercepts of helical axes to define joint centers (Blankevoort et al. 1990) or by estimating the HJC to be the center of a sphere described by the three dimensional rotation of a point on a rigid body, the thigh (Cappozzo, 1984). These approaches are not accurate for small angular movements and velocities that may be prevalent in many gait patterns. Also, it may not be feasible to conduct maximum range of motion trials prior to data collection to

determine hip joint center on some patients (i.e. the elderly, arthritic, severely contracted).

Estimating the position of HJC from bony palpable landmarks is another procedure used by researchers (Andriacchi et al. 1980; Tylkowski et al. 1982). Andriacchi et al. estimated HJC as 1.5-2.0 cm distal to the midpoint of a line between the pubic symphysis and the anterior superior iliac spine in the frontal plane and along a line directly medial to the greater trochanter in the sagittal plane. Andriacchi's group did not report how their approach was devised. Tylkowski et al. studied five museum cadaveric pelvic specimens of undetermined sex and age, and AP and lateral pelvic radiographs of 200 children followed in a growth study. Tylkowski's group predicted HJC by translations along a pelvic coordinate system in fixed percentages of anthropometric measurements. The distance of HJC medial and posterior to the anterior superior iliac spines (ASIS) was calculated as a constant proportion of the distance between the ASIS: 11% medial and 21% posterior to the respective ASIS. The distance to HJC inferior from the ASIS was found to be 12% of the distance between the ASIS and the ipsilateral knee joint line (Tylkowski et al. 1982).

Bell et al. (1989) compared Andriacchi's and Tylkowski's approaches to find HJC. Bell's group obtained AP pelvic radiographs of 39 children and 31 adults of known sex. HJC was defined in these groups as the center of a series of concentric circles matched to the size of the femoral head shadow. Measurements were taken of bony landmarks on the AP pelvic x-rays using a Graf/Pen Sonic Digitizer. Since the ASIS and pubic tubercles (PT) were not radiographically distinct landmarks their locations had to be estimated. AP and right lateral biplanar radiographs were taken in a fixed reference frame of 20 adult dry pelves (unknown sex) with

radiopaque markers on bony prominences. These were used to establish the ASIS and PT locations on the aforementioned AP radiographs and were also pooled into the data of HJC location. For the 20 adult pelves, HJC was located at the center of a plastic half-sphere matched to the size of the acetabulum. In summary, Bell's group had AP x-rays of 51 adults and 39 children and right lateral x-rays of 20 adults to establish the location of HJC. HJC location was established by a percentage of pelvic width (the distance between ASIS), and they found HJC to be 14% medial, 30% distal, and 22% posterior to the ASIS in adults. The results of the location of HJC medial and posterior to the ASIS were different from those reported by Tylkowski et al. Comparison of the different approaches of HJC estimation was done by measuring the differences of actual HJC measured on the x-rays to the estimated location using Andriacchi's and Tylkowski's methods. In this study, Bell et al. concluded that the approach suggested by Andriacchi et al. was the most accurate method of predicting HJC in the frontal plane and the approach suggested by Tylkowski et al., using the figure of 22% of pelvic width, best predicted AP location of HJC in the sagittal plane.

Bell et al. (1990) then compared the accuracy of Cappozzo's (1984) rotational method of HJC localization to Andriacchi's and Tylkowski's methods of HJC estimation. AP and lateral radiographs of seven healthy adult males with reflective skin markers over bony landmarks were taken in a reference frame to find the actual location of HJC and to check the estimation of HJC of Andriacchi's group and Tylkowski's group.

Cappozzo's rotational method of HJC localization utilized the application of the least squares method of spherical analysis. To check this method, the seven healthy males were required to stand on one limb and then to

continuously and sequentially flex, extend, and abduct the hip with the knee extended and then return to the normal position without rotating the femur during the three-second video data collection. Two to three trials were required to calculate the HJC for each side. In comparing the methods of the estimated HJC to the actual HJC, Bell et al. (1990) concluded that Cappozzo's method was the least accurate of the three and that a combination of Andriacchi's and Tylkowski's methods was most accurate to find HJC. However, Bell et al. (1990) reversed their previous conclusions (Bell et al. 1989) in this study by concluding that the method suggested by Andriacchi et al. most accurately predicted the AP HJC location and that Tylkowski's approach was better for the frontal plane location of HJC, but with the percentages of ASIS width based on their subjects' pelves (14% medial and 30% distal).

The present study was designed to directly measure pelvic cadaveric anatomy utilizing a large sample size to establish the location of hip joint center accurately. The objectives were to find a correlation between HJC and pelvic geometry, to study if HJC could be estimated by taking percentages of pelvic width alone, and to investigate if there are any significant differences in locating HJC in males vs. females.

B. The kinetics of biomechanics

The studies of the kinetics of the body during locomotion has progressed over time with the increase in knowledge of the basic equations of motion and the advancement of technology.

1. The basic kinetic equations

The objective of this study was focused on the kinetics of the hip, namely the hip moments and power, during the stance phase of gait. The computations of the moments at the hip joint requires the modeling of the human body as a set of rigid bodies. In classical mechanics, the dynamics problem involving rigid bodies is solved for the motions of the bodies, since all the driving forces, both internal and external to the body, are usually well defined. In biomechanics, however, the problem is reversed. The forces and the moments at the joints are internal and cannot be experimentally measured; whereas, the motions are obtainable through the use of special targets on body segments and advanced camera systems.

The equations of motion that define both of these problems are expressed in translational and rotational components. The translational (Newtonian) equation of the rigid body is

$$\vec{F} = m \vec{a}_{cm}$$

where \vec{F} is the sum of the external forces on the body, m is the mass of the body, and \vec{a}_{cm} is the acceleration of the body at its center of mass. The rotational (Euler) equation of motion for a rigid body is

$$\vec{M} = \vec{I} \cdot \dot{\vec{\omega}} + \vec{\omega} \times (\vec{I} \cdot \vec{\omega})$$

where \vec{M} is the sum of the moments of the body about its center of mass, \vec{I} is the inertia tensor, $\vec{\omega}$ is the angular velocity of the body, and $\dot{\vec{\omega}}$ is the angular acceleration of the body. These equations can be simplified by

expressing them with respect to the principal axes of the body (Figure 3). These Newton-Euler equations can then be written as

$$F_{x} = m a_{cm_{x}}$$

$$F_{y} = m a_{cm_{y}}$$

$$F_{z} = m a_{cm_{z}}$$

$$M_{x} = I_{xx}\dot{\omega}_{x} + \omega_{y}\omega_{z} \left(I_{yy} - I_{zz}\right)$$

$$M_{y} = I_{yy}\dot{\omega}_{y} + \omega_{z}\omega_{x} \left(I_{zz} - I_{xx}\right)$$

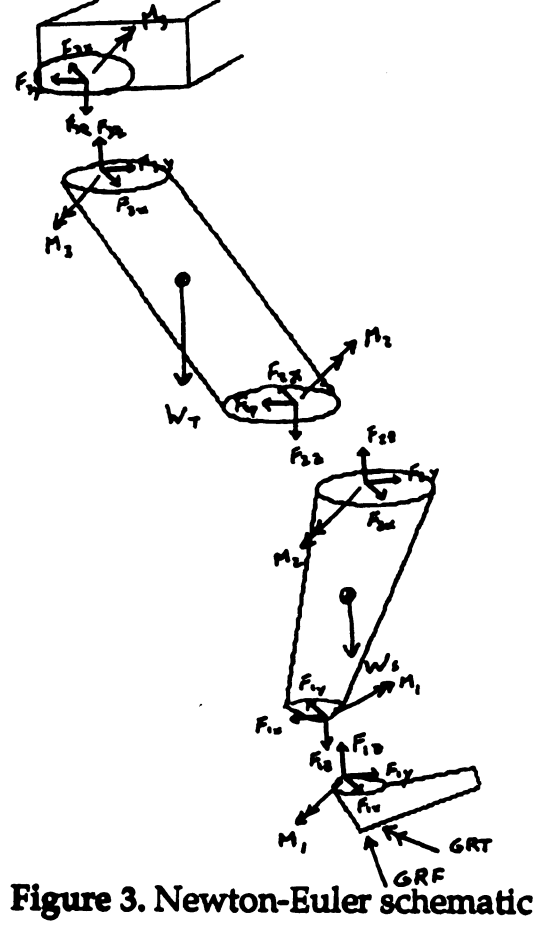
$$M_{z} = I_{zz}\dot{\omega}_{z} + \omega_{x}\omega_{y} \left(I_{xx} - I_{yy}\right)$$

where x, y, and z are the principal axes of the body (Greenwood,1988).

In walking, the magnitude of the effects of the inertial terms of the lower limbs on the moments at the joints are questionable and often ignored. This allows the moments about the joints to be computed at each instance of time as a quasi-static solution (Figure 4). The equation for the moments at the hip then becomes

$$\vec{M} = \vec{p} \times \overline{GRF} + \overline{GRT} + \vec{t} \times \overline{WT} + \vec{s} \times \overline{WS}$$

where \vec{p} is the moment arm between the ground reaction force (\overrightarrow{GRF}) and hip joint center (HJC), \overrightarrow{GRT} is the ground reaction torque, \vec{t} is the moment arm between the center of the gravity of the thigh and HJC, \overline{WT} is the



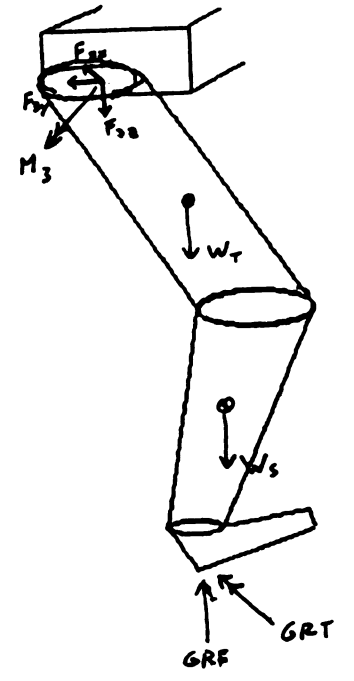


Figure 4. Quasi-static schematic

15

weight of the thigh, \bar{s} is the moment arm between the center of the gravity of the shank and HJC, and \overline{WS} is the weight of the shank.

Whether or not the inertial and gravitational terms are needed to precisely calculate the moments at the hip during stance phase of walking is still a matter of debate in the literature.

2. The history of kinetic analysis

As far back as Leonardo da Vinci, scientists have been investigating the movements, forces, and moments of the body. All of the early studies were done by the process of observation. In 1680, however, Borelli began to apply Galileo's scientific methods to the study of human locomotion. Muybridge (1887) and Marey (1885) advanced the observational kinematical studies of biomechanics with the use of photography. Braune and Fisher (1895) began to use the process of stereophotogrammetry (photographical representation of bodies in three dimensions) and were the first to study the human body as a classical mechanics problem of a system of rigid bodies. This was considered the start of modern biodynamics.

As technology increased, the science of biomechanics advanced as well, and the process and accuracy of the three-dimensional analysis of joints became more reliable. Early studies of ground reaction forces on the foot during walking were attempted by the use of subjects walking on plaster of Paris and finely spaded garden soil to study their foot imprints. This, however, only gave information on the shape of the subject's foot and not the amount of pressure distributed (Soutas-Little, 1987). Elftman (1939) used a force platform (developed by himself) that measured the magnitudes of the three components of force, from which he derived the

point of application of the force of the foot on the ground. Elftman also captured motion by taking "cinematic" records at 92 exposures per second of a subject walking behind a rectangular grid. Timing was obtained by using a vibrating reed of known period placed in the photographic field. His force plate data, coupled with his cinematic records, enabled him to calculate "reversed effective torques" (rudimentary moments) at the joints.

The most widely cited paper on the moments at the lower limb joints while walking was written by Bresler and Frankel (1950). They modeled the lower limb during walking with the free-body diagram shown in Figure 5. They used D'Alembert's principle of equilibrium of bodies in motion to express internal forces and moments at joints directly in terms of ground reaction forces, gravity forces, and inertial forces.

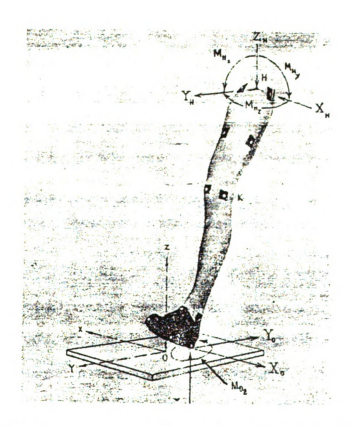


Figure 5. Bresler and Frankel's free-body diagram of the lower limb

Figure 6 shows the results of their calculations. Bresler and Frankel were interested in the significance of the inertial and gravitational effects on the moment equations, and also calculated the moments without these terms. The results of the "fore-and-aft" (flexion/extension) moments with and without inertial and gravitational terms are shown in Figure 7.

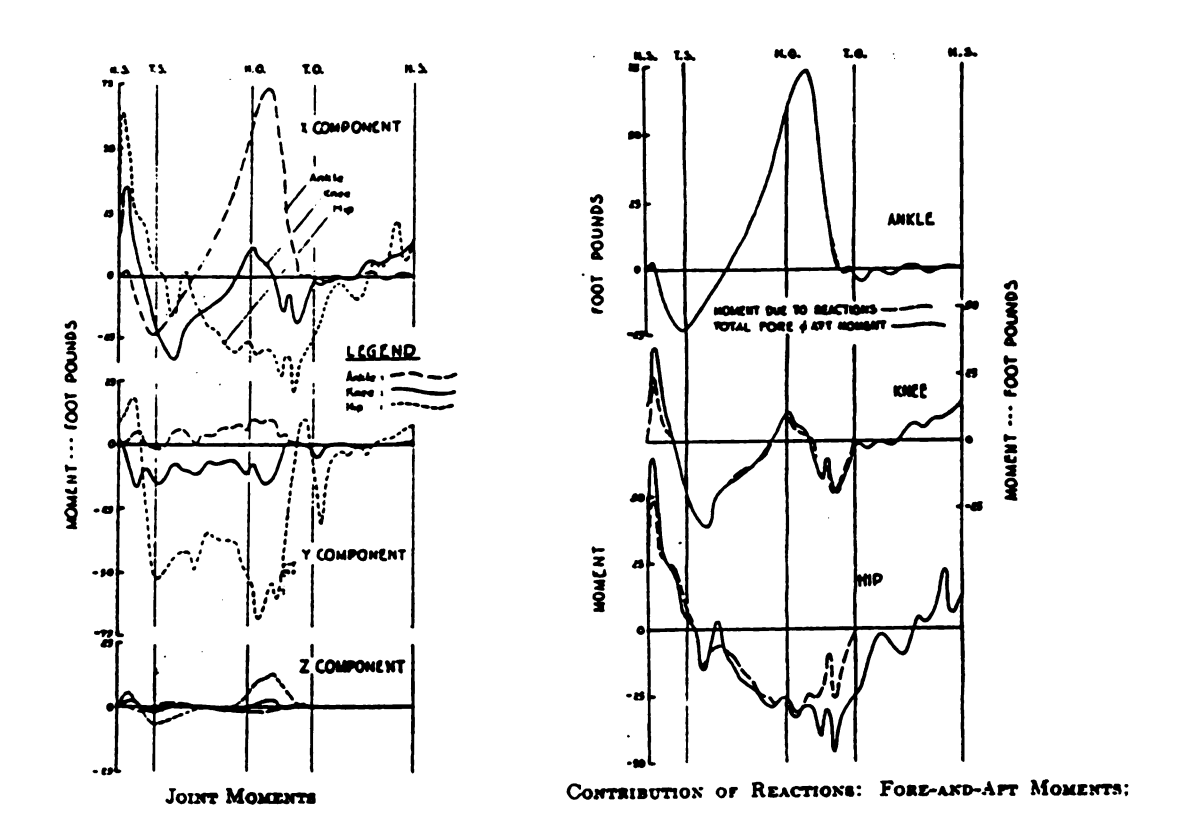


Figure 6. Joint moment results Figure 7. Contribution of reactions for (Bresler and Frankel, 1950) flex/extension moment

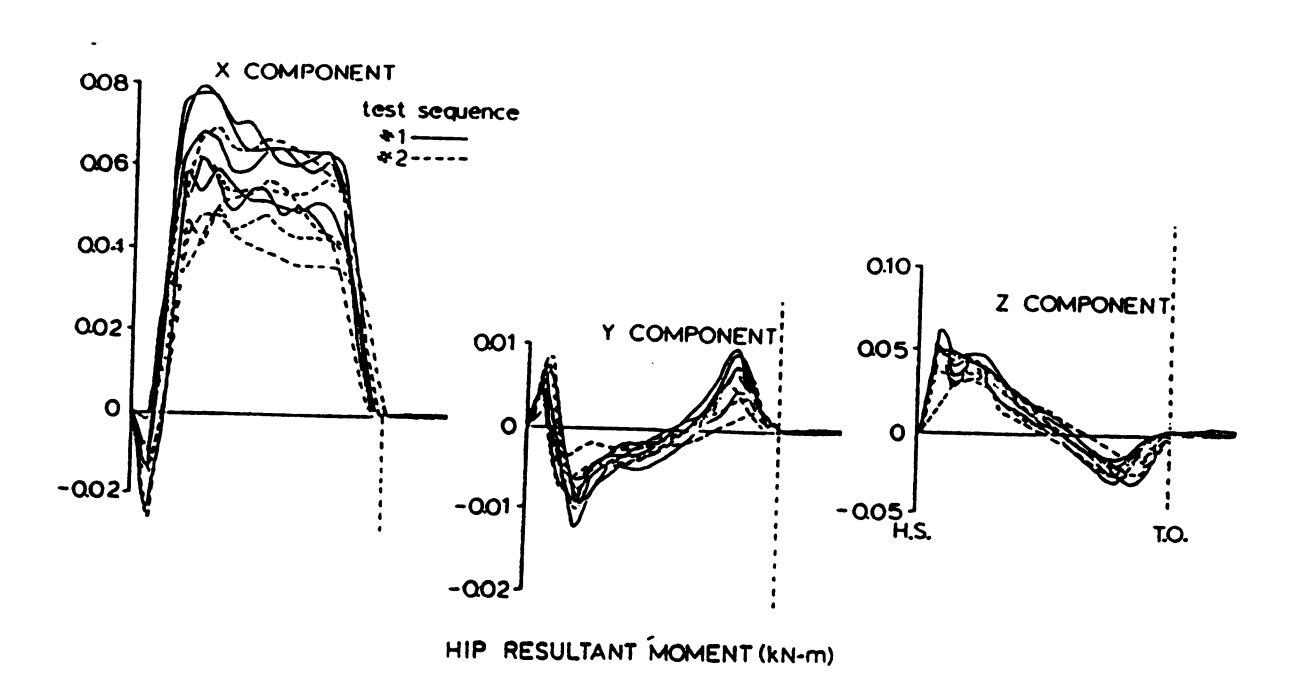
Bresler and Frankel concluded that "the effect of gravity and inertia on the fore-and-aft moments is very small for the ankle and the knee moments, and relatively small on the hip moments throughout most of stance phase."

Crowninshield et al. (1978) also solved the inverse dynamics

Problem (calculating the forces and moments from position data) for the

Luip during walking. This was achieved by modeling the body as a system

of rigid links, experimentally measuring the locations of the body segments through time, and using the kinetic data from a force plate. Once the resultant moments and forces were calculated, they were transformed to local joint coordinates (Figure 8).



x - abduction/adduction; y - internal/external rotation; z - flexion/extension

Figure 8. Hip resultant moments (kN-m) (Crowninshield et al. 1978)

Boccardi et al. (1981) studied moments at the lower limb joints by an on-line processing of kinematic data and ground reaction data. This was done by superimposing images of the resultant vector of force with images showing the position of the hip, knee, and ankle joints. They defined the muscular moment "as the product of the force exerted by a muscle and the distance from its articular axis." Specifically, the moment at the hip was calculated by the cross product of the perpendicular distance between the

projection of the ground reaction force and the joint center with the ground reaction force itself. This neglected gravitational and inertial effects.

Boccardi et al. only studied the results in the sagittal (flexion/extension) and frontal (abduction/adduction) planes (Figure 9).

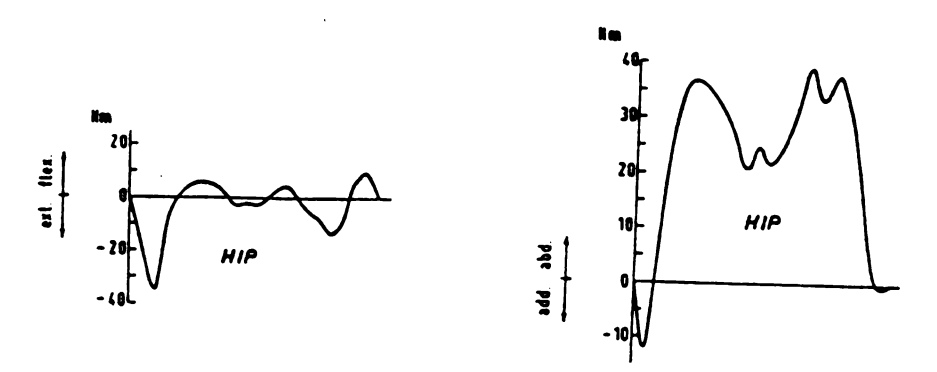


Figure 9. Boccardi's flexion/extension and abduction/adduction hip moments due to ground reaction effects alone.

They concluded that "both the general shapes of the diagrams and the numerical maximum and minimum values are very similar to those obtained by other means." The magnitudes, however, appear to be half of what Crowninshield, 1978, reported. Although the hip joint moments had consistent shape and similar values with and without inertial and gravitational terms, they had some discrepancies during the end of stance phase compared to the other joints. This is due to the inertial components of deceleration and acceleration of the leg at the push-off part of stance. These results were also taken for subjects walking at a "relatively" high speed, and it was concluded that the patients or subjects with typically slower gait would have even less contributions from the inertial terms.

Wells (1981) did a study on the projection of the ground reaction force as a predictor of joint moments. He claimed that computing

moments about joints as the cross product of the moment arm to the ground reaction force from joint center with the ground reaction force is an approximation and a potential source of error. As this method is used for joints more superior, the source of error is assumed to increase (Figure 10). Wells calculated the moments in a similar manner as Bresler and Frankel (1950) and compared these results with the moments calculated due to ground reaction force alone. He pointed out that the link segment model's use of gravitational and inertial terms requires the approximations of various anthropometric data and is a source of error. For slow cadence (1.4 m/s), the results of both methods are shown in Figure 11. Wells concluded that "the projection of the ground reaction force is a good predictor of net joint moments for slow walking (more typical of patients than of normals). Increasing the velocity of gait results in increasing errors, especially at the hip. It can be concluded that it is a useful estimate, but care must be taken when using the method in normal or faster speed walking, or for moments at the hip joint."

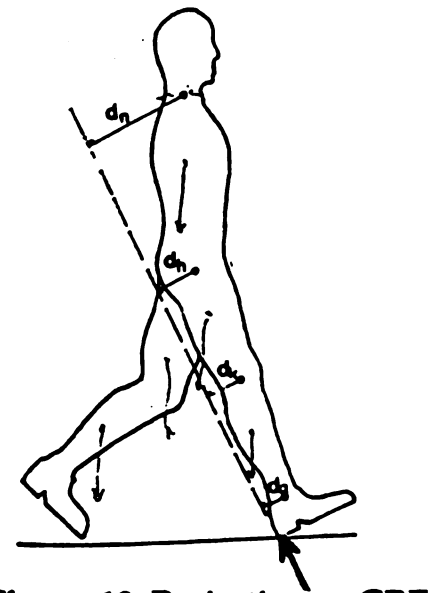


Figure 10. Projection of GRF up the body (Wells 1981).

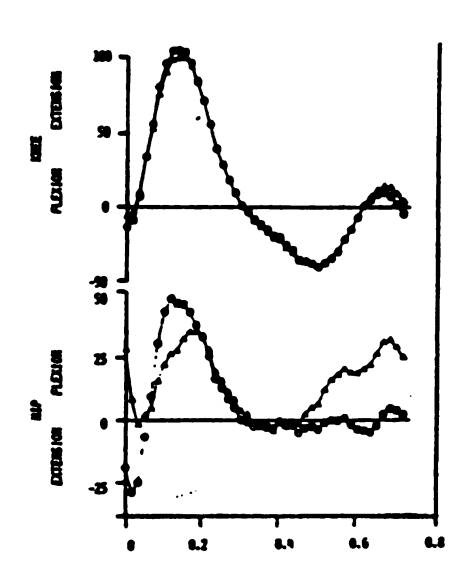


Figure 11. Net joint moments, N-m (Wells 1981).

Winter (1981, 1984) performed comprehensive studies on the flexion/extension forces and moments of the lower limb during gait. Winter (1981) states that the time history of the moments of force at the joints is "one of the most valuable biomechanical variables to have for the assessment of any human movement." He also points out that the main function of the lower limb during stance is to resist collapse and then to extend for limb push-off. Support of the body is achieved by extensor moments at every joint of the lower limb during stance. He concludes that the variability of each joint moment (ankle, knee, and hip) forces the use of a new parameter for gait analysis — the support moment (M_s) . This is simply the summation of the ankle, knee, and hip extensor moments. The pattern and magnitude of Mg was found to be consistent and useful for gait interpretation. The individual flexion/extension (sagittal plane) moments were calculated using Bresler and Frankel's (1950) equations, including the inertial and gravitational terms. Winter used a projection of the greater trochanter medially as his location of hip joint center for moment calculations. Figure 12 shows two examples of the flexion/extension moments and the typical support moments.

Cappozzo (1984) computed moments by Bresler and Frankel's (1950) approach. He also pointed out that when expressing joint moments, a point of application must be chosen. The functional significance of the moment depends upon its location and "this point should be defined either as the point through which the resultant articular surface contact force acts or, in the absence of friction, could be taken as the center of rotation" of the joint. An example of his joint coordinate system moments are shown in Figure 13.

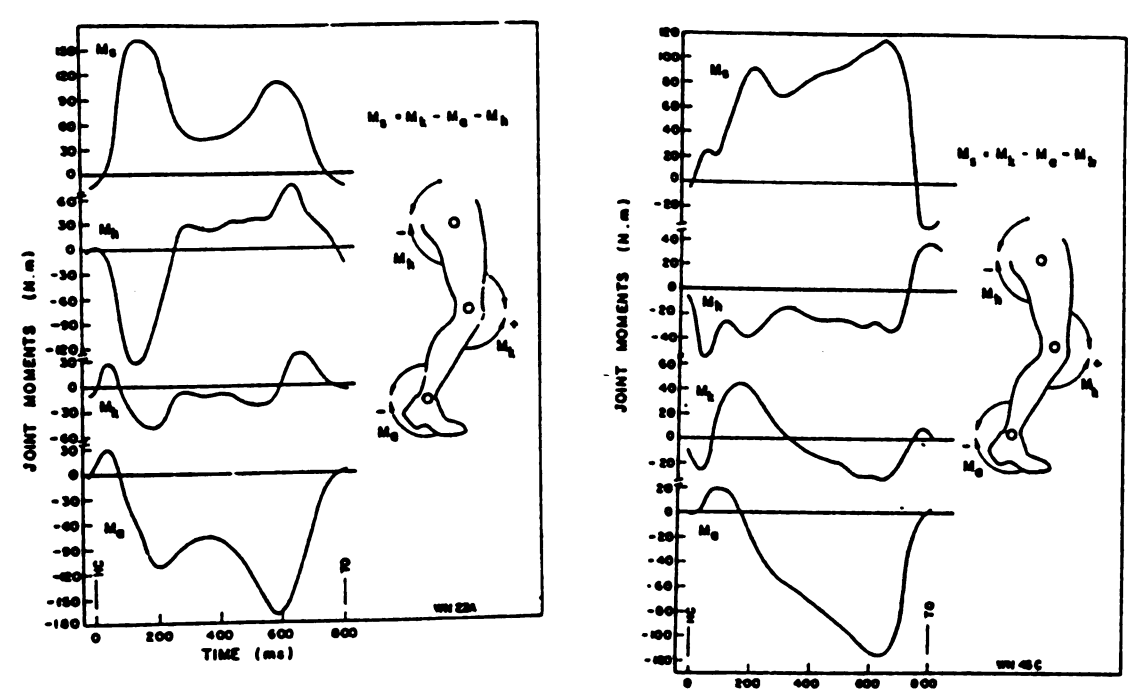


Figure 12. Flexion/extension moments: ankle (M_a) , knee (M_k) , hip (M_h) , and total support (M_s) (Winter, 1980)

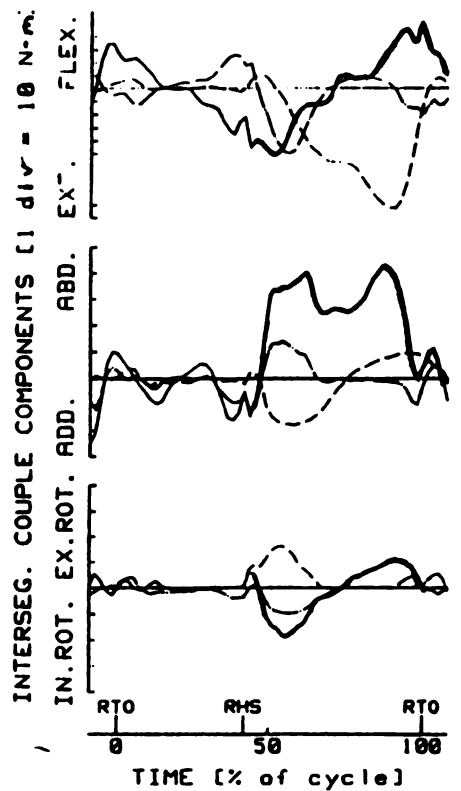


Figure 13. Moments in joint coordinate system (dark solid line indicates hip moment) (Cappozzo, 1984)

In 1990, Ramakrishnan et al. did a study on lower extremity joint moments and ground reaction torques to establish a "normal" data base of adults. They used a VICON motion analysis system, a force plate, and foot switches to obtain the data needed to compute three-dimensional moments of the hip, knee, and ankle joints and ground reaction torques of 40 adults (18-40 yrs old) and 10 aged adults (55-70 yrs old). The moments were calculated using three-dimensional linear motion, angular motion, velocities, accelerations of body segments, and external ground reaction forces. The inertial components of the moments were calculated by the Euler equations of rotation about principal axes described earlier. Moments were normalized as percent body weight and limb length. Figure 14 displays sample results and Table 1 shows magnitude comparisons between their results, Winter's (1984) results and Cappozzo's (1984) results. Ramakrishnan attributed the difference in magnitudes to normalization techniques and different estimations of hip joint center locations.

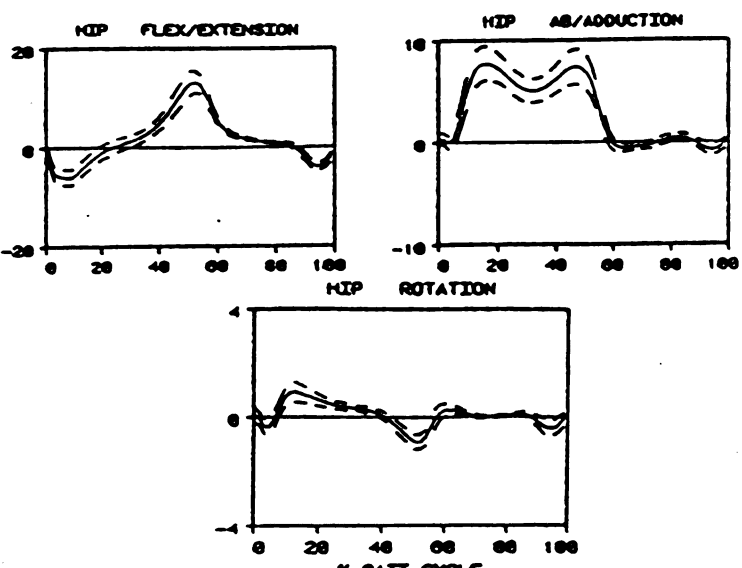


Figure 14. Hip moments of walking normalized to % body weight limb length (Ramakrishnan, 1990)

Table 1. Comparison of maximum moments (Ramakrishnan, 1990)

Comparison of maximum moment with previous authors

No. of Subjects:	Present N=40	Winter 1 N=16	Cappozzo 1 N=1
(120	evaluations		
Hip flexion	13.2(2.3)	6.5(2	.9) 8.0
Kneeextension	6.9(1.5)	5.5(2	
Ankle plantarflexion	13.5(1.2)	17.0(•
Hip abduction	7.7(1.6)	-	6.0
Knee abduction	3.2(1.4)	-	2.3
Hip rotation (external)	0.9(0.4)	-	3.1
Knee rotation (external)	0.4(0.1)	-	1.5
Ankle rotation (external)	1.3(0.3)	-	1.5
Ground reaction torque		-	-

Normalized to unit leg length. Values shown are mean (standard deviation) and were interpolated from the published graphs.

Ounpuu et al. (1991) established a data base for pediatric (ages 5 - 14) gait of three-dimensional lower extremity joint kinetics. They used Euler's equations to calculate the net joint moments relative to each body segment coordinate system. Ounpuu used Dempster's (1959) anthropometric estimates for adults because of the lack of data for children. They believed that this would not be a source of error because "the contribution of the inertial components to the joint kinetic data in the stance phase is small." They also calculated power defined to be the angular velocity of a particular segment times the moment of that segment. Graphs of hip moments and power for the sagittal and frontal plane are shown in Figure 15. Their results were similar to the adult data results of Bresler and Frankel (1950) and Ramakrishnan et al. (1990). From this, they inferred that "children typically establish their mature gait as early as age 5 years."

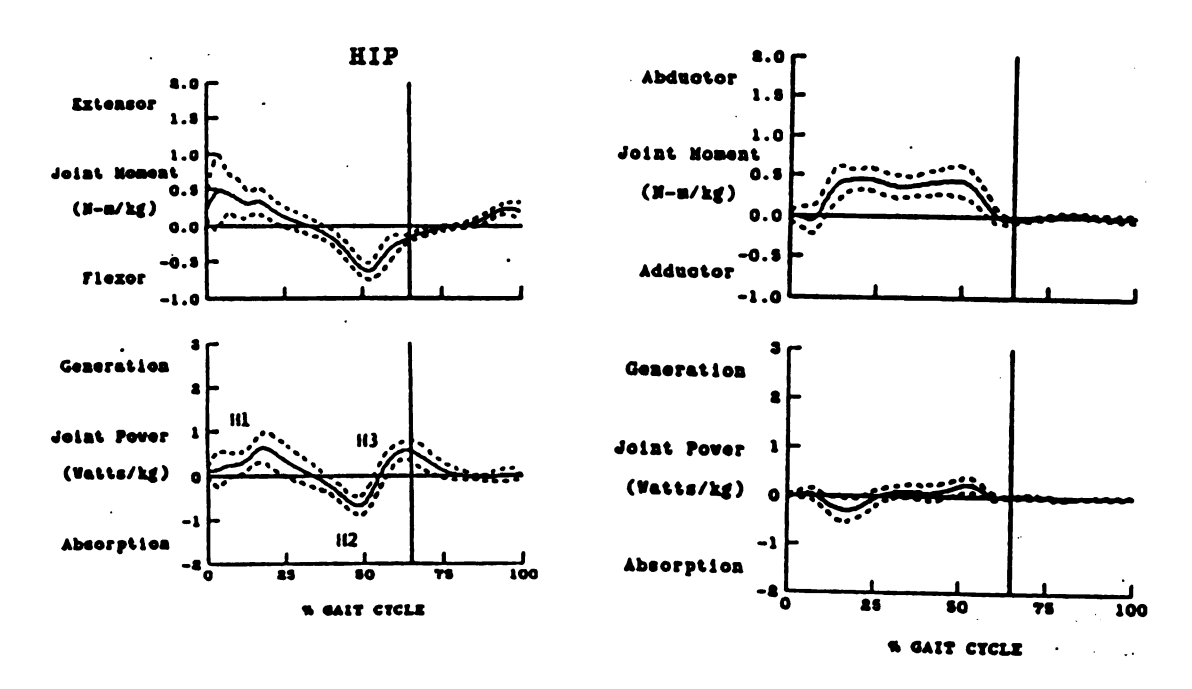


Figure 15. Frontal and sagittal plane hip moments and power (Ounpuu et al. 1991)

The methods of calculating moments at the hip are well established by using the laws of classical mechanics. The question still remains as to whether or not inertial terms are needed to obtain accurate results. Most authors (Bresler and Frankel (1950), Boccardi (1981), Wells (1981), and Ounpuu (1991)) stated that the inertial effects on joint moments were small but started to become significant at the hip joint, especially with a fast gait. However, with inertial terms, care must be taken to compute accurate angular velocities and accelerations about the axes of the moments studied. Since only displacement data of angular motion is directly obtained, differentiation must be applied twice to generate velocity and acceleration terms. Estimations of anthropometric data (body segments' inertias, weights, and center of gravity locations) are based upon average data, not individual subjects. Subjects seen in clinical gait laboratories are

26

patients with constrained, slow gait, and the effect of inertial terms are minimal. For these reasons, the moments in this study were calculated without the inertial terms. However, since the weight of the lower limb is roughly one-sixth body weight, the gravitational effects were considered.

Power is defined as the rate of doing work. Most authors express power at a joint during gait as the power associated with the individual planes of motion. They (Ounpuu, 1992; Winter 1992) compute this 'power' as the magnitude of the moment multiplied by the angular velocity of the planar angle in question. If the model being studied is planar, then this is logical, such as Winter's (1992) study of the biomechanics in the sagittal plane. However, when three-dimensional kinetics are being studied, the true definition of power is $\bar{\mathbf{M}} \cdot \bar{\mathbf{w}}$ and individual components cannot be separated in a scalar quantity. This planar 'pseudo-power' is, however, used as a clinical tool to help describe muscle activity. Therefore, in this research, power in the sagittal plane was calculated as the flexion/extension moment multiplied by the angular velocity of flexion/extension; true power at the hip was calculated as $\bar{\mathbf{M}} \cdot \bar{\mathbf{w}}$.

III. METHODS OF DATA COLLECTION

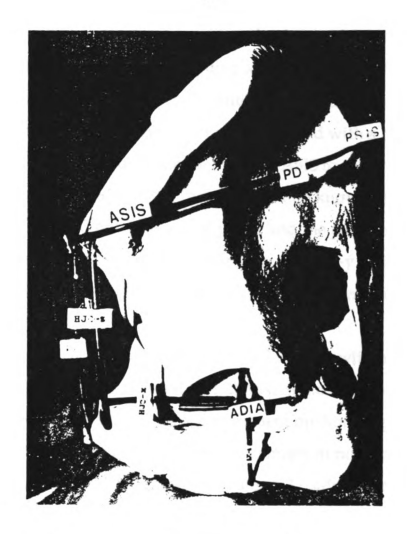
This chapter is divided into two major sections. The first section is a description of the methods utilized to define the location of HJC based on pelvic geometry. This was completed through an extensive cadaver study performed by the author and Geoffrey Seidel, M.D. of the Rehabilitation Institute of Michigan, Wayne State University, Detroit, Michigan. The second section of this chapter is a general description of the experimental methods used to collect the kinematic and kinetic data of a subject walking. This work was performed at the Biomechanics Evaluation Laboratory, Saint Lawrence Health Science Pavilion, East Lansing, Michigan.

A. Hip Joint Center Location

All human cadavers used for anatomical instruction at Wayne State University School of Medicine, Detroit, Michigan from April 1991 through January 1993 were examined after anatomical dissection. The Wayne State University mortuary acquires voluntarily donated cadavers from three counties of southeastern Michigan. Those cadavers with intact pelves were entered into the study group and available demographic data recorded. Sixty-four cadavers were examined, 35 female and 29 male. The ages ranged from 53 to 99 (mean 75.1, sd 12.6) representing skeletally

mature adults. Intact cadaveric pelvic specimens were excluded from the study if there was a pelvic fracture, acetabular surgery, severe degenerative changes with osteophytosis, and obvious pelvic asymmetry. If an orthopedic procedure was performed unilaterally, the other side was included in the study group. This left a total of 122 sides examined.

Pelves were removed from the cadavers and defleshed to allow accurate measurement of bony landmarks. Each pelvis was placed on a flat surface with both ASIS and the pubis in contact with a data recording sheet. To establish a pelvic coordinate system, the frontal plane was defined as the plane passing through both ASIS and the pubic symphysis. The coordinate system was defined with: its origin at the respective ASIS side that was being measured; y-axis mediolateral (positive medial); z-axis superoinferior (positive inferior); and x-axis anteroposterior (positive posterior). The point of contact of both the ASIS and the pubis were traced on the data recording sheet to ensure the pelvis did not move during the pelvic measurement procedure. All measurements were made with a millimeter ruler or calipers from bony surfaces, not compressible soft tissue structures. Measurements were made of acetabulum depth and diameter to ensure that the acetabulum could be considered a hemisphere and HJC was defined as the center of the acetabular rim (labrum removed). HJC-x (depth measurement) was defined and measured as the perpendicular distance from the frontal plane to the center of the bony acetabular rim (Figure 16). The pelvis was lifted and the specific contact points of each ASIS and the pubis were noted within the traced areas on the data recording sheet. The position of the projection of HJC-x on the frontal plane was recorded on the data sheet.



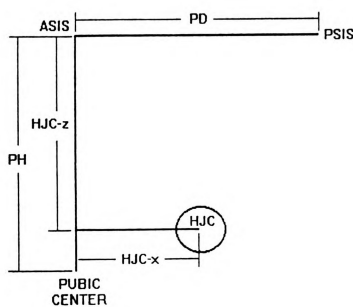
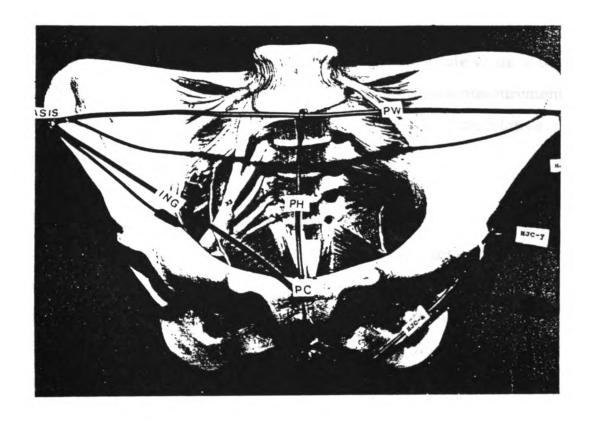


Figure 16. Medial/lateral view of pelvic measurement

Other pelvic measurements included pelvic width (ASIS to ASIS), pelvic height (perpendicular from pubic center to the inter-ASIS line), ASIS to pubic center, and ASIS and pubic center to the intersection of HJC-x with the frontal plane. Pelvic depth was measured with a caliper accurate to a millimeter in an oblique fashion from the ASIS to the posterior superior iliac spine (PSIS). With the ASIS location known, the HJC-x projection of the HJC onto the frontal plane, and the pubic center (PC) defined as the center of the pubic symphysis, the HJC-y (medial measurement) and the HJC-z (height measurement) were calculated (Figure 17).

All measurements were made by Dr. Seidel, to within a millimeter. Interrater reliability was assessed with the assistance of two additional raters who were instructed in the measurement methodology and then each allowed to select a group of pelvic specimens at random to reproduce all measurements (rater 1: 20 sides and rater 2: 17 sides). Dr. Seidel's measurements were compared to those of each rater. Mean interrater differences for each measurement were less than one millimeter. An analysis of interrater differences with data plot analysis failed to reveal any significant systematic or random error. Interrater reliability correlation coefficients of the pelvic measurements were high for pelvic measurements indicating a reliable measurement procedure.

Parametric analysis of interval measurement data and Pearson product-moment correlation analysis was performed with SPSS/PC+ statistical package. No violations of normality were observed and outlier data were included in analysis. Power analysis established the sample sizes adequate for systematic analysis. The student's paired t-test was utilized to compare male and female data. Measured distances from the



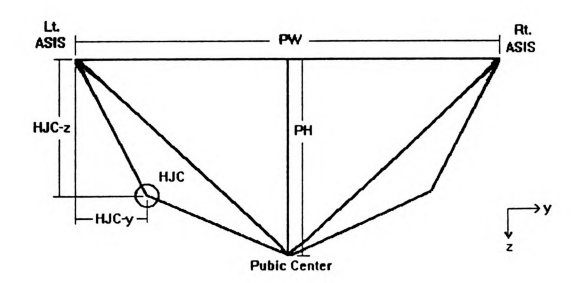


Figure 17. Frontal view of pelvic measurements

ASIS to ipsilateral HJC along x, y, and z axes were divided by pelvic width (ASIS separation), pelvic depth, and pelvic height and were intercorrelated and compared to previously reported data. The absolute value of the differences between estimated and true HJC coordinate measurements were made and analyzed with Student's t-test to assess the relative accuracy of HJC location.

B. Kinematic and Kinetic Data Collection

In order to calculate the moments at the hip joint during gait, the external forces acting on a subject while walking and the positions of the subject's body segments must be measured throughout the gait cycle. Therefore, both kinematic and kinetic data were collected of a subject walking.

1. Equipment

The kinematic data were collected using four solid state, shuttered 60 Hz NEC video cameras and a Motion Analysis Corporation VP-320 model dynamic image processor. Prior to collecting subject walking data, a calibrated space of $150 \times 100 \times 160$ cm centered over the force plate was defined by sixteen control points (Figure 18). The cameras were positioned to encompass the control points (spherical targets covered with 3M retroreflective tape) such that the entire space could be viewed by each camera. The targets were illuminated by incident light provided by flood lights mounted 2.0 cm away from the camera lens, and the target's light image was reflected back to the camera. The kinematic coordinate system is referred to as 'lab space' (ls) and is also shown in Figure 18. The Expertvision three-dimensional (EV3D) digitizing program, utilizing

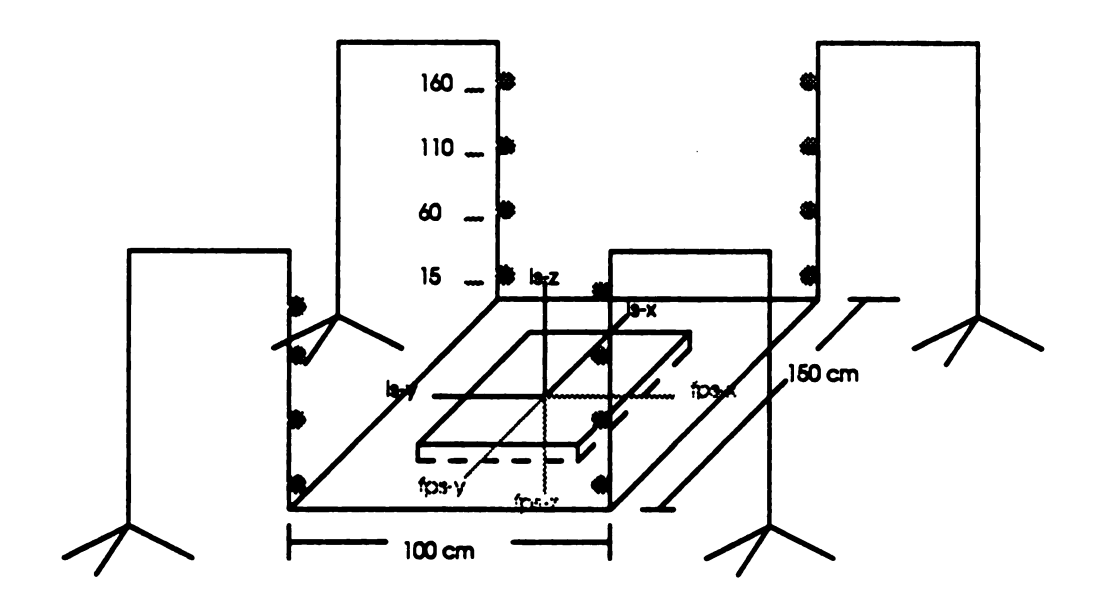


Figure 18. Calibration set-up with lab space (ls) and force plate space (fps) coordinate systems

direct linear transformations, was used to compute the three-dimensional positions of the targets. The norm of residuals (the accuracy of the input location of a target compared to the computed position of the target) ranged from .38 to .47, indicating an accurately calibrated space.

Stance phase ground reaction data were collected using an AMTI Biomechanics Platform Model OR6-6. This force plate simultaneously measures the foot-ground forces (F_X, F_y, F_z) and the moments (M_X, M_y, M_z) and M_z about its instrument center at a collection rate of 1000 Hz. The forces and moments are measured through the use of strain gages attached to load cells at the four corners of the plate. Sample force data for a walking trial is shown in Table 2. The force plate is flush with the laboratory floor and the instrument center is 4.05 cm below the top surface. The orientation of the force plate coordinate system is different from that of lab space and is shown in Figure 18.

2. Walking data collection

Kinematic and kinetic data were collected simultaneously for two subjects walking through lab space at comfortable stride. The subjects used for this test were 24 and 26 year old males with no known pathologies. The subjects signed an informed consent form approved by UCHRIS (IRB #89-559). Using hypo-allergenic tape, nine retro-reflective targets were attached to the subject (Figure 19) over the following bony landmarks:

left anterior superior iliac spine (LASIS) right anterior superior iliac spine (RASIS) posterior superior iliac spine (PSIS) greater trochanter (GT) lateral femoral epicondyle (LATCOND)

Table 2. Sample force plate data for walking

-	Fz(N)	Fx(N)	Fy(N)	Mz (N-m)	Mx (N-m)	M (N)
. 0			•		•	• • •
0	45.596 60.363	1.877 2.628	-1.828 -3.328	0.397	4.611	4.328
2	86.945	2.628	-6.328	0.246 0.700	6.080 8.137	6.089 8.437
3	122.388	4.130	-8.578	0.851	11.076	11.665
4	163.738	4.130	-11.578	1.003	14.897	15.773
5	213.949	3.379	-15.328	1.457	19.599	21.056
6	267.113	1.877	-17.578	1.911	23.420	25.751
7	311.416	-2.628	-18.328	2.365	26.947	29.566
8	340.952	- 7.885	-19.828	2.971	29.004	32.207
9	358.673	-13.141	-20.578	3.425	30.180	33.674
10	367.534	-17.647	-22.078	4.030	30.180	34.261
11	361.627	-22.904	-23.578	4.636	29.592	34.555
12	355.720	-26.658	-24.328	5.090	28.710	33.968
13	346.859	-29.662	-27.328	5.392	27.828	33.087
14 15	335.045 329.138	-31.164 -32.666	-28.828 -30.328	5.847 5.998	26.653	32.207
16	329.136	-33.417	-32.578	6.149	25.771 25.183	31.620 31.033
17	317.323	-34.167	-34.078	6.452	24.596	30.740
18	314.370	-32.666	-36.328	6.603	24.008	30.446
19	311.416	-33.417	-37.828	6.603	24.008	30.153
20	311.416	-31.915	-38.578	6.755	23.420	30.153
21	311.416	-31.915	-40.078	6.755	23.714	30.446
22	314.370	-31.164	-41.578	6.755	23.714	30.446
23	317.323	-29.662	-41.578	6.603	24.008	30.740
24	317.323	-28.911	-42.328	6.755	24.008	30.740
25	323.231	-27.409	-44.578	6.755	23.714	31.033
26	326.184	-25.907	-44.578	6.603	24.008	31.620
27	332.091	-24.405	-45.328	6.603	24.596	31.620
28	335.045	-22.904	-46.828	6.603	24.889	31.913
29 30	337.998 340.952	-21.402 -19.149	-47.578 -48.328	6.452 6.452	24.889 24.889	31.913 32.207
31	340.952	-17.647	-49.828	6.452	24.596	31.913
32	340.952	-16.145	-49.828	6.452	24.596	31.913
33	340.952	-14.643	-50.578	6.301	24.302	31.913
34	337.998	-13.141	-52.828	6.301	24.008	31.620
35	335.045	-12.391	-53.578	6.149	23.420	31.327
36	332.091	-10.889	-53.578	5.998	23.420	31.033
37	332.091	-10.889	-53.578	5.998	23.420	30.446
38	326.184	-8.636	-52.828	5.847	23.420	30.446
39	326.184	-6.383	-52.828	5.695	22.538	29.859
40	323.231	-6.383	-52.828	5.544	22.538	29.859
41	323.231	-5.632	-52.078	5.544	22.244	29.566
42	323.231	-4.881	-51.328	5.392	22.244	29.272
43	323.231	-3.379	-51.328	5.090	22.244	29.272
44	320.277	-2.628	-50.578	5.090	21.950	29.272

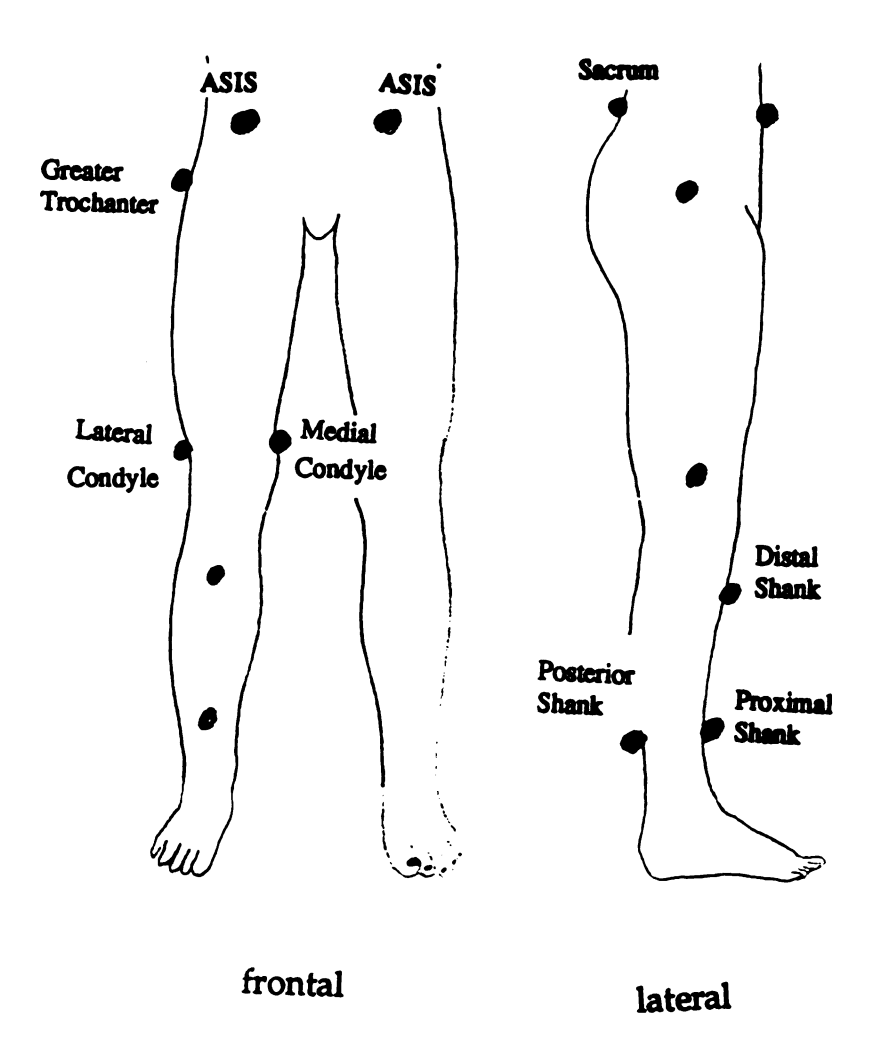


Figure 19. Targeting scheme

medial femoral epicondyle (MEDCOND) proximal anterior tibia (PROX) distal anterior tibia (DIST) distal posterior tibia (POST)

At least three non-collinear targets were placed on each body segment studied so segment anatomical planes and axes could be formed.

Anthropometric measurements were taken of the distance between the inter-ASIS line and the pubic symphysis (ps), of pubic depth (ASIS to PSIS) and of the shank length (LATCOND to calcaneus).

The subjects were instructed to walk through the calibrated space at a "normal" cadence. Trials were saved if the subject successfully struck the force plate with the entire foot of the targeted side and nothing else. The reproducibility of the force data is shown for three trials in Figure 20. Data were collected for walking with both left and right sides targeted. In all, five trials of each condition were saved. Using EV3D, all trials were tracked and edited to establish the three-dimensional trajectories of the targets as the subject walked through lab space (Table 3). With the subject standing erect in the middle of lab space standing measurements were taken to correct for any misalignment of targets (Figure 21). A completed tracked and edited walking file is shown in Figure 22.

Biomechanics Evaluation Laboratory

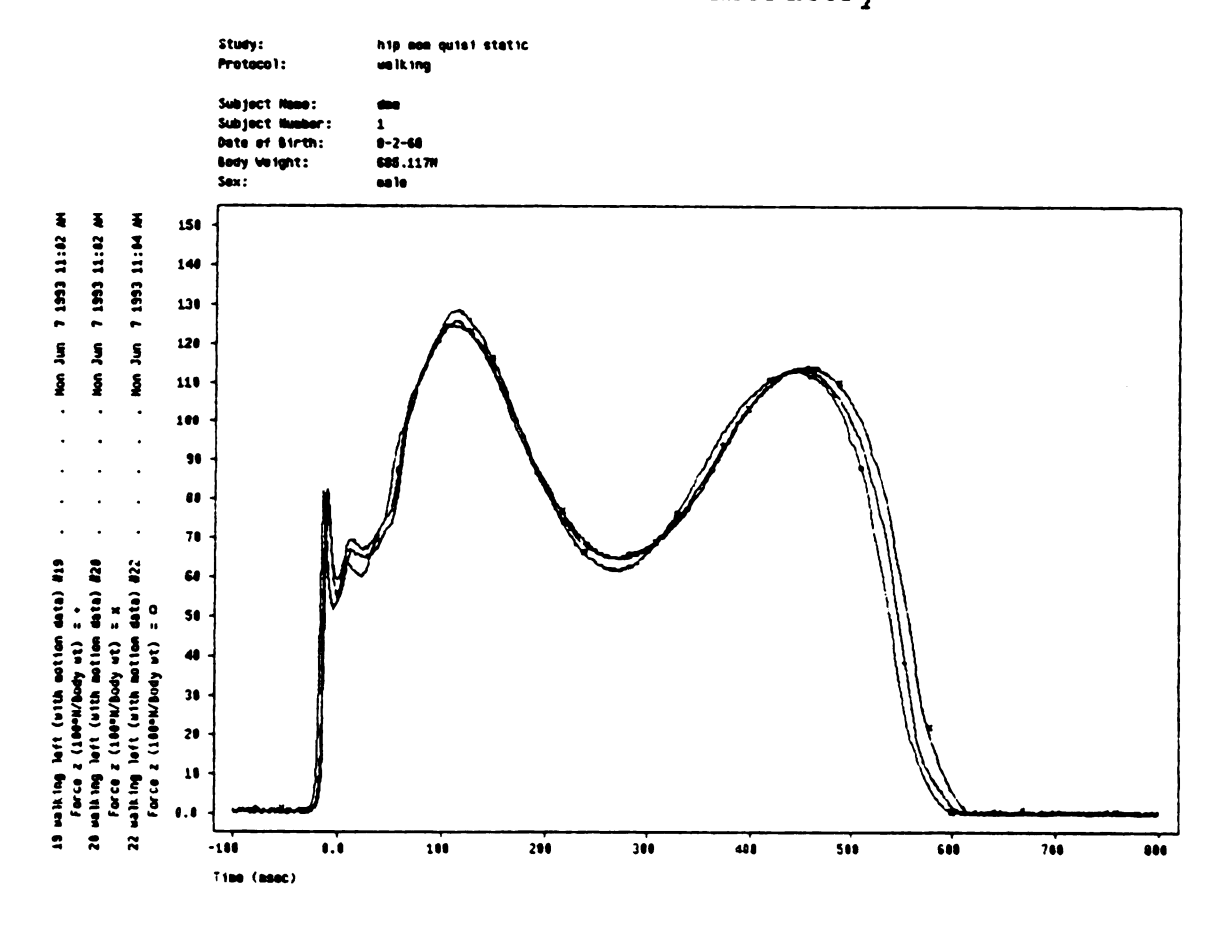


Figure 20. Vertical ground reaction force (F_Z) of three trials

Table 3. Sample motion data

```
SKILL 1:
 FOR WHICH THERE IS (ARE) 1 TRIAL(S).
 TRIAL
         1:
 INITIAL TIME
                           0.000000 SECS.
 TIME INCREMENT =
                        16666*10-6 SECS.
 CUTOFF FREQ'S:
 OBSERVATION
                  1 FOR WHICH T =
                                      0.000000
 LT ASIS
                         IS AT X -
                                        -53.7131 Y =
                                                           16.6629 Z =
                                                                               98.1406
                                                                         .12
.30.35.
86.771
87.5132
50.5237
50.2506
39.25
 RT ASIS
                         IS AT X =
                                         -47.2895 Y =
                                                            -6.6110 z =
                                                                               97.7227
 PSIS
                         IS AT X =
                                        -72.0099 Y =
                                                            -4.4761 Z =
                      IS AT X = -47.4855 Y = 6.3542 Z =

IS AT X = -53.2762 Y = -14.3585 Z =

IS AT X = -29.1295 Y = -8.2870 Z =

IS AT X = -30.6517 Y = 3.1821 Z =

IS AT X = -24.1522 Y = -2.4788 Z =

IS AT X = -21.7351 Y = -0.9415 Z =

IS AT X = -35.1483 Y = -1.3715 Z =
 PUBIC SYMPH
 GR TROC
 CONDYLE LAT
 CONDYLE MED
PROX SHANK
                IS AT X =
IS AT X =
IS AT X =
 DIST SHANK
POST SHANK
                                                                               22.3886
OBSERVATION 2 FOR WHICH T = 0.016667
IS AT X =
LT ASIS
                                      -50.0936 Y -
                                                            16.5952 Z =
                                                                               98.0593
                                                            -6.8167 z =
                                                                               98.0319
                                                            -4.4377 Z =
                                                                              100.5000
                                                             6.1335 z =
                                                                               86.9013
                                                           -14.6527 Z =
                                                                               87.8699
                                                        -8.1218 Z =
                                                                               50.7285
                                                            3.1890 Z =
                                                                               50.4429
                                                            -2.3525 z =
                                                                               39.1517
                                                            -0.8387 z =
                                                                               24.5000
                                                            -1.5312 Z =
                                                                               22.7333
 OBSERVATION 3 FOR WHICH T = 0.033333
                         IS AT X = -46.4443 Y = IS AT X = -40.4418 Y =
 LT ASIS
                                                            16.4538 z =
                                                                               98.0612
 RT ASIS
                         IS AT X =
                                                            -7.1014 Z =
                                                                              98.4025
                         IS AT X =
 PSIS
                      IS AT X = -65.1557 Y =
IS AT X = -40.1842 Y =
IS AT X = -46.4512 Y =
IS AT X = -22.4307 Y =
IS AT X = -24.6236 Y =
                                      -65.1557 Y =
                                                            -4.3538 Z =
                                                                              100.7019
                                                             5.8039 z =
 PUBIC SYMPH
                                                                               87.1212
                                       -46.4512 Y =
                                                           -14.9987 z =
                                                                               88.2897
 GR TROC
                                                           -7.9684 z =
                                        -22.4307 Y =
 CONDYLE LAT
                                                                               50.8828
                                       -24.6236 Y = 3.1098 Z =

-18.8933 Y = -2.2087 Z =

-18.1619 Y = -0.7200 Z =

-31.5276 Y = -1.7496 Z =
 CONDYLE MED
                                                                               50.6384
 PROX SHANK
                        IS AT X =
                                                                               39.0623
 DIST SHANK
                         IS AT X -
                                                                               24.3399
 POST SHANK
                         IS AT X =
                                                                               23.1249
 OBSERVATION 4 FOR WHICH T = 0.050000
                                                          16.2669 Z =
                                                                               98.1380
 LT ASIS
                         IS AT X = -42.8189 Y =
 RT ASIS
                                                            -7.4092 Z =
                                                                               98.7967
                         IS AT X =
                                         -37.2354 Y =
                        -4.2599 z =
 PSIS
                                                                              100.9201
PUBIC SYMPH
                      IS AT X =
                                                                               87.3940
 GR TROC
                                                                               88.7205
CONDYLE LAT
                                                                               50.8944
CONDYLE MED
                                                                             50.7670
                                                             2.9768 Z =
PROX SHANK
                                                                                38.9279
```

example of walking barefoot right ted file

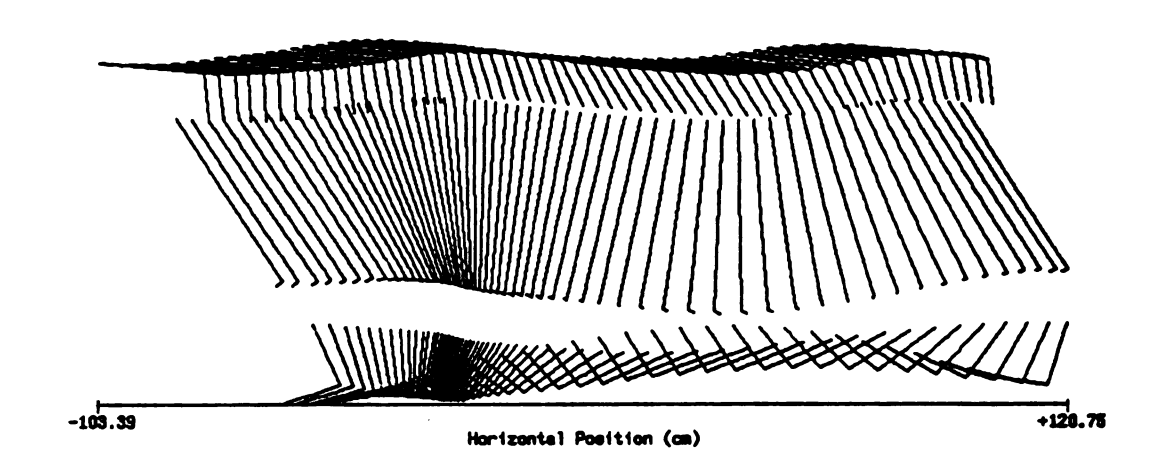


Figure 21. EV3D stick figure of standing subject

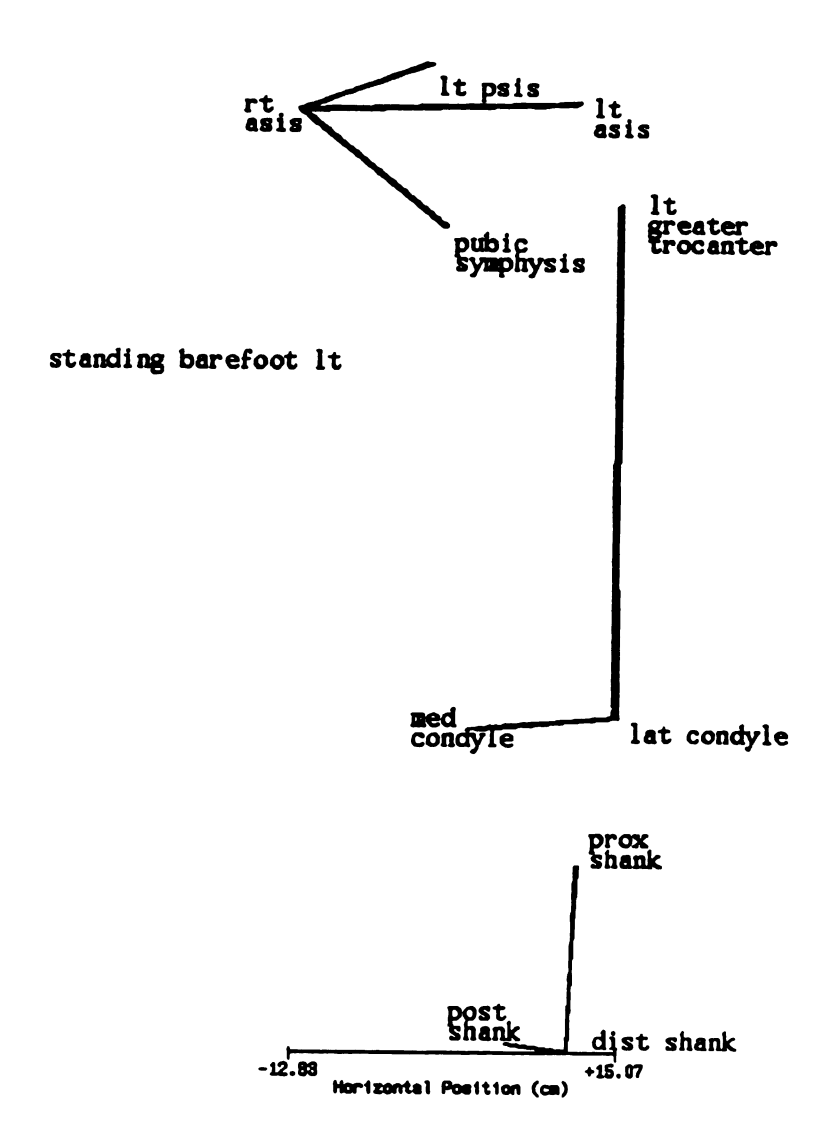


Figure 22. EV3D stick figure of walking subject

IV. ANALYTICAL METHODOLOGY

This chapter is presented in two major sections: the first describing the mathematical methods of calculating hip joint center and the correlations to pelvic geometry; and the second describing the analytical methods to calculate the hip moments and power during gait.

A. Hip Joint Center

Only the posterior measurement (HJC-x) of hip joint center could be obtained by direct measurements on the defleshed pelves. HJC-y (medial measurement) and HJC-z (inferior measurement) had to be calculated from the other measurements taken using trigonometric functions (Figure 23). The measured distances taken from the cadaver study were the distance between the ASIS and the midline of the inter-ASIS line (a), the pelvis height (b), the distance between the ASIS and pubic center (c), and the distances between the projection of HJC-x on the frontal plane and the ASIS (e) and the pubic center (d). These distances are related by the following trigonometric identities:

$$d^2 = e^2 + c^2 - 2ec(\cos \theta)$$
 $b^2 = a^2 + c^2 - 2ac(\cos \theta)$

yielding, the following values of ϕ and θ :

$$\phi = \cos^{-1} \left(\frac{-d^2 + e^2 + c^2}{2ec} \right) \qquad \theta = \cos^{-1} \left(\frac{-b^2 + a^2 + c^2}{2ac} \right)$$

where ϕ and θ are intermediate angles needed to calculate the values:

HJC-z =
$$-esin(\phi + \theta)$$

HJC-y = $-ecos(\phi + \theta)$

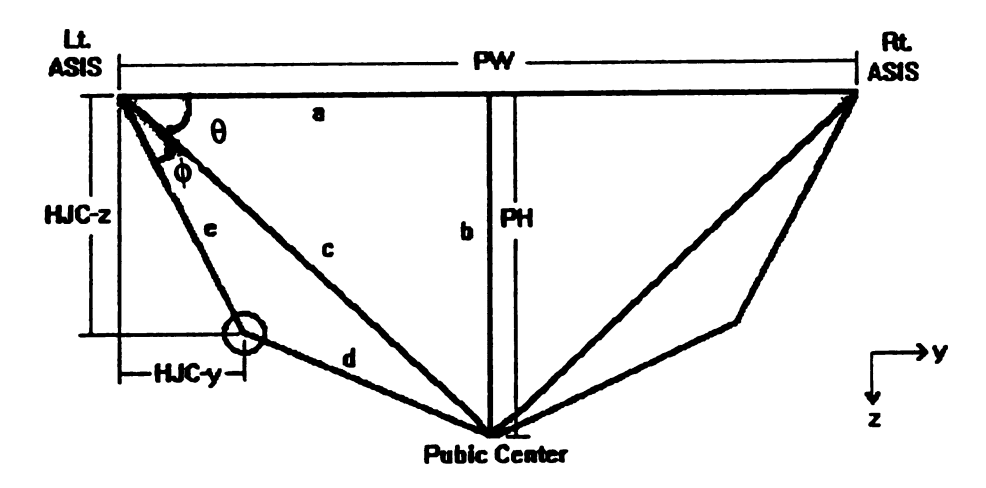


Figure 23. Pelvic geometry of frontal plane

The location of the HJC has now been determined from pelvic measurements.

Pearson product-moment correlations were performed to evaluate the relationship between HJC values and pelvic anthropometric measurements. For example, the correlation (r) of HJC-y with PW was calculated as

$$r = \frac{\sum (HJC - y - \overline{HJC - y})(PW - \overline{PW})}{N(S_{HJC - y})(S_{PW})}$$

where,

$$S_{HJC-y} = \sqrt{\frac{\sum (HJC-y - \overline{HJC-y})^2}{N}}$$

and,

$$S_{PW} = \sqrt{\frac{\sum (PW - \overline{PW})^2}{N}}$$

are the standard deviations of the HJC-y and PW measurements, with HJC-y equal to the mean HJC-y measurement, PW equal to the mean PW measurement, and N equal to the number of pelvis sides measured.

B. Moments and Power

Calculating the moments and power at the hip joint during gait involves the interaction of the force plate data, the kinematic data, and anthropometric data.

1. Force plate calculations

The forces and moments of the reaction between the foot and the ground create forces and moments at each joint throughout the body in the quasi-static model. The force plate data includes the magnitudes of the interactive forces and the moments about instrument center but does not directly give the position of those forces on the foot. The position of the resultant forces on the foot is needed to calculate the moment arm between

the GRF and the HJC. This can be solved as a system of general forces. The position of the resultant force on the force plate is called the center of pressure (COP):

In order to solve for the COP, a force and a couple about the vertical axis had to be formed and a point along the resultant line of action had to be defined. The point of interest was the intercept of the line of action with the floor surface. The force plate surface was 4.05 cm (zht) above the instrument center of the force plate. This problem can be solved by resolving the forces and moments into a single reaction force and a vertical torque, T.

The force and moments about the instrument center are:

$$\vec{R} = Fx\hat{i} + Fy\hat{j} + Fz\hat{k}$$

 $\vec{M} = Mx\hat{i} + My\hat{j} + Mz\hat{k}$

We want an equivalent force system

$$\vec{M} = \vec{p} X \vec{R} + T_z \hat{k}$$

where, \vec{p} is a vector from the instrument center to the intercept of the line of action with the force plate surface (Figure 24):

$$\vec{p} = x \cos \hat{i} + y \cos \hat{j} + z h t \hat{k}$$

then.

$$\bar{M} = [\{(ycop)(Fz) - (zht)(Fy)\}\hat{i} - \{(Fz)(xcop) - (zht)(Fx)\}\hat{j} + \{(xcop)(Fy) - (ycop)(Fx)\}\hat{k} + T_z\hat{k}$$

and, by equating the vector components:

$$xcop = \frac{(zht)(Fx) - My}{Fz}$$
 $ycop = \frac{Mx + (zht)(Fy)}{Fz}$

$$T_z = Mz - xcop(Fy) + ycop(Fx)$$

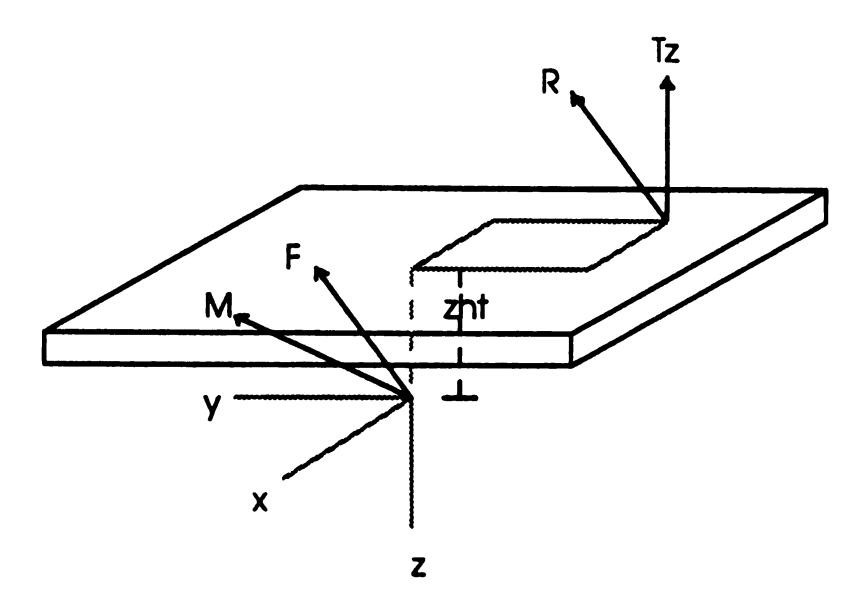


Figure 24. Equivalent force system of force plate

2. Kinematic analysis

For each instance of time ($\Delta t = 1/60$ sec), the raw kinematic data is transformed from trajectory data to the form of three-dimensional positions of targets in lab coordinate space, where the origin is floor level in the center of the force plate (Figure 18). With at least three targets on each body segment between articulating joints, a local coordinate system could be defined for each segment.

Pelvis coordinate system (Figure 25):

The y-axis of the pelvis coordinate system was defined as

$$\overline{LASIS} - \overline{RASIS} = i_{yp}$$

where LASIS equals the position vector whose components are the coordinates of the target LASIS in lab space (Figure 26). The unit base vector is:

$$\hat{i}_{yp} = \frac{i_{yp}}{|i_{yp}|}$$

The z-axis was formed by the cross product of the two vectors formed in the transverse plane of the pelvis:

$$(\overline{LASIS} - \overline{RASIS}) \times (\overline{PSIS} - \overline{RASIS}) = i_{zp}$$

$$\hat{i}_{zp} = \frac{i_{zp}}{|i_{zp}|}$$

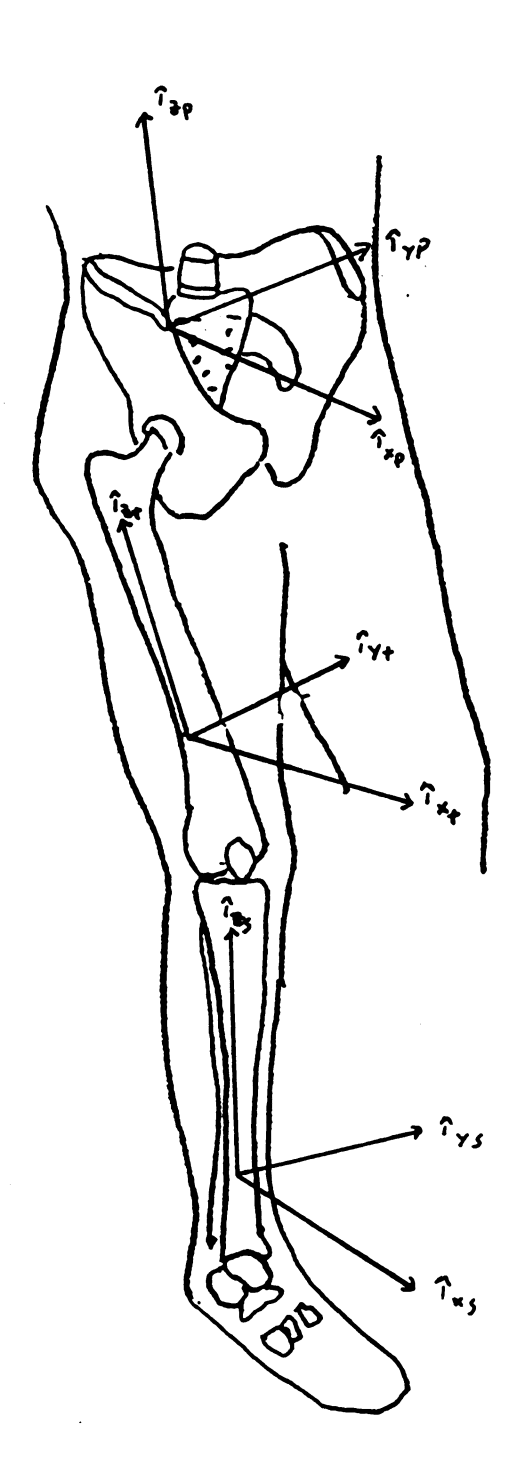


Figure 25. Local segment coordinate systems

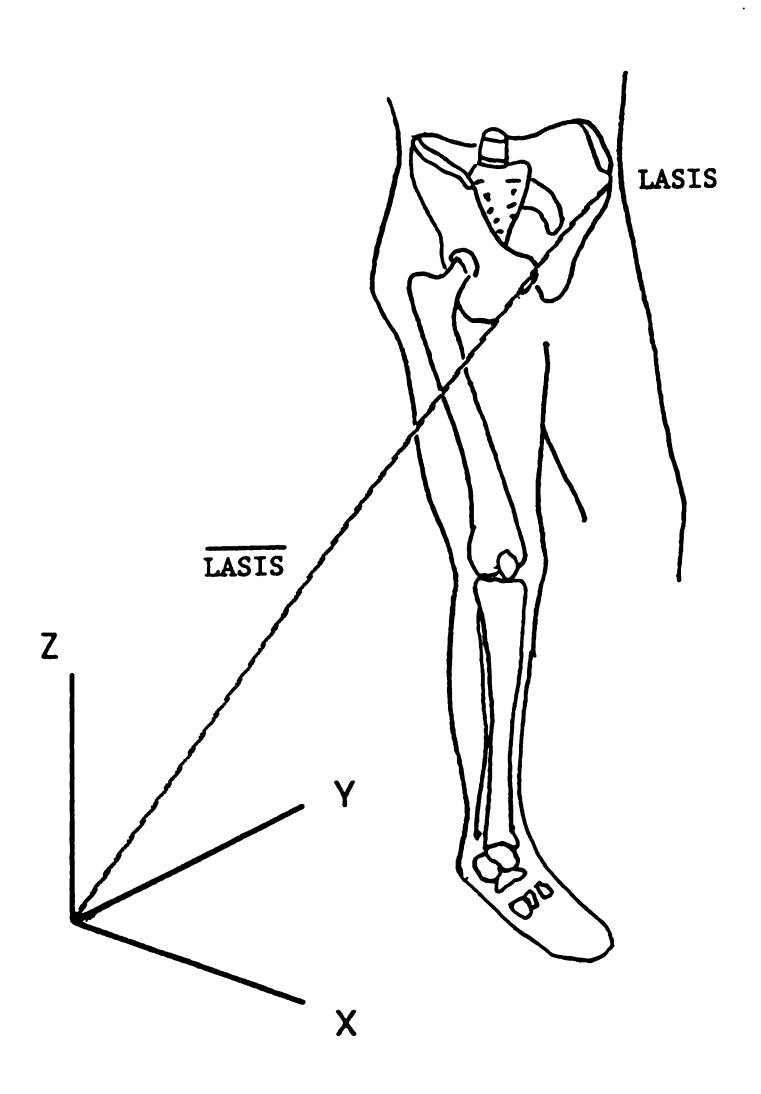


Figure 26. Position vector in lab space

The x-axis was formed as the final vector axis orthogonal to the y-axis and z-axis:

$$\hat{i}_{xp} = \hat{i}_{yp} \times \hat{i}_{zp}$$

Thigh coordinate system (Figure 25):

The z-axis of the thigh coordinate system was defined as

$$\overline{GT} - \overline{LATCOND} = i_{zt}$$

$$\hat{i}_{zt} = \frac{i_{zt}}{|i_{zt}|}$$

The x-axis was derived by the cross product of the two vectors defined in the frontal plane of the thigh:

Right side:

$$(\overline{MEDCOND} - \overline{LATCOND}) \times (\overline{GT} - \overline{LATCOND}) = i_{xt}$$

Left side:

$$(\overline{LATCOND} - \overline{MEDCOND}) \times (\overline{GT} - \overline{LATCOND}) = i_{xt}$$

$$\hat{i}_{xt} = \frac{i_{xt}}{|i_{xt}|}$$

The y-axis was formed as the final vector axis orthogonal to the x-axis and the z-axis:

$$\hat{i}_{yt} = \hat{i}_{zt} \times \hat{i}_{xt}$$

Shank/Foot complex coordinate system (Figure 25):

The z-axis of the shank/foot coordinate system was defined as

$$\overline{PROX} - \overline{DIST} = i_{ZS}$$

$$\hat{i}_{zs} = \frac{i_{zs}}{|i_{zs}|}$$

The y-axis was formed by the cross product of the two vectors formed in the sagittal plane of the shank:

$$(\overline{POST} - \overline{DIST}) \times (\overline{PROX} - \overline{DIST}) = i_{ys}$$

$$\hat{i}_{ys} = \frac{i_{ys}}{|i_{ys}|}$$

The x-axis was formed as the final vector axis orthogonal to the y-axis and z-axis:

$$\hat{i}_{xs} = \hat{i}_{ys} \times \hat{i}_{zs}$$

Using the pelvic coordinate base vectors, HJC was defined in lab space for both the right and left targeted sides:

$$\overline{RHJC} = \overline{RASIS} - al\hat{i}_{xp} + a2\hat{i}_{yp} - a3\hat{i}_{zp}$$

$$\overline{\text{LHJC}} = \overline{\text{LASIS}} - a1\hat{i}_{xp} - a2\hat{i}_{yp} - a3\hat{i}_{zp}$$

where,

$$a1 = .34 | \overline{PSIS} - \overline{RASIS} |$$
 $a2 = .14 | \overline{LASIS} - \overline{RASIS} |$
 $a3 = .80 | PS |$

(.34 is the percentage of pelvic depth to HJC, .14 is the percentage of pelvic width to HJC, and .80 is the percentage of pelvic height to HJC. These were the results of the cadaver study, and will be discussed later.)

Using the thigh coordinate base vectors, the center of gravity of the thigh (CGT) in lab space was calculated for both the right and left targeted sides:

$$\overline{RCGT} = \overline{GT} + b1\hat{i}_{xt} + b2\hat{i}_{yt} - b3\hat{i}_{zt}$$

$$\overline{LCGT} = \overline{GT} + b1\hat{i}_{xt} - b2\hat{i}_{yt} - b3\hat{i}_{zt}$$

where,

$$b1 = 0.0$$

 $b2 = .5 | \overline{MEDCOND} - \overline{LATCOND} |$
 $b3 = .433 | \overline{GT} - \overline{LATCOND} |$

(.433 is the percentage of the thigh length measure from GT to CGT as reported by Winter (1990), .5 is the estimated percentage of thigh width to CGT.)

Using the shank/foot coordinate base vectors, the center of gravity of the shank/foot complex (CGS) was calculated for both the right and left targeted sides:

$$\overline{RCGS} = \overline{LATCOND} + c1\hat{i}_{xs} + c2\hat{i}_{ys} - c3\hat{i}_{zs}$$

$$\overline{LCGS} = \overline{LATCOND} + c1\hat{i}_{xs} - c2\hat{i}_{ys} - c3\hat{i}_{zs}$$

where,

$$c1 = 0.0$$

 $c2 = .5 | \overline{MEDCOND} - \overline{LATCOND} |$
 $c3 = .606 | \overline{LATCOND} - \overline{CALCANEUS} |$

(.606 is the percentage of the shank length measure from LATCOND to CGS as reported by Winter (1990), .5 is the estimated percentage of shank width to CGS.)

3. Combining motion and force data

In order to use the force plate data and kinematic data together, they both had to have the same coordinate systems. Therefore, the force data was transformed from force plate space (fps) to lab space (ls):

and the applied forces on the force plate become reaction forces:

$$Rx(ls) = Fy(fps)$$

 $Ry(ls) = Fx(fps)$
 $Rz(ls) = Fz(fps)$

$$GRT(ls) = T_Z(fps)$$

The kinematic data were collected at 60 Hz and the force plate data at 1000 Hz. Therefore, the kinematic data had to be interpolated to be able to combine it with force data. A cubic spline was used to perform this interpolation. As defined by Cheney (1988), "a spline function is a function consisting of polynomial pieces on subintervals, joined together with certain smoothness conditions." In order to have a continuous second derivative of the interpolated data, a spline of degree three was chosen. From Cheney (1988),

With data points of the form $x = t_1, t_2,, t_n$ and $y = y_1, y_2, ..., y_n$ a function S, was constructed with n-1 cubic polynomial pieces $(S_1, S_2, ..., S_{n-1})$, with the following conditions:

Interpolating conditions: $S(t_i) = y_i \quad (1 \le i \le n)$

Continuity conditions:

$$\lim_{x \to t_{i}^{-}} S^{(k)}(x) = \lim_{x \to t_{i}^{+}} S^{(k)}(x) \quad (0 \le k \le 2, 2 \le i \le n-1)$$

In order to satisfy all of the degrees of freedom, it was decided to use a natural spline with,

$$S''(t_1) = S''(t_n) = 0$$

The resulting cubic spline function was solved as,

$$S_{i}(x) = \frac{z_{i+1}}{6h_{i}}(x - t_{i})^{3} + \frac{z_{i}}{6h_{i}}(t_{i+1} - x)^{3} + \left(\frac{y_{i+1}}{h_{i}} - \frac{z_{i+1}h_{i}}{6}\right)(x - t_{i}) + \left(\frac{y_{i}}{h_{i}} - \frac{z_{i}h_{i}}{6}\right)(t_{i+1} - x)$$

where,

$$h_i = t_{i+1} - t_i$$

and,

$$z_{i} = 6 \left(\frac{y_{i+1} - y_{i}}{t_{i+1} - t_{i}} - \frac{y_{i} - y_{i-1}}{t_{i} - t_{i-1}} \right) \qquad (2 \le i \le n-1)$$

 $\mathbf{z_i}$ is a n by n matrix that is a symmetric tridiagonal system and was solved by forward elimination and back substitution.

4. Solution of moments at the hip expressed in lab coordinates

The quasi-static hip moments are composed of three parts. The first part is the moment at the HJC due to the ground reaction force and torque (\vec{M}_R) . This was calculated by computing the cross product of the moment arm of the HJC to the COP with the GRF and then adding the GRT.

$$\vec{M}_{R} = (\overline{COP-HJC}) \times \overline{R(ls)} + \overline{GRT(ls)}$$

The second part of the moment at HJC is due to gravity acting on the thigh at its center of gravity (\vec{M}_T) . This was calculated by computing the cross

product of the moment arm from HJC to the thigh center (CGT) with the weight of the thigh.

$$\vec{M}_T = (\overline{CGT - HJC}) \times (\overline{-W_T}) \hat{k}$$

where,

$$W_T = 0.1(BW)$$

(the thigh is approximately 10% of body weight (Winter, 1990))

The third part of the moment at HJC is due to gravity acting on the shank/foot complex at its center of gravity (\bar{M}_S). This was calculated by computing the cross product of the moment arm from HJC to the shank/foot center (CGS) with the weight of the shank and foot.

$$\vec{M}_S = (\overline{CGS-HJC}) \times (\overline{-W_S}) \hat{k}$$

where,

$$W_S = 0.061(BW)$$

(the shank/foot is approximately 6.1% of body weight (Winter, 1990))

Therefore, the total moments at hip joint center in lab space are

$$\overline{\text{HIPMOM(ls)}} = \overline{M_R} + \overline{M_T} + \overline{M_S}$$

5. Joint Coordinate System and angle calculations

The hip moments are expressed in lab space coordinates but, it is more practical to express them in the joint coordinate system at the hip joint. This allows the definition of the moments to apply to body axes (i.e. moment about y-axis is the flexion/extension moment). A joint coordinate system was derived between the pelvis and thigh as suggested by Grood and Suntay (1983). The joint coordinate system (JCS) is formed by choosing two body axes (one from each body) and taking the cross product of them to create the third axis of the coordinate system (Figure 27). The body axes were chosen as

$$\hat{e}_2 = \hat{i}_{yp}$$
 (y axis unit vector of pelvis)

$$\hat{e}_3 = \hat{i}_{zt}$$
 (z axis unit vector of thigh)

The common perpendicular to both body axes, called the floating axis, was

defined as

$$\hat{\mathbf{e}}_1 = \frac{\hat{\mathbf{e}}_2 \mathbf{X} \, \hat{\mathbf{e}}_3}{\left|\hat{\mathbf{e}}_2 \mathbf{X} \, \hat{\mathbf{e}}_3\right|}$$

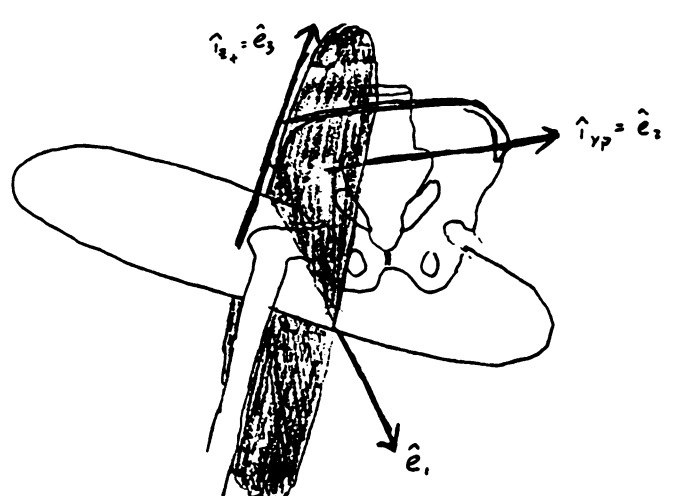


Figure 27. Joint coordinate system

These three axes form a non-orthogonal joint coordinate system from which the three angles of the joint motion could be computed at each instance of time:

flexion / extension =
$$\sin^{-1}(\hat{e}_1 \cdot \hat{i}_{pz})$$
 {flexion(+)/extension(-) } external / internal rotation = $\sin^{-1}(\hat{e}_1 \cdot \hat{i}_{ty})$ {ext. rot. (+) for right side} {ext. rot (+) for left side } abduction / adduction = $\sin^{-1}(\hat{e}_2 \cdot \hat{e}_3)$ {abduction(+) for right } {abduction(-) for left}

6. Transformation of moments from lab space to joint coordinate space

To analyze the moments as a driving force that produce angular displacements at the hip, the lab space moments were transformed to the joint coordinate system.

Again, the joint coordinate system was defined as

$$\hat{e}_1 = \hat{e}_{1x} + \hat{e}_{1y} + \hat{e}_{1z}$$

$$\hat{e}_2 = \hat{e}_{2x} + \hat{e}_{2y} + \hat{e}_{2z}$$

$$\hat{e}_3 = \hat{e}_{3x} + \hat{e}_{3y} + \hat{e}_{3z}$$

and the moments in lab space ($\overline{HIPMOM(ls)}$) as M_X , M_Y , and M_Z .

The relationship between moment components in joint coordinate space with the moments in lab space were derived as follows:

$$M_x = M_1 e_{1x} + M_2 e_{2x} + M_3 e_{3x}$$

 $M_y = M_1 e_{1y} + M_2 e_{2y} + M_3 e_{3y}$
 $M_z = M_1 e_{1z} + M_2 e_{2z} + M_3 e_{3z}$

where M_1 , M_2 , and M_3 are the moment components in joint coordinate space.

In matrix form,

$$\begin{bmatrix} M_{x} \\ M_{y} \\ M_{z} \end{bmatrix} = \begin{bmatrix} e_{1x} & e_{2x} & e_{3x} \\ e_{1y} & e_{2y} & e_{3y} \\ e_{1z} & e_{2z} & e_{3z} \end{bmatrix} \begin{bmatrix} M_{1} \\ M_{2} \\ M_{3} \end{bmatrix}$$

or

$$[M(ls)] = A[M(jcs)]$$

then,

$$[M(jcs)] = A^{-1}[M(ls)]$$

This 3X3 system of linear equations was solved by Cramer's rule.

$$A^{-1} = \left(\frac{1}{\det A}\right) A dj A$$

where,

$$\det A = e_{1x}(e_{2y}e_{3z} - e_{2z}e_{3y}) - e_{2x}(e_{1y}e_{3z} - e_{1z}e_{3y}) + e_{3x}(e_{1y}e_{2z} - e_{1z}e_{2y})$$

and AdjA is the transpose of the matrix of cofactors (α_{ij}) of a_{ij} in A and $\alpha_{ij} = (-1^{i+j}) detA_{ij}$

Therefore,

$$[M(jcs)] = \left(\frac{1}{\det A}\right) Adj A[M(ls)]$$

then,

$$M_1 = M(jcs-x) = \frac{\det A_1}{\det A}$$

$$M_2 = M(jcs-y) = \frac{\det A_2}{\det A}$$

$$M_3 = M(jcs-z) = \frac{\det A_3}{\det A}$$

where,

$$\mathbf{A_{1}} = \begin{bmatrix} \mathbf{M_{x}} & \mathbf{e_{2x}} & \mathbf{e_{3x}} \\ \mathbf{M_{y}} & \mathbf{e_{2y}} & \mathbf{e_{3y}} \\ \mathbf{M_{z}} & \mathbf{e_{2z}} & \mathbf{e_{3z}} \end{bmatrix} \mathbf{A_{2}} = \begin{bmatrix} \mathbf{e_{1x}} & \mathbf{M_{x}} & \mathbf{e_{3x}} \\ \mathbf{e_{1y}} & \mathbf{M_{y}} & \mathbf{e_{3y}} \\ \mathbf{e_{1z}} & \mathbf{M_{z}} & \mathbf{e_{3z}} \end{bmatrix} \mathbf{A_{3}} = \begin{bmatrix} \mathbf{e_{1x}} & \mathbf{e_{2x}} & \mathbf{M_{x}} \\ \mathbf{e_{1y}} & \mathbf{e_{2y}} & \mathbf{M_{y}} \\ \mathbf{e_{1z}} & \mathbf{e_{2z}} & \mathbf{M_{z}} \end{bmatrix}$$

7. Power

With the angles defined, and the moments in joint coordinate space, power in the plane of progression (sagittal, flexion/extension plane) and the true mathematical power at the hip during stance were computed. Power is defined as the rate of doing work. In biomechanics applications, it equals the dot product of the moment and the angular velocity of the segment, when describing the power generated or absorbed by the muscle activity at the joint. If the contribution from internal/external rotation and

abduction/adduction were considered to be negligible, the 'power' in the plane of progression as a function of time is solved as:

Power(t) =
$$M_2(t) \cdot (\omega_{fe}(t))$$

= (flex/ext moment)(angular velocity of flex/ext at the hip)

The angular velocity of the flexion/extension at the hip ($\omega_{fe}(t)$) was computed from the time history of the angular displacement. This was done by forward, central, and backward differentiation of the angle file.

$$\omega_{\text{fe}}(t_1) = \frac{-3(\text{fe}(t_1)) + 4(\text{fe}(t_2)) - \text{fe}(t_3)}{2(t_2 - t_1)}$$

$$\omega_{fe}(t_1 \le i < N) = \frac{fe(i+1) - fe(i-1)}{2(t_{i+1} - t_i)}$$

$$\omega_{fe}(t_N) = \frac{3(fe(t_N)) - 4(fe(t_{N-1})) - fe(t_{N-2})}{2(t_N - t_{N-1})}$$

However, the true power at the hip during stance phase is actually defined as:

$$P = \vec{M} \cdot \vec{\omega}$$

where \bar{M} is the hip joint moment vector expressed in the hip joint coordinate system (jcs) and $\bar{\omega}$ is the angular velocity vector of the hip expressed in jcs.

The actual time derivative of the angle velocity is expressed as:

$$\frac{d}{dt}\bar{\theta} = \frac{d}{dt}(\theta_1\hat{e}_1 + \theta_2\hat{e}_2 + \theta_3\hat{e}_3) = \frac{d\theta_1}{dt}\hat{e}_1 + \theta_1\frac{d\hat{e}_1}{dt} + \frac{d\theta_2}{dt}\hat{e}_2 + \theta_2\frac{d\hat{e}_2}{dt} + \frac{d\theta_3}{dt}\hat{e}_3 + \theta_3\frac{d\hat{e}_3}{dt}$$

where the time derivatives of the unit vectors are ignored because they are small.

The angular velocity of abduction/adduction (ω_{ab}) and external/internal rotation (ω_{ci}) were calculated in the same manner as the flexion/extension angular velocity.

For each time = t_i the power was calculated as follows:

$$P = (M_1\hat{e}_1 + M_2\hat{e}_2 + M_3\hat{e}_3) \cdot (\omega_1\hat{e}_1 + \omega_2\hat{e}_2 + \omega_3\hat{e}_3)$$

where M_1 , M_2 , and M_3 are the flexion/extension, abduction/adduction, and external/internal rotation moments at the hip respectively and ω_1 , ω_2 , and ω_3 are the respective angular velocities.

The moment and angular velocity terms are expressed in a non-orthogonal joint system. That is, $\hat{e}_1 \perp \hat{e}_2$ and $\hat{e}_1 \perp \hat{e}_3$ but \hat{e}_2 is not necessarily $\perp \hat{e}_3$.

Therefore, when expanding the dot product,

$$\hat{\mathbf{e}}_1 \cdot \hat{\mathbf{e}}_2 = \hat{\mathbf{e}}_1 \cdot \hat{\mathbf{e}}_3 = 0$$

but,

$$\hat{\mathbf{e}}_2 \cdot \hat{\mathbf{e}}_3 \neq 0$$

Power was then calculated as:

$$P = M_1 \omega_1 + M_2 \omega_2 + M_3 \omega_3 + (M_2 \omega_3 + M_3 \omega_2) \hat{e}_2 \cdot \hat{e}_3$$

V. RESULTS AND DISCUSSION

This chapter is composed of two sections. The first section includes the results of the hip joint cadaver study and an explanation of its accuracy and value. The second section includes and discusses the results of the hip joint moments and power calculations during the stance phase of gait using the new hip joint center location.

A. Hip Joint Center

A total of 64 cadaver pelves were studied to find a correlation between pelvic geometry and the location of hip joint center.

Measurements were taken on only skeletally mature adults so the results of HJC location on children is unknown. Of the data taken, interrater reliability correlation coefficients were high indicating a reliable measurement procedure. Female pelves were significantly smaller than male pelves in all measurements except the distance from ASIS to HJC along the y-axis (HJC-y). However, Student's t-test analysis of female and male location of HJC as a function of pelvic geometric parameters (HJC-x/pelvic width (PW), HJC-y/PW, HJC-z/PW, HJC-x/pelvic depth (PD), and HJC-z/pelvic height (PH)) revealed no significant differences. Female pelvic measurements were proportionally smaller than those of males (consistent with Brinckmann et al., 1981) making the ratios of HJC location as a function of pelvic volume measurements constant for both sexes.

Therefore, pelvic measurement data of both sexes were pooled for analysis. This gave us a large data sample size (N=122 sides) for statistical analysis. The female and male mean measurements are shown in Table 4 with their standard deviations (sd) and standard error of the mean (sem) results. Combined male and female pelvic measurement data are presented in Table 5.

The mean acetabular depth was measured to be 49% of the acetabular diameter. This supported the assumption that the acetabulum was a hemisphere and that the location of HJC could be defined as the center of the acetabular rim.

Pearson product-moment correlations were performed to evaluate the relationship between HJC measurements and pelvic anthropometric measurements (Table 6). HJC-x was poorly correlated with PW at 0.22 (N = 122; p < 0.009), HJC-y was highly correlated with PW at 0.80 (N = 122; p < 0.0001), while HJC-z was not correlated with PW at -0.02 (N = 122; p = NS) suggesting that HJC-x and HJC-z cannot be accurately located as a function of PW. A Pearson product-moment correlation analysis of pelvic volume measurements was performed to evaluate the inter-relationship of pelvic geometric measurements. No significant relationship was found between PW and PH (N = 122) or PH and PD (N = 68). PW was correlated with PD at 0.55 (N = 68; p < 0.0001). The apparent relationship between PW and PD may reflect the skew measurement of PD (ASIS to PSIS). This measurement contains a component of the y-axis (width) of the pelvis and is not a true perpendicular PD measurement.

As previously stated, Bell et al. (1989 & 1990) compared the methods of locating the HJC by bony palpable landmarks of Tylkowski's group and Andriacchi's group. Bell et al. also calculated new PW percentages to

Table 4. Comparison of female and male pelvic measurements

	Female				Male			
	Mean (cm)	sd	sem	N	Mean (cm)	sd	sem	N
PW	23.4	1.14	0.20	34	24.30	1.71	0.23	27
PH	8.7	0.73	0.09	34	9.20	0.80	0.11	27
PD	16	1.01	0.17	34	16.80	0.58	0.10	34
ADIA	4.6	0.35	0.05	53	5.20	0.27	0.04	44
ADEP	2.2	0.22	0.03	53	2.50	0.24	0.04	44
ING	14.6	0.78	0.09	68	15.30	0.88	0.12	54
HJC-x	5.5	0.51	0.06	68	5.90	0.45	0.06	54
HJC-y	3.2	0.87	0.11	68	3.40	0.81	0.11	54
HJC-z	6.9	0.68	0.08	68	7.40	0.79	0.11	54

Table 5. Mean pelvic measurements and interrater reliability (IRR) coefficients

	Mean (cm)	\$d	sem	Number	IRR
PW	23.8	1.72	0.16	64	.99***
PH	8.9	0.80	0.07	64	.98***
PD	16.4	0.89	0.11	68	.94***
ADIA	4.9	0.44	0.04	97	.95***
ADEP	2.4	0.27	0.03	97	.90***
ING	14.9	0.89	0.08	122	.98***
HJC-x	5.7	0.52	0.05	122	.97***
HJC-y	3.4	0.90	0.08	122	.93***
HJC-z	7.1	0.77	0.07	122	.91***
HJC-x/PW	0.24	0.02	0.00	122	.97***
HJC-y/PW	0.14	0.03	0.00	122	.90***
HJC-z/PW		0.04	0.00	122	.93***
HJC-x/PD	0.34	0.02	0.00	68	.90***
HJC-z/PH		0.05	0.00	122	.76***

Table 6. Pearson product-moment correlations of HJC related to pelvic geometry

	PW	PH	PD
HJC-x	.22 (.009)	.17 (NS)	.61 (.000)
HJC-y	.80 (.000)	04 (NS)	.14 (NS)
HJC-z	02 (NS)	.80 (.000)	.11 (NS)
PH	.13 (NS)	1.00	.18 (NS)
PD	.55 (.000)	.18 (NS)	1.00

estimate the position of HJC. In 1989, they calculated HJC to be located as a percentage of PW 30% distal, 14% medial, and 22% posterior, relative to the ASIS for adults. These values were found using 51 AP and 20 right lateral adult pelvis x-rays. In 1990, they calculated HJC to be located as a percentage of PW 30% distal, 14% medial, and 19% posterior, relative to the ASIS for adults. These values were found using 7 AP and right lateral x-rays of adult males with skin markers to indicate bony landmarks. Bell's group's conclusion in 1989 was that the most accurate method of predicting HJC location was to use Andriacchi's approach to estimate the position in the frontal plane and Tylkowski's approach, but with the new posterior percentage of PW, in the sagittal plane. In 1990, they concluded that the most accurate method to locate HJC would be to use Tylkowski's approach, but with new PW percentages, for the frontal plane and Andriacchi's approach for the AP location. These contradictory conclusions drawn in the two studies could be due to the small sample size of pelves studied in fixed reference frames (N=20 & N=7). Differences, also, could have come from the errors of taking measurements from marker placements on soft tissue (Bell et al., 1990). However, the Pearson product-moment correlation analysis in our study revealed that

HJC-x was poorly correlated at 0.22 with PW and that HJC-z was not correlated at all with PW, which would indicate that errors should be prevalent when trying to relate HJC to pelvic width on any axis except the medial/lateral axis.

To find a more accurate approach of defining HJC, the components of HJC were compared to their respective pelvic geometric parameters. HJC-y was highly correlated to PW at 0.80 (N = 122; p < 0.0001). HJC-z was highly correlated with pelvic height at 0.80 (N = 122; p < 0.0001). HJC-x was found to be correlated with pelvic depth (PD) at 0.61 (N = 68; p < 0.0001). HJC-x (N = 122) and HJC-y (N = 122) were not significantly correlated with PH and HJC-y (N = 122), and HJC-z (N = 122) were not significantly correlated with PD.

To compare the location of HJC using a function of pelvic width alone versus using a function of pelvic volume, HJC location as a function of both were calculated. As a percentage of PW, our study revealed that HJC was located 24% (sd 2%) of PW posteriorly, 14% (sd 3%) of PW medially, and 30% (sd 4%) of PW inferiorly. The differences in the posterior percentage as compared to Bell's groups could be contributed to the difference in sample size and the differences in taking direct pelvic measurements versus radiographic measurements. The average percentages were, however, rather similar to Bell et al. (1989 and 1990). Although this confirms an average location of HJC as a function of pelvic width, it does not hold on a subject specific case since the correlation of HJC-x and HJC-z with PW is highly scattered (Figure 28). As a function of pelvic volume, we found that HJC was located 34% (sd 2%) of PD posteriorly, 14% (sd 3%) of PW medially, and 80% (sd 5%) of PH inferiorly.

The above ratios were used to assess the relative error in HJC

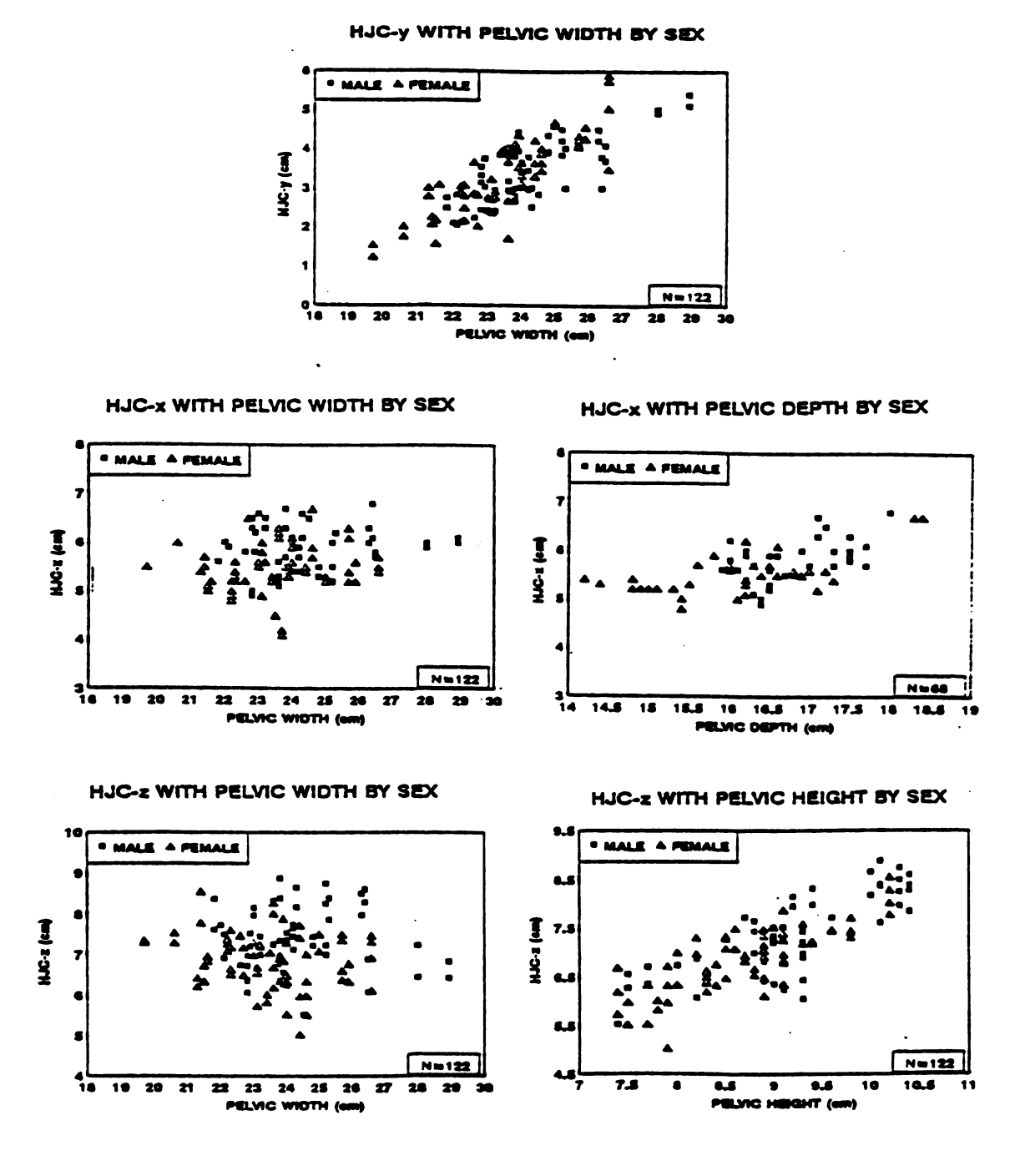


Figure 28. Scatter plots of HJC vs. pelvic measurements

estimation along their axes in this study. Using our specimens with Bell's group's (1990) value to calculate HJC-x as 19% of PW resulted in a mean error (absolute value of estimated value minus true measured value of our pelves) of 1.2 centimeters (cm) (sd 0.5; range: -1.1 to 1.5) and Bell's (1989) value of HJC-x as 22% of PW yielded a mean error of 0.6 cm (sd 0.4; range: -0.4 to 2.2). Using our calculated location of HJC-x as 24% of PW resulted in a mean error of 0.5 cm (sd 0.3; range: -1.6 to 1.1). This mean error based on pelvic width was significantly larger t = 0.0001 than calculating HJC-x as 34% of PD which yielded a mean error of 0.3 cm (sd 0.2; range: -0.7 to 0.9). Overall, the calculation of HJC-x as a function of pelvic depth resulted in a smaller error than calculation of HJC-x as a function of pelvic width (Table 7).

Table 7. Errors of HJC-x location estimation

HJC-x calculation	N	Mean(cm)	sd	sem	Max
1 0.19 PW - true 1	122	1.2	0.52	0.05	2.2
1 0.22 PW - true 1	122	0.6	0.44	0.04	1.5
1 0.24 PW - true 1	122	0.5	0.34	0.03	1.6
1 0.34 PW - true 1	68	0.3	0.21	0.03	0.9

The absolute value of the error associated with calculating HJC-z as a function of pelvic width (30%) revealed a mean error of 0.7 cm (sd 0.6, sem 0.05, range -2.1 to 2.3), while calculation as a function of pelvic height (80%) revealed a mean error of 0.3 cm (sd 0.3, sem 0.03, range -0.8 to 1.4). The pelvic height method of calculating HJC-z reduced the mean error by a mean of 0.4 cm and represented a significant reduction at t = 0.0001.

There were no differences in the calculation of HJC-y in comparing Bell's results (1989 and 1990) and our results. The absolute value of the error associated with calculating HJC-y as a function of pelvic width (14%) yielded a mean error of 0.6 cm (sd 0.4, sem 0.04, range -1.4 to 2.2).

Overall, the mean error of the location of HJC measurements using PW alone was significantly higher than locating HJC relative to pelvic volume measurements. The calculation of HJC-x as a function of pelvic depth and HJC-z as a function of pelvic height resulted in a significantly smaller error than the calculation of both HJC-x and HJC-z as a function of pelvic width.

Accurate location of HJC is critical in gait analysis studies for accurate computation of hip muscle moments, joint intersegmental resultant forces, and joint motion. A subject specific technique for locating HJC is crucial to reduce the errors associated with HJC displacements from actual positions. Cappozzo's method of determining HJC by assuming the thigh was a rigid body and calculating HJC as the center of a sphere described by three-dimensional rotations using a least square analysis was studied by Bell et al. (1990). The errors associated with this method were attributed to several factors. Namely, several of the healthy adult males studied had difficulty obtaining sufficient abduction to establish HJC making this approach of questionable value in the study of gait where subjects are unable to perform large amplitude angular movements at the hip, have low endurance for pretest and test gait analysis trials, or are unable to stand on a single limb. Also, excessive care must be taken to control velocity and specific position of the limb during rotations to ensure accurate results. It was concluded that the most accurate and efficient way of determining HJC on a subject specific basis was by relating HJC to palpable bony landmarks.

The Pearson product-moment correlations calculated to compare HJC location to pelvic geometry indicated strong linear relationships between the HJC components and their respective geometric parameter measurements. The correlation between HJC-x and pelvic depth (PD) was 0.61 (N = 68; p < 0.0001). Although this correlation was not as high as the HJC-y and HJC-z correlations, it is markedly higher than the correlation between HJC-x and PW. This "lower" correlation is most likely due to the fact that the measurement of PD (ASIS to PSIS) was not a true pelvic depth measurement. A better pelvic depth measurement would be measured from the inter-ASIS line to either the PSIS or the second sacral spinous process. This would give a more perpendicular parameter to the frontal plane to compare the HJC-x measurement with. This also explains the correlation of 0.51 between PW and PD.

The high correlations between HJC components and their respective pelvic dimensions plus the lower mean error involved in using the pelvic volume relationships indicate that HJC cannot be located relative to ASIS as a function of pelvic width alone. Translation from the ASIS to HJC along the y-axis (mediolateral) can be made as a function of pelvic width; however, translations along the x-axis (anteroposterior) and the z-axis (superoinferior) cannot be made without corresponding pelvic volume measurements. Pelvic volume measurements are needed to normalize the subject specific location of HJC. Therefore, HJC is located relative to the ASIS 14% pelvic width medial, 34% pelvic depth posterior, and 80% of pelvic height inferior.

B. Moments and power at the hip during stance

The kinematic and kinetic data of two subjects walking were collected using the methods described in chapter III. A series of computer programs were written to solve for the center of pressure (COP) during stance, the hip joint position, angles, angular velocities during gait, the applied quasi-static hip moments, and the power in the plane of progression and the true power at the hip joint during stance. In order to link the motion and force data, the motion data was interpolated using a cubic spline and sampled at 100 Hz. An example of the results of this spline is shown with the position of HJC-z in lab space for a gait cycle (Figure 29).

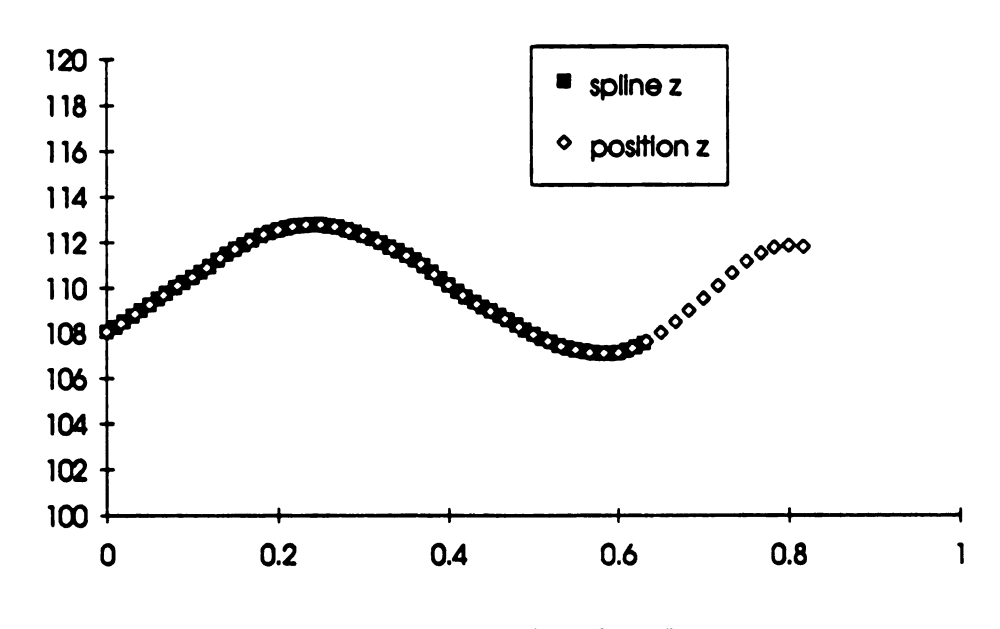


Figure 29. Splined HJC-z

The kinematic results for the hip during walking were computed in degrees for the angles and rads/sec for the angular velocities and were plotted as functions of time. The angles at the hip during walking for

subject 1 and 2 are shown in Figures 30 and 31, respectively. At initial foot contact, the hip is flexed 35 degrees. It then extends fully to near the end of stance, at which point it flexes again through swing phase to the initial contact again. Through stance, the hip adducts while loading occurs and then abducts as the load diminishes when double stance phase and then swing phase occur. External rotation was prevalent at the hip towards the end of stance phase and into the beginning of swing at which point internal rotation of the hip occurs and continues until initial contact occurs again.

The three external forces on the body resulting from foot-to-floor contact are shown in Figure 32 for subject 1 and Figure 33 for subject 2. Subject 1 had a maximum deceleration force of 115 %BW (% body weight) and a maximum acceleration force of 108 %BW. His maximum braking force was 20 %BW and his maximum propulsion force was 25 %BW. Subject 2 was a little more conservative in his gait with a deceleration force of 104 %BW and an acceleration force of 110 %BW. His maximum braking force was 15 %BW and his maximum propulsion force was 18 %BW. Both patterns were consistent with normative data.

The applied quasi-static hip moments and power were calculated at the hip joint center location determined by the cadaver study. The moments were normalized by body mass to reduce inter-subject variability, as suggested by Kadaba, 1989, and were expressed in units of N-m/kg. Power was calculated as both the power in the plane of progression $(M_{flex} \cdot \omega_{flex})$ and true power $(\bar{M} \cdot \bar{\omega})$ and was expressed in the units of Watts/kg. Both the moments and the power were presented as functions of percent stance phase. This allowed subjects with different

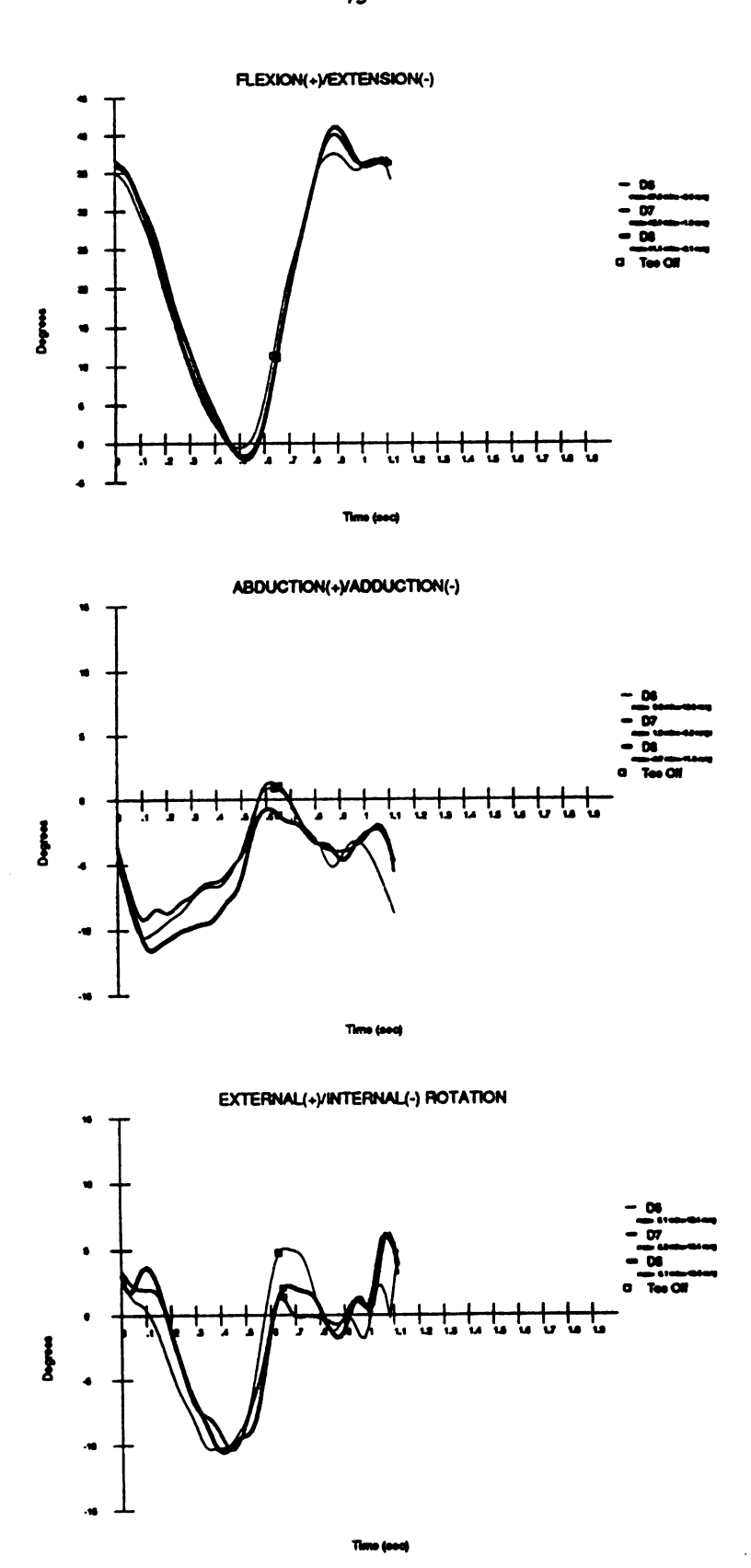


Figure 30. Hip angles during gait - subject 1

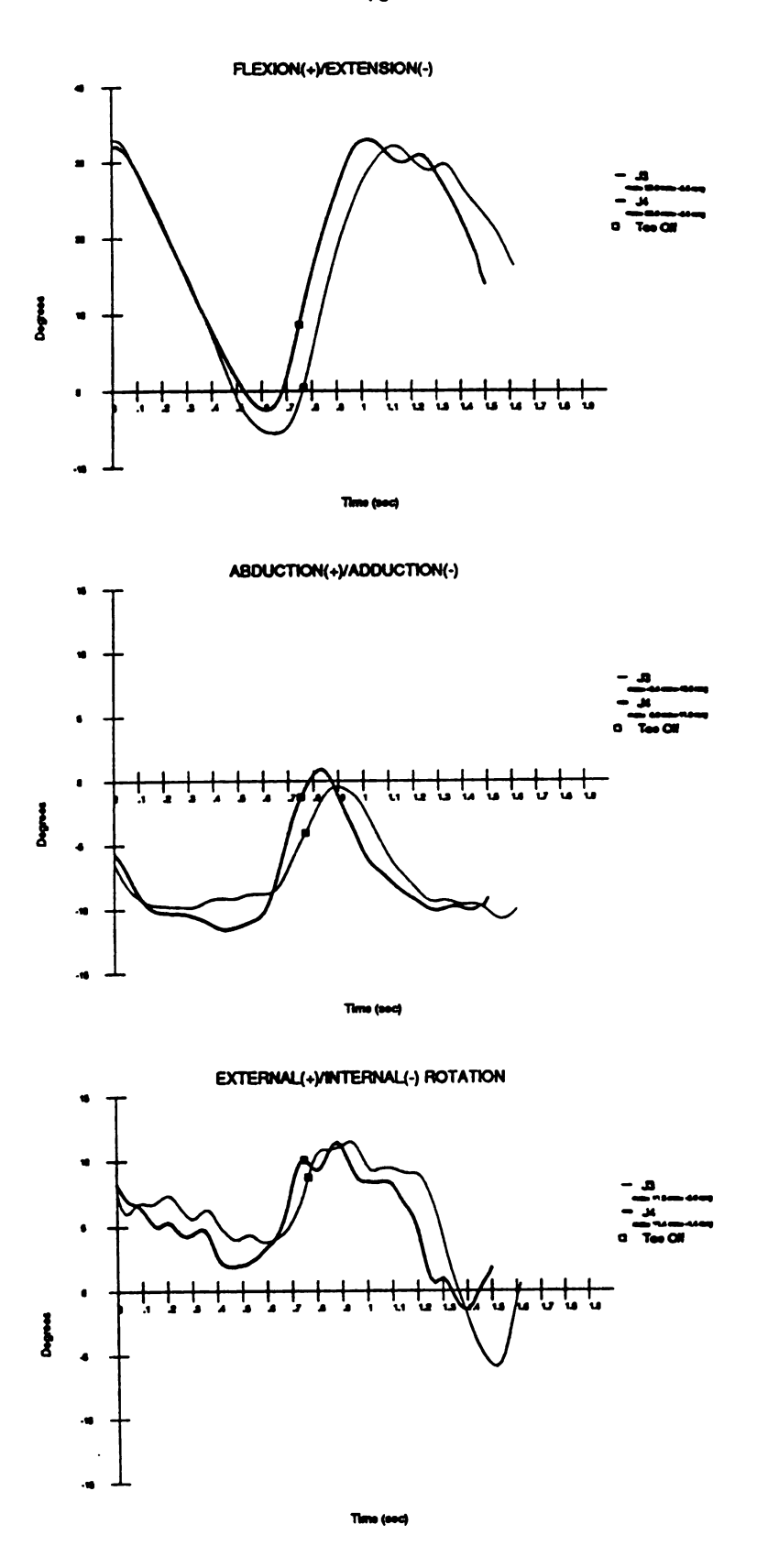


Figure 31. Hip angles during gait - subject 2

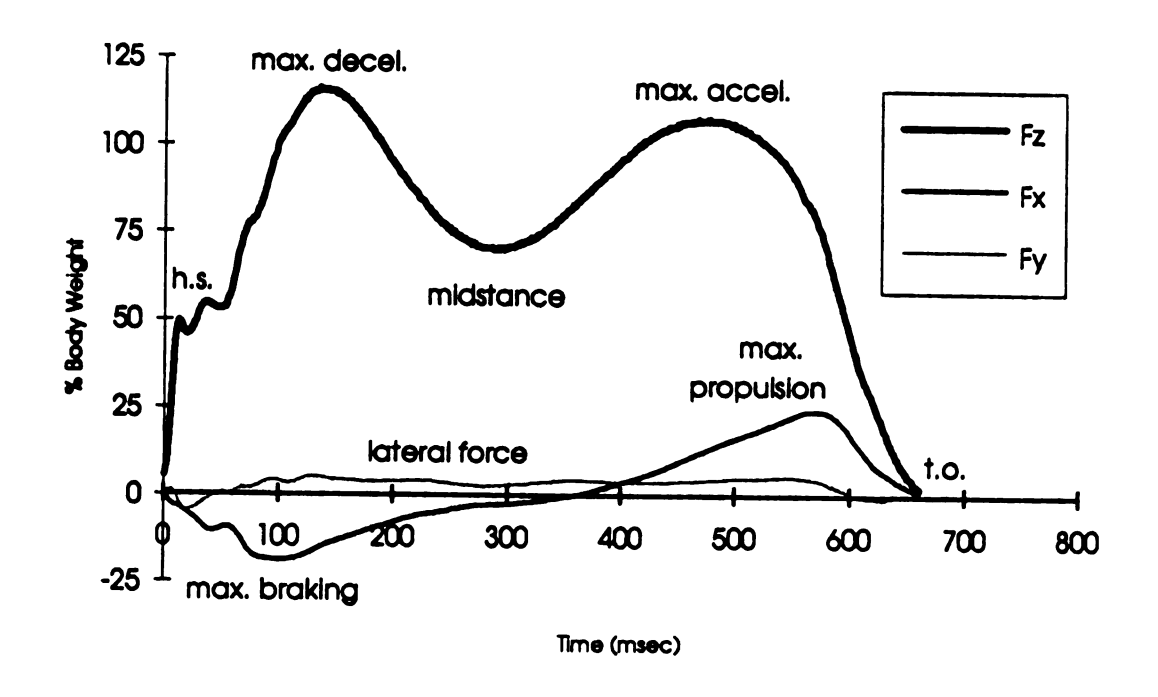


Figure 32. Forces in lab space - subject 1

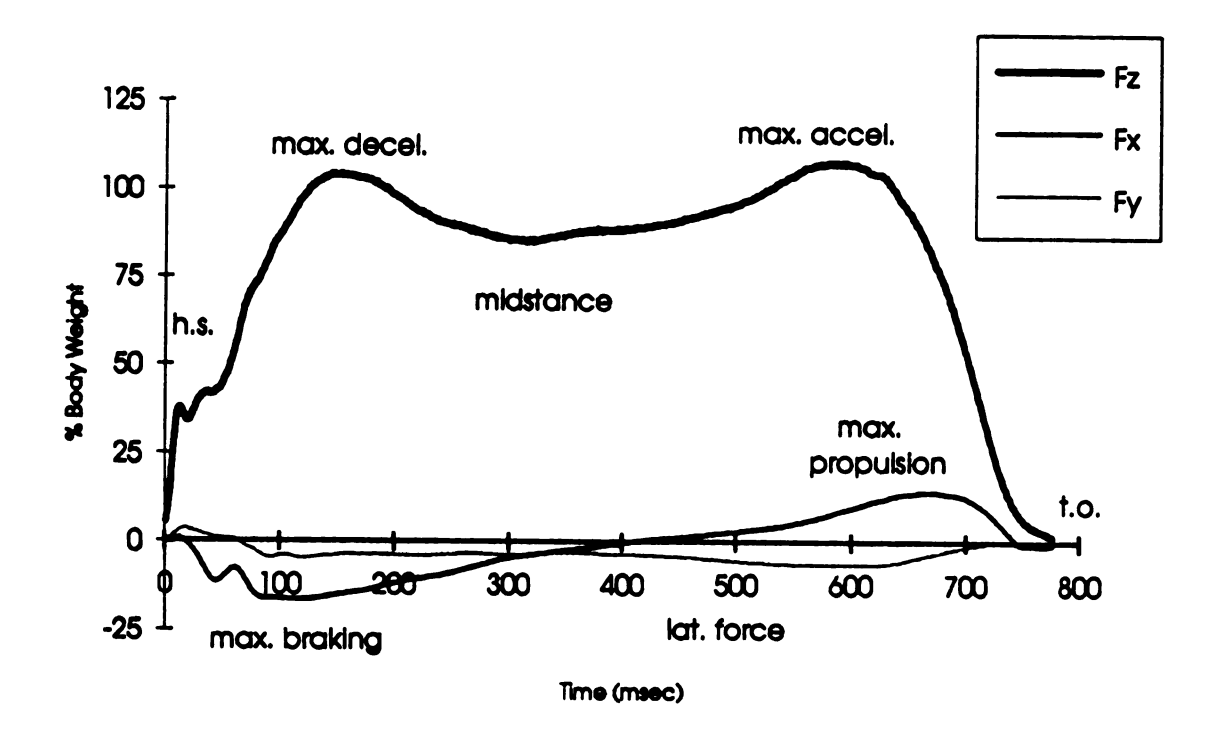


Figure 33. Forces in lab space - subject 2

stance times to be compared. The angles, angle velocities, moments and power were computed in the joint coordinate system described in the analytical methods chapter.

The applied quasi-static moments for three trials are shown in Figure 34 for three trials of subject 1 and Figure 35 for two trials of subject 2. Although the applied moments were calculated and presented, it is more conceptual to discuss them as muscle moments (internal, driving moments) at the hip. Therefore, a flexor moment at the hip is shown as an applied extension moment in the figures. An abductor moment at the hip is shown as an applied adduction moment. And an internal (medial) rotator moment at the hip is shown as an applied external (lateral) rotation moment. The trends of the two subjects are quite similar to each other and to literature, except for a slight difference in the flexion/extension moment at the beginning of stance. Since the subjects' data follows closely to the general trends as reported in the literature (Bresler and Frankel, 1950, Cappozzo, 1984), a general overview of the hip moments during gait (Whittle, 1991) will be discussed first and then the minor discrepancies of both subjects' results with literature will be addressed.

At heel strike, there is a sudden extensor moment (applied flexion) at the hip which diminishes quickly. The motion data shows the hip is extending resulting from concentric contraction (shortening of muscle) of the hip extensors. As the hip continues to extend, the resultant force passes behind the HJC, and the upper body passes over the COP, the hip joint moment becomes a flexor (applied extension). This occurs at around midstance, that is 50% of stance phase. During the second half of stance phase, the flexor activity is eccentric contraction (lengthening of muscle) in order to decelerate the hip extension until the opposite foot comes down

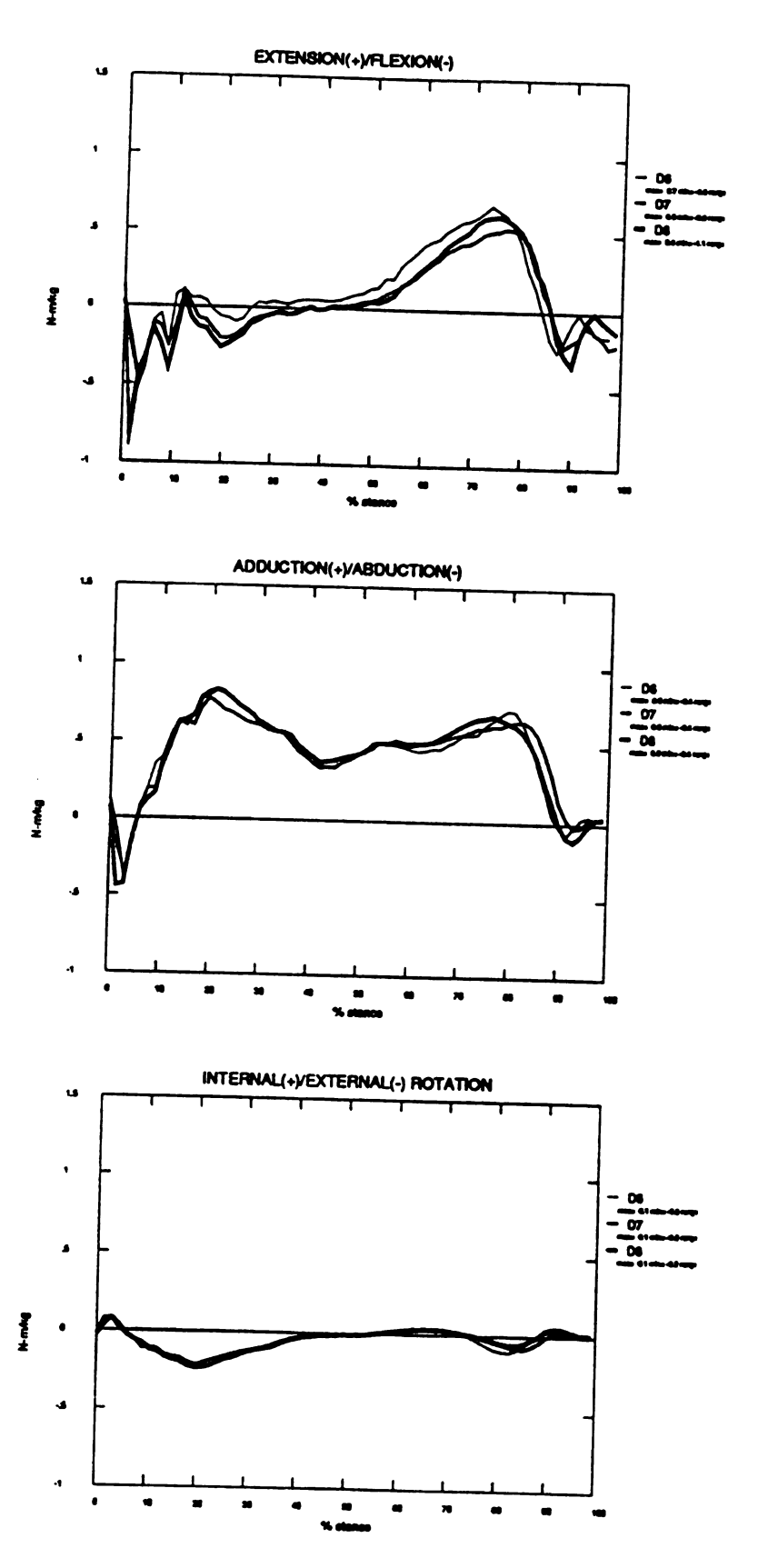


Figure 34. Applied quasi-static hip moments - subject 1

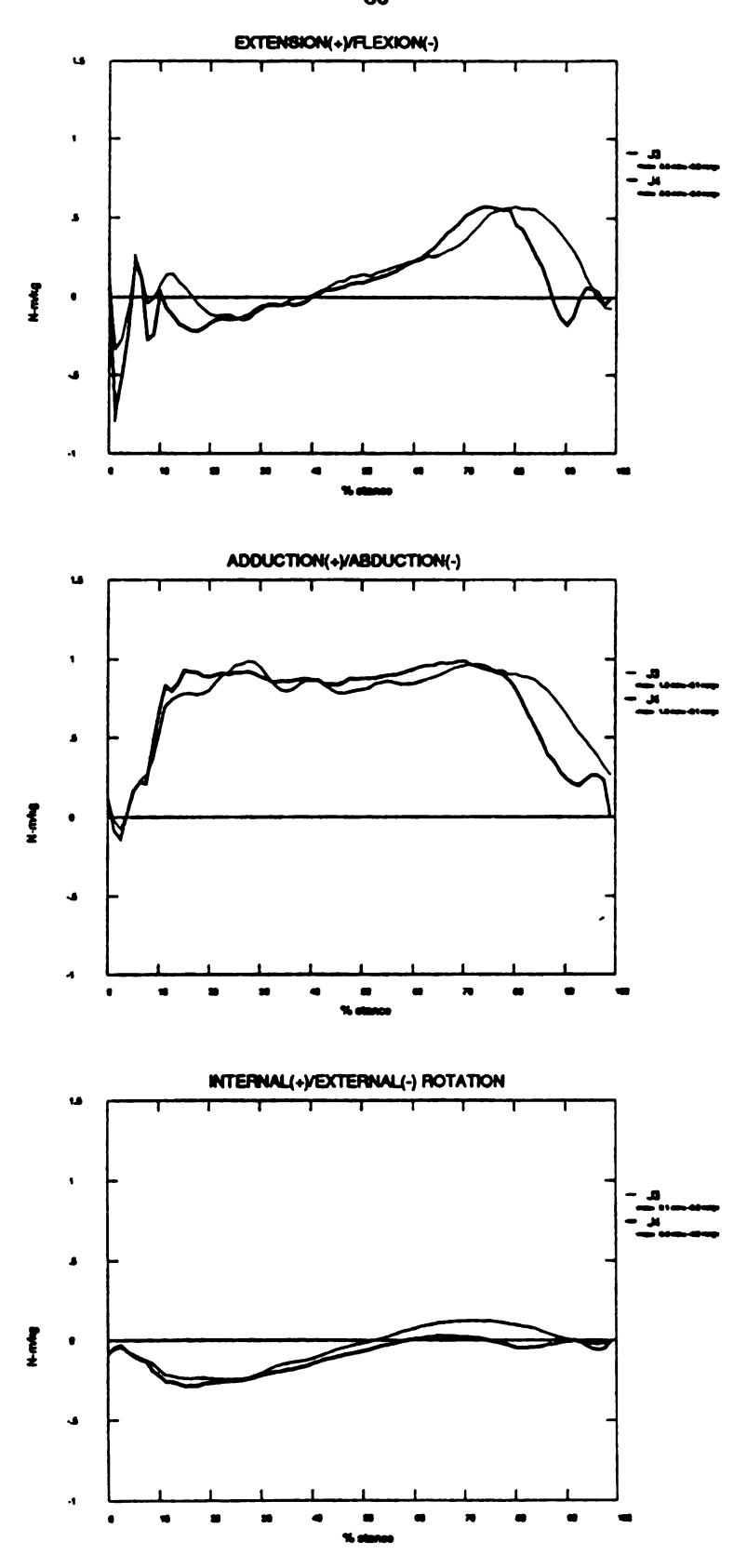


Figure 35. Applied quasi-static hip moments - subject 2

into double stance and then concentric flexor contraction occurs to bring the thigh forward and upward. The extensor moment at the beginning of stance also acts to decelerate the upper body's forward rotation and switches to a flexor moment to accelerate forward rotation of the upper body at the end of stance.

The applied adduction/abduction moments occur primarily as a result of the cyclic pattern of shifting weight from one foot to the other which occurs during walking. There is an abductor moment (applied adduction) throughout the entire stance phase of gait. During the first part of stance, the hip abductors fire eccentrically to hold the pelvis up while there is no support under half of it. After midstance the abductors switch to concentric contractures to raise the pelvis up again. The sharp decrease of abductor activity at the end of stance is due to the beginning of double stance and then swing phase.

There is little information in literature on the external/internal rotator moments at the hip during gait, but the pattern is consistent with what has been previously reported (Bresler and Frankel, 1950, Cappozzo, 1984). At the beginning of stance, an internal moment (applied external) occurs until midstance and then external concentric contraction occurs, resulting in an external (applied internal) moment.

The results of the maximum moments occurring during gait are compared to literature and presented in Table 8. All literature moment results were converted to N-m/kg, and all results are presented as internal moments. The literature result averages fell between the two subjects' results for all the moments except for the extensor (applied flexion) moment at the beginning of stance. The low value obtained for this extensor moment could be contributed to a couple of factors that will be

Table 8. Comparison of maximum moments (N-m/kg)

	B&F '50	Crow '78	Cap '84	Win '84	Oun '92	AVG	subject 1	subject 2
abductor 1	0.94	1.16	0.63		0.50	0.81	0.80	1.00
abductor 2	1.26	0.94	0.71		0.50	0.85	0.70	1.00
extensor	0.80	0.87	0.79	0.50	0.65	0.72	0.30	0.30
flexor	0.73	0.51	0.79	0.50	0.60	0.63	0.70	0.60
Internal rot	0.27	0.17	0.32			0.25	0.20	0.30
external rot	0.18	0.14	0.17			0.16	0.10	0.20

(B&F = Bresler and Frankel, Crow = Crowninshield, Win = Winter, and Oun = Ounpuu; abductor 1 = 1st peak of abd/add moment and abductor 2 = 2nd peak of abd/abd moment)

discussed below.

An example of the position of the body segments at the maximum extensor (applied flexion) moment and maximum flexor (applied extension) moment in stance is depicted by a stick figure shown in Figure 36. The maximum extensor moment occurred at around 20% of stance and the maximum flexor moment at around 75% of stance for subject 1. The vertical force (Fz) for 20% of stance was 786 N with a moment arm to HJC at 13.6 cm. The braking (Fx, horizontal) force was 109 N with a moment arm of 91 cm to HJC. These forces and moment arms, coupled with the thigh and shank weights produced an applied flexion moment of 14 N-m. At 75% of stance, with a vertical force of 721 N and moment arm of 15.7 cm and a propulsion (Fx, horizontal) force of 112 N with a moment arm of 90 cm, the applied extension moment was 35 N-m. Since the ratio of horizontal to vertical forces during the maximum moment times in stance phase did not vary greatly and the vertical moment arm to HJC was basically constant, the one factor that essentially drove the moment results was the x-direction (horizontal) moment arm.

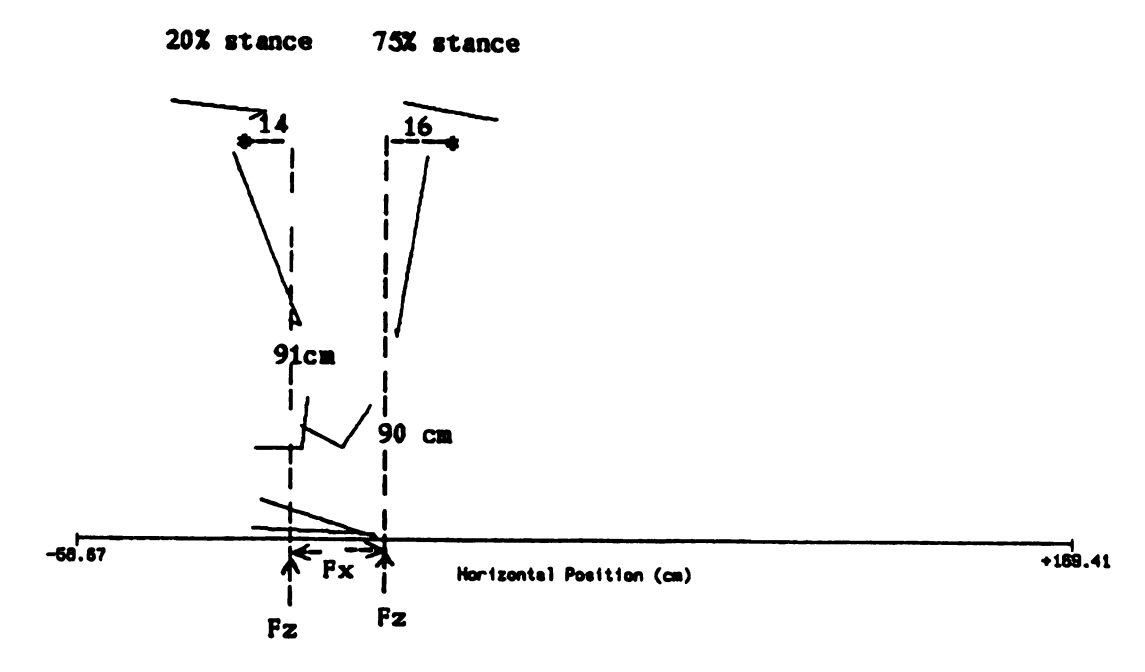
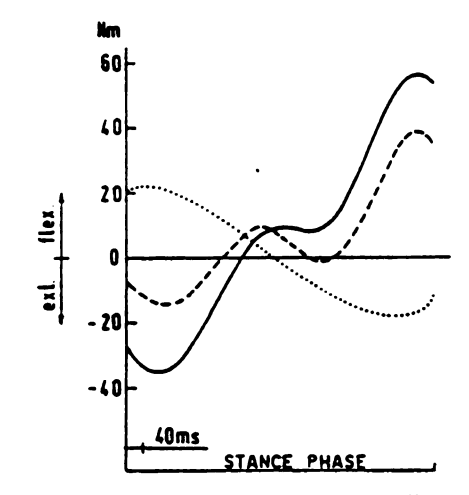


Figure 36. Stick figure depicting forces and moment arms in the sagittal plane - subject 1

Precise location of HJC and proper synchronization of force plate data with motion data were crucial in obtaining the most accurate representation of hip joint moments.

Although, it has been reported that the inertial terms are minimal, they do effect the results. Bresler and Frankel's (1950) comparison of inertial terms and no inertial terms in moments (Figure 7) match the results in the end of stance for the flexion/extension moments of subjects 1 and 2 (Figure 34 and Figure 35). When Boccardi (1981) calculated the moments at the lower joints in walking due to ground reaction force alone, he did not include the inertial or gravitational terms (lower limb weights). He showed that the gravitational effects and inertial effects worked opposite of each other and therefore minimized their contributions (Figure 37).



Time courses of the inertia (continuous line) gravity (dotted line) moments and their sum (dash line) computed at the hip joint of the lower left limb.

Figure 37. Inertial and gravitational terms in moments (Boccardi, 1981)

To study the effects on the applied moments at the hip with no gravity terms, the moments were calculated with and without the weights of the thigh and shank/foot complex for one trial of subject 1 (Figure 38) and one trial of subject 2 (Figure 39). This had the effect of increasing the applied adduction moments in both peaks for subject 2. This subject's combined center of gravity of the thigh and shank was located lateral to HJC. Therefore, when the gravity terms were removed, the effect was to remove applied adduction moments. Ignoring the gravity terms also had the effect of increasing the extensor (applied flexion) moment at the beginning of stance and increasing the flexor (applied extension) moment at the end of stance, considerably (66.7% increase for subject 1, 33.3% increase for subject 2). The weight terms act inferiorly and at the beginning of stance, they are located anterior to HJC and produce an applied extension (internal flexor) moment. At the end of stance, they are located posteriorly and produce an applied flexion (internal extensor)

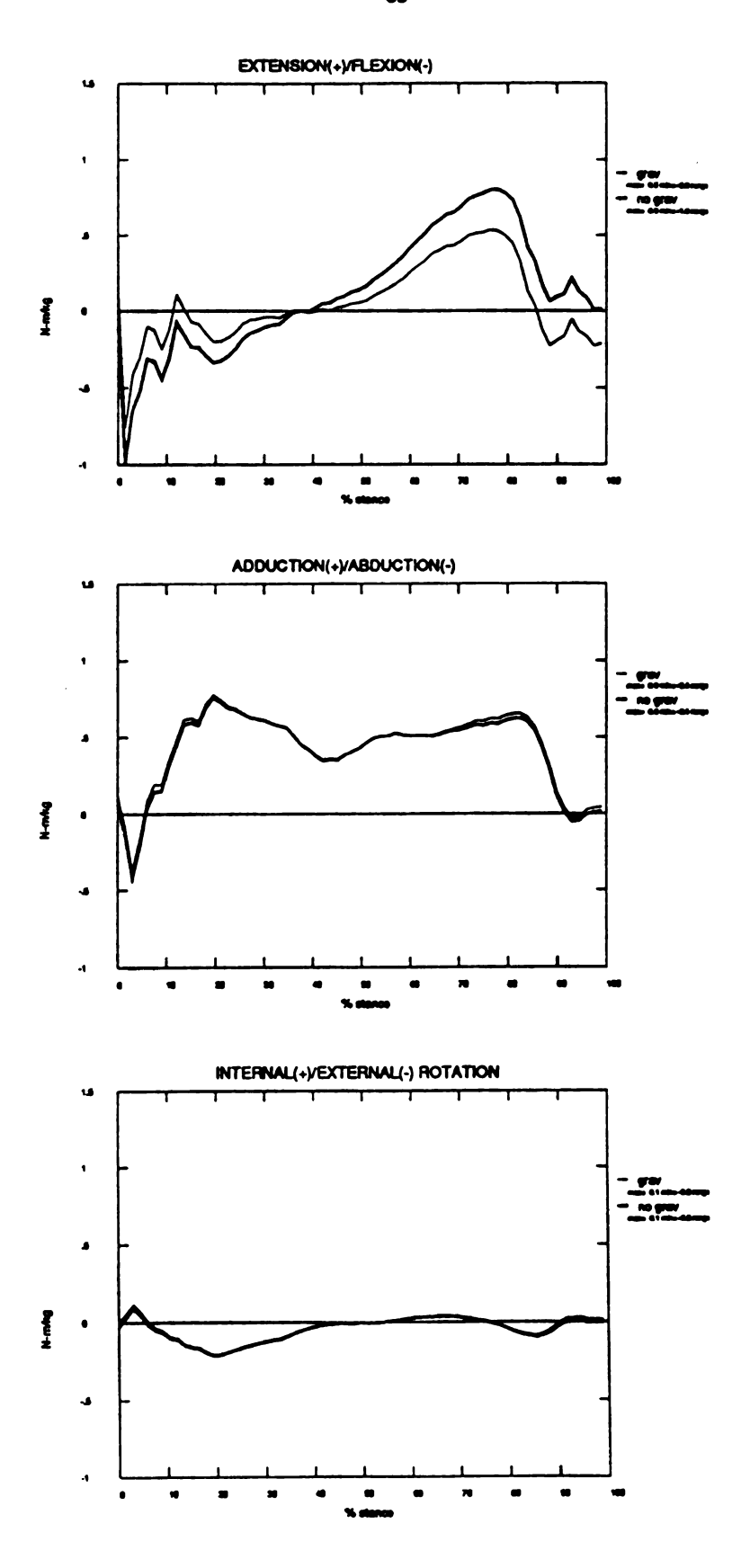


Figure 38. Applied hip moments with and without gravity terms -subject 1

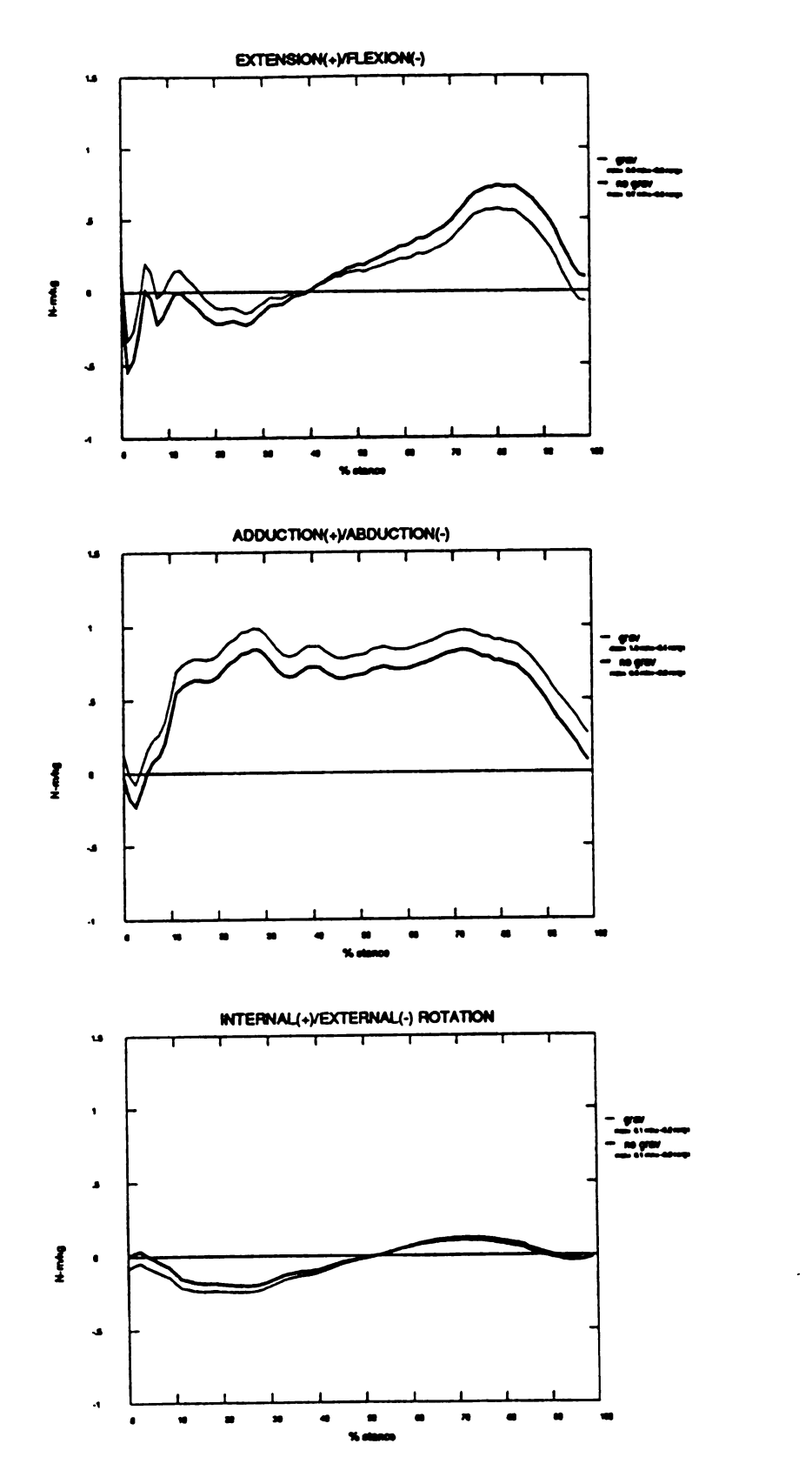


Figure 39. Applied hip moments with and without gravity terms -subject 2

moment. These observations coincide with the effects of taking the gravity terms out of the moment equations. The applied moment results without the gravity terms also match the results of the inverse dynamics equations presented in literature more closely. Since the Newton-Euler equations were not formulated, it is not possible to accurately describe the results of the moment equations with inertial effects.

Since the moment arms, in calculating any moments, have a large effect on not only the magnitudes of the results but also on the polarity of the results, the location of HJC had to be accurately defined. Since a new method of locating HJC was used in this study, differences arose in the moment results. To compare with Winter's (1984) data, moments were calculated in the sagittal plane using his definition of HJC (a projection of the greater trochanter medially to the sagittal plane). In the sagittal plane, this has the effect of moving the hip joint center lateral, posterior, and inferior to its actual location. The results of using the greater trochanter as HJC for the computation of flexion/extension moments is shown in Figure 40 for subject 1 and for subject 2. The flexion/extension moment is highly sensitive to the moment arm in the x-direction of lab space. Thus, a shift of the HJC in the posterior direction increases the x-direction moment arm during the first part of stance and decreases it in the later half of stance. For subject 1, this had the result of adding 0.2 to 0.3 N-m/kg applied flexion moment in the first half of stance and decreasing applied extension moment in the second half of stance by 0.2 to 0.3 N-m/kg. With the position of the greater trochanter as HJC, subject 2 had a 0.2 N-m/kg added applied flexion moment in the first half of stance but little change in the moments in the second half of stance. This was due to subject 2's higher proportion of anterior force to vertical force at this stage of gait. In



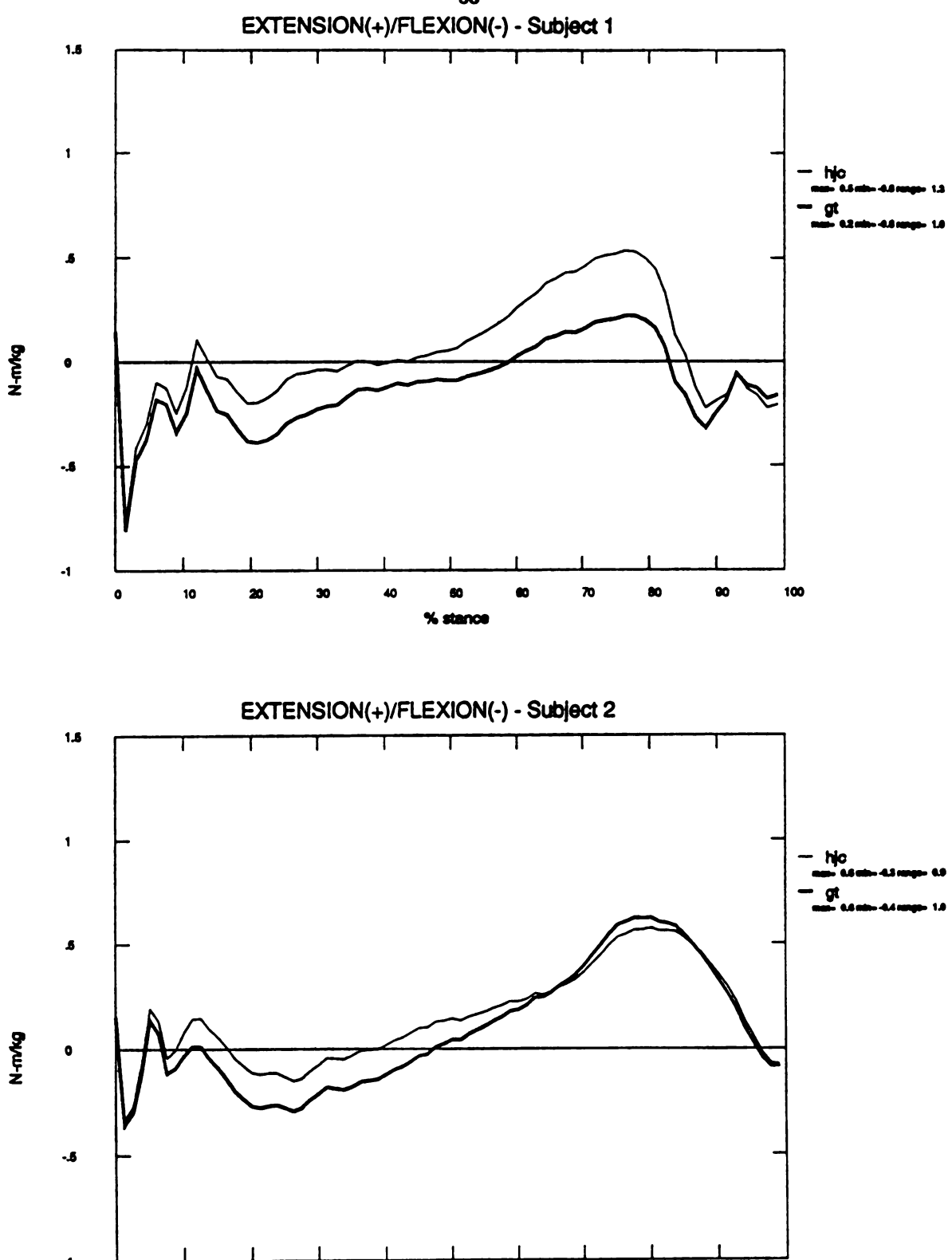


Figure 40. Flexion/extension moments at HJC and greater trochanter

both cases, however, the results were brought more in line with literature, which shows an equal proportion of flexion to extension moments throughout stance and higher magnitudes of extensor and moments. This demonstrates how crucial the position of HJC is in calculating hip joint moments.

With the moments calculated and the angles at the hip during gait previously defined, power was then calculated. Most literature reports a "pseudo-power" in the individual planes of motion. Therefore, both this power and the true power were calculated. The angular velocities of hip motion are shown in Figure 41 for subject 1 and in Figure 42 for subject 2. The largest angular velocities occurred, as expected, for flexion/extension. At the end of stance, subject 1 achieved a maximum angular velocity of 3.2 rads/s and subject 2 achieved a maximum angular velocity of 2.5 rads/s. The abduction/adduction velocities remained low during most of stance, but at the end of stance subject 1 abducted his thigh at 1.4 rads/s and subject 2 abducted at 1.3 rads/s. Also, at the end of stance, subject 1 was externally rotating at 2.0 rads/s and subject 2 at 1.4 rads/s.

Power is defined as the rate of doing work. In human movement studies, it is used as a parameter to define energy absorption and generation associated with muscle activity. The power was calculated as internal values (opposite of the applied moments) at the joint. Positive values indicate power generation (concentric muscle contraction) and negative values indicate power absorption (eccentric muscle contraction). The power results are shown in Figure 43 for subject 1 and figure 44 for subject 2. The 'power' curve in the plane of progression matched quite closely to literature (Ounpuu, 1992, Figure 15). Subject 1 had a maximum power generation of 0.5 Watts/kg and a maximum power absorption of

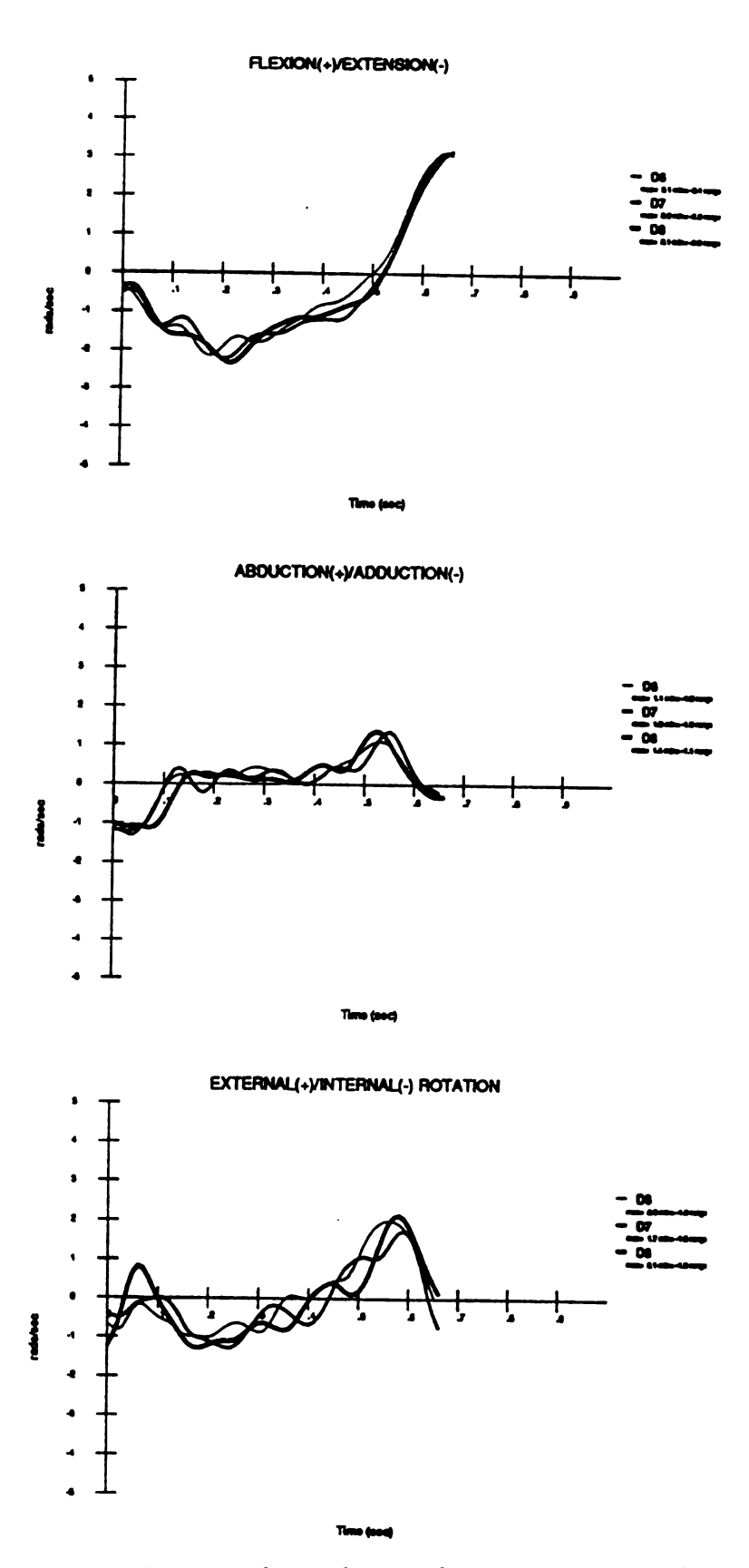


Figure 41. Hip angular velocity during stance - subject 1

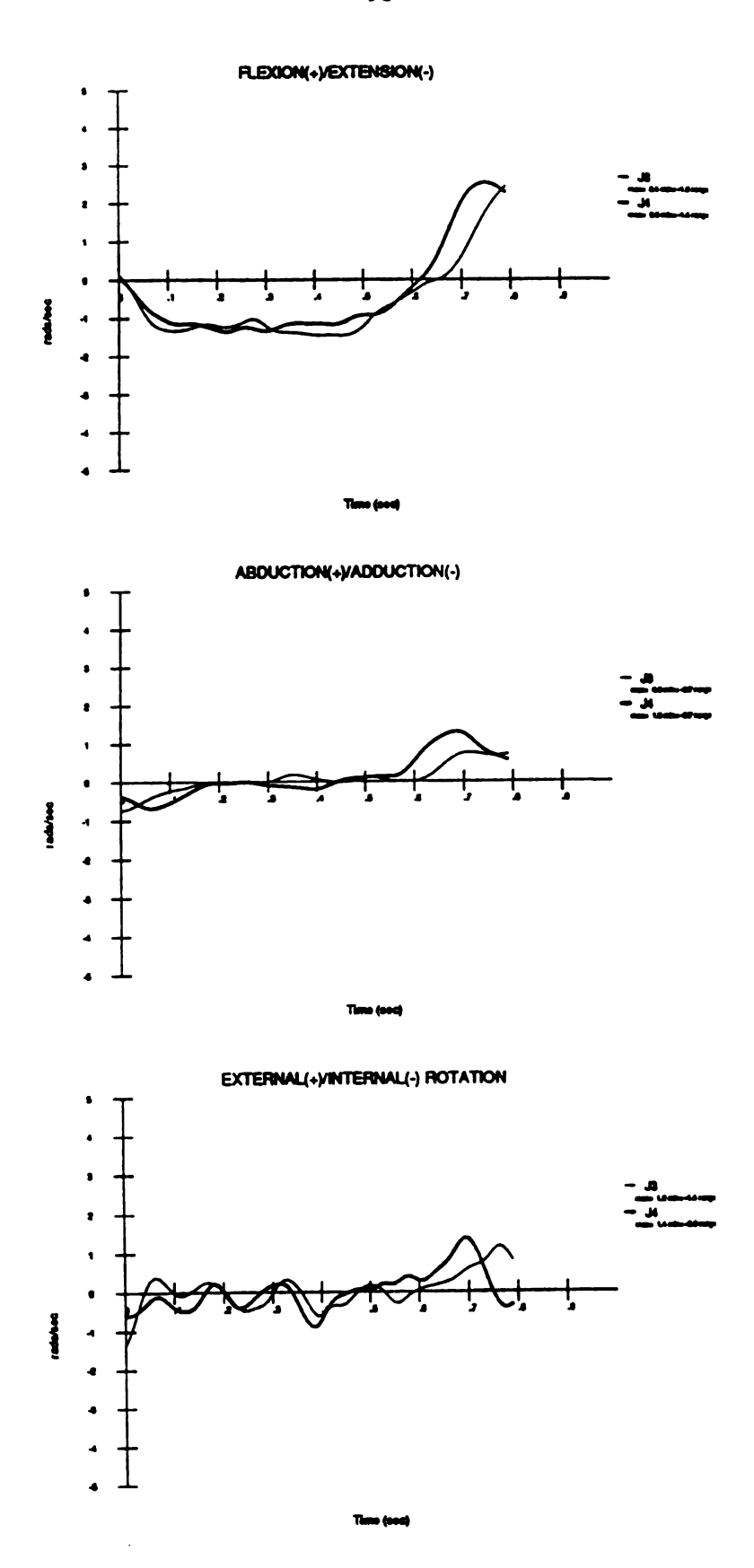
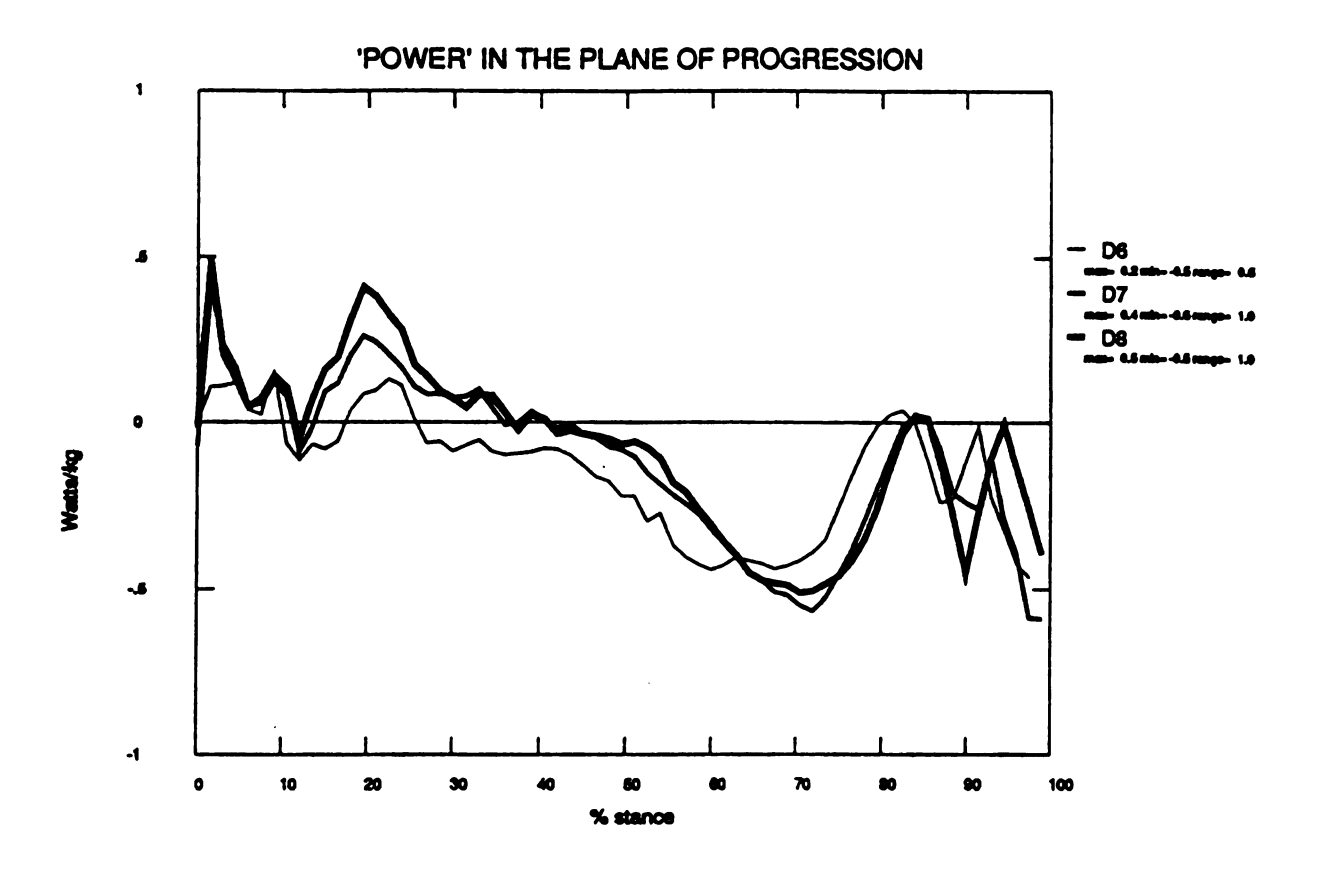


Figure 42. Hip angular velocity during stance - subject 2



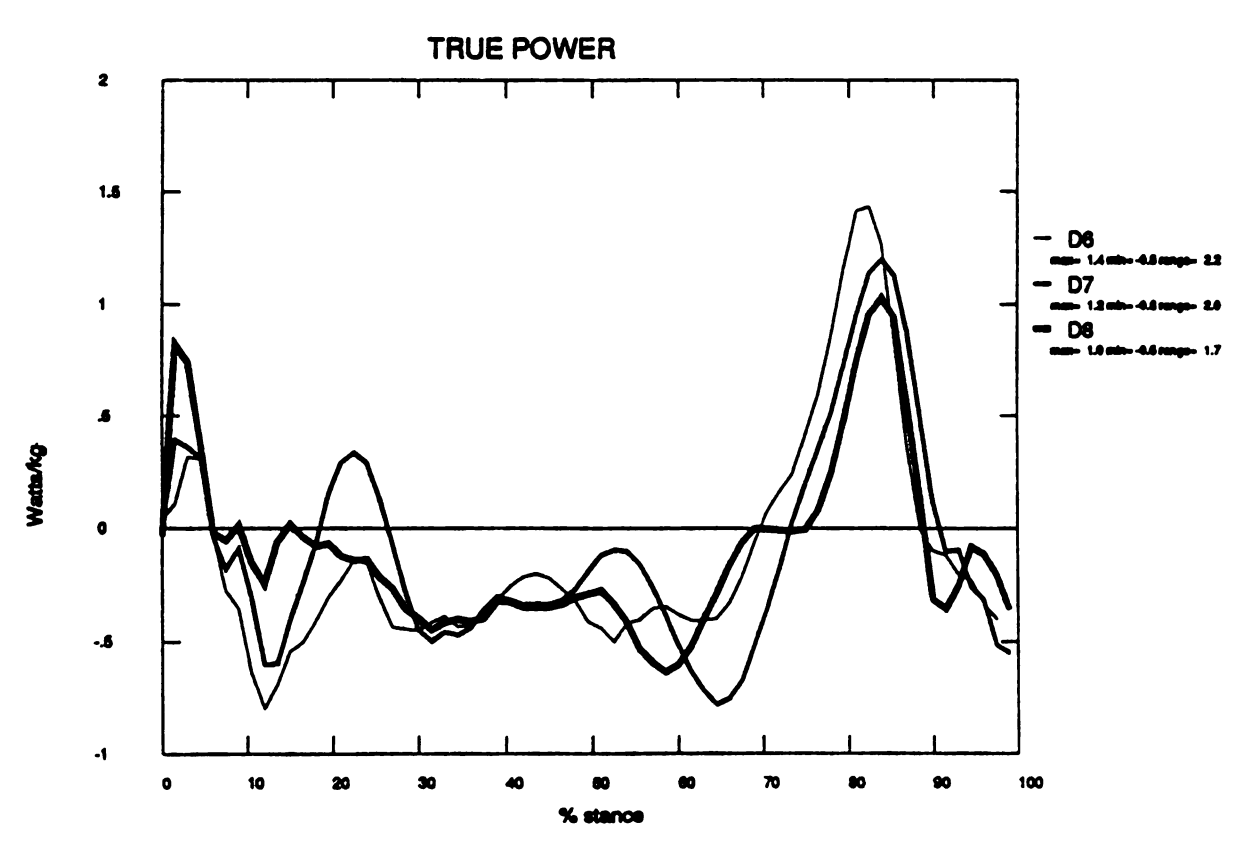


Figure 43. Hip power during stance phase - subject 1

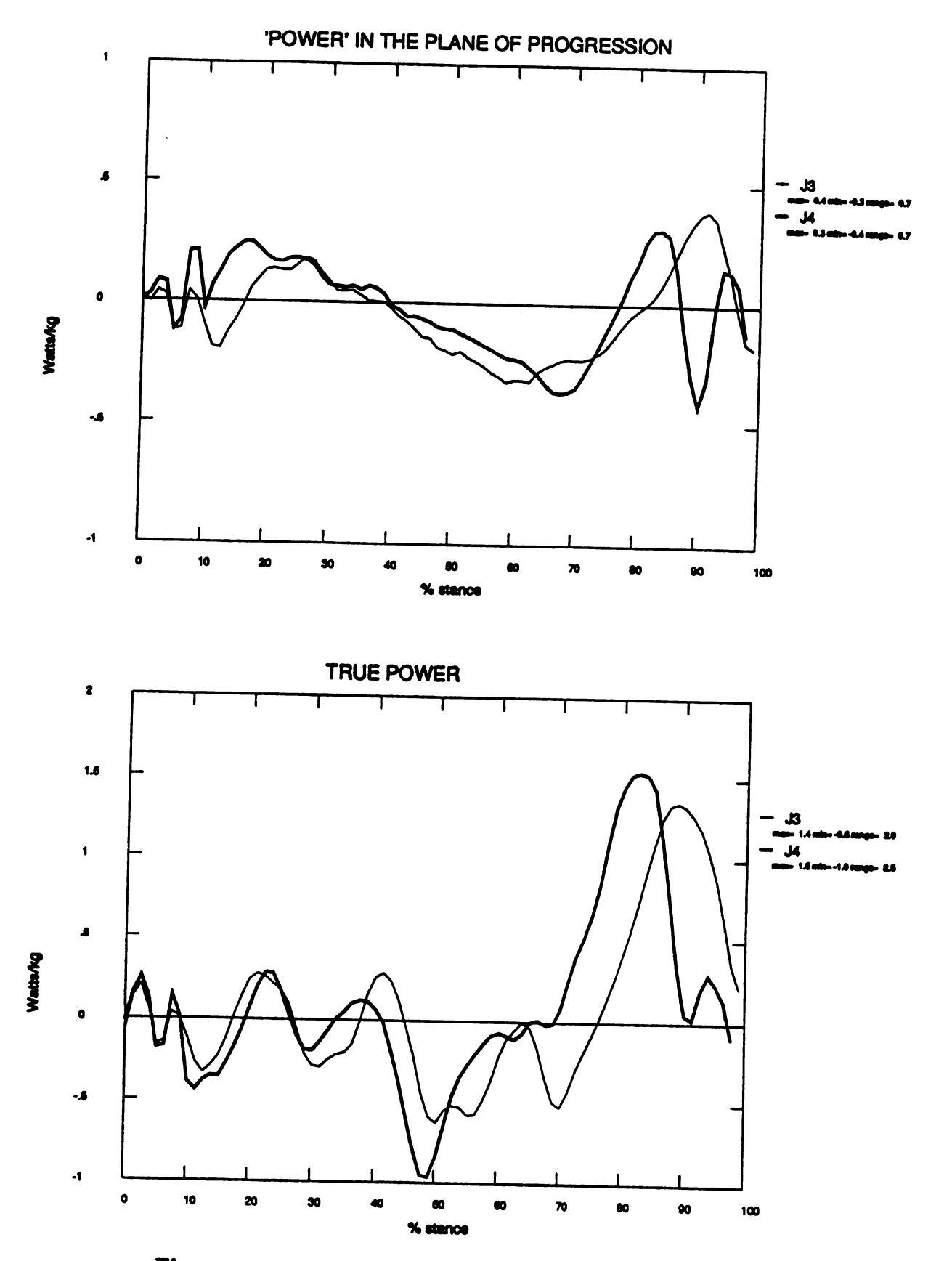


Figure 44. Hip power during stance phase - subject 2

0.5 Watts/kg. The cross-over from power absorption to generation occurred at midstance. At the end of stance, power was again generated. Subject 2 had slightly lower maximum values but similar trends.

The results of the 'power' calculated in the plane of progression is used in literature to describe the muscle activity during flexion/extension in the sagittal plane. During the first part of stance, the hip extensors fire concentrically and are acting as power generators and then power absorption occurs as the flexors contract eccentrically. When the flexors switch to concentric contractions to move the thigh upward and forward, power generation again occurs.

There are marked differences between the results of 'pseudo-power' and true power, as defined mathematically. At the knee, where power measurements are also computed, abduction/adduction and external/internal rotations are small and are not resisted by muscles. However, the angular velocities at the hip out of the plane of progression (abduction/adduction angular velocity and external/internal angular velocity) are not small enough during stance to ignore. At the end of stance, these velocities obtained magnitudes up to 2.0 rads/s (115 degs/s). The trends of the true power curve matched for both subjects but with different magnitudes. There was also no literature on this type of power calculation to compare the results with. The differences in magnitudes between the two subjects is most likely due to the different angular velocities of both subjects. Subject 1 completed stance in about 0.66 seconds and it took subject 2 just about .80 seconds. At the end of stance when the leg is coming forward and upward for toe off, there is a large generation of power at the hip. Subject 1 had a maximum power generation of 0.7 Watts/kg and subject 2 had a maximum power

generation of 1.1 Watts/kg.

VI. CONCLUSIONS

The high correlations between HJC components and their respective pelvic dimensions plus the lower mean error involved in using the pelvic volume relationships indicate that HJC cannot be located relative to ASIS as a function of pelvic width alone. Translation from the ASIS to HJC along the y-axis (mediolateral) can be made as a function of pelvic width; however, translation along the x-axis (anteroposterior) and the z-axis (superoinferior) cannot be made without corresponding pelvic volume measurements. Pelvic volume measurements are needed to normalize the subject specific location of HJC. Therefore, HJC is located relative to the ASIS 14% pelvic width medial, 34% pelvic depth posterior, and 80% of pelvic height inferior.

The quasi-static moments were accurately calculated at the hip during the stance phase of gait. Both the general trends and magnitudes of the quasi-static solution agreed with previous literature results that utilized the true inverse dynamics equations. The one difference in the results was that a decrease in extensor activity at the hip in the beginning of stance was found by the quasi-static method. It was shown that the moment calculation is highly sensitive to the anterior/posterior moment arm to the reaction forces. Locating true HJC accurately is crucial in calculating the precise moments at the hip during gait. The results of the quasi-static moment formulation are sufficient if ranges and magnitudes of

moments are desired, but caution should be used when studying the polarity of the moments at the initial foot contact in stance and at the toe off in stance where dynamic effects are more prevalent.

Power at the hip during stance was calculated both in the plane of progression and as the actual total power. The 'power' in the plane of progression compared favorably with literature and could be used in a clinical setting in aiding in the understanding of the activity of the flexion/extension muscles. However, the correct definition of power yielded marked differences in the results and should be studied further to establish basic trends and magnitudes during stance. This result of true power could be used as a parameter to quantify the total absorption or generation of energy at the hip during gait, instead of trying to limit the analysis to individual planes.



LIST OF REFERENCES

- 1. Andriacchi, T.P., Andersson, G.B.J., Fermier, R.W., Stern, D. and Galante, J.O. (1980) A study of lower-limb mechanics during stair-climbing. *Journal of Bone and Joint Surgery* 62-A, 749-757.
- 2. Bell, A.L., Brand, R.A., and Pederson, D.R. (1989) Prediction of hip joint centre location from external landmarks. *Human Movement Science*, 8, 3-16.
- 3. Bell, A.L., Pederson, D.R., and Brand, R.A. (1990) A comparison of the accuracy of several hip center location prediction methods. *Journal of Biomechanics* 23, 617-621.
- 4. Blankevoort, L., Huiskes, R. and de Lange, A. (1990) Helical axes of passive knee joint motions. *Journal of Biomechanics* 23, 1219-1229.
- 5. Boccardi, S., Pedotti, A., Rodano, R., and Santambrogio, G.C. (1981) Evaluation of muscular moments at the lower limb joints by an on-line processing of kinematic data and ground reaction. *Journal of Biomechanics* 14, 35-45.
- 6. Borelli, G.A., (1680) De motu animalium. Roma
- 7. Braune, C.W. and Fisher, O. (1895) Der Gang des Menschen. Internationale Abhandlungen der Mathematisch Physisch Koniglich Sachsischen Gesellschaft fur Wissenchaften 21, 151-324.
- 8. Bresler B, Frankel JP. (1950) The forces and moments in the leg during level walking. *Transactions of the ASME* 72, 27-36.
- 9. Brinckmann, P., Hoefert, H. and Jongen, H. Th. (1981) Sex differences in the skeletal geometry of the human pelvis and hip joint. *Journal of Biomechanics* 14, 427-430.

- 10. Cappozzo, A. (1984) Gait analysis methodology. Human Movement Science 3, 27-50.
- 11. Cheney, W. and Kincaid, D. *Numerical Mathematics and Computing*. Monterey, California: Brooks/Cole Publishing Company, 1980, 147-157.
- 12. Crowninshield, R.D., Johnston, R.C., Andrews, J.G., and Brand, R.A., (1977) The effects of joint cnter location on hip kinetics. *Proceedings from the* 23rd annual ORS convention 47-49.
- 13. Crowninshield, R.D., Johnston, R.C., Andrews, J.G., and Brand, R.A., (1978) A biomechanical investigation of the human hip. *Journal of Biomechanics* 11, 75-85.
- 14. Delp. S.L., Maloney, W. (1993) Effects of hip center location on the moment-generating capacity of the muscles. *Journal of Biomechanics* 26, 485-499.
- 15. Dempster, W.T., Grabel, W.C., and Felts, W.J.L. (1959) The anthropometry of manual work space for the seated subject. *Am J Phys Anthrop* 17, 289-317.
- 16. Elftman, H. (1939) Forces and energy changes in the leg during walking. *Am. J Physiol* 125, 339-356.
- 17. Ellis, M.I., Seedhom, B.B., Amis, A.A., Dowson, D. and Wright, V. (1979) Forces in the knee joint whilst rising from normal and motorized chairs. *Engng Med.* 8, 33-40.
- 18. Greenwood, D.T. *Principles of dynamics, Second Edition*. New Jersey: Prentence-Hall, 1988, 389-393.
- 19. Grood, E.S. and Suntay, W.J. (1983) A joint coordinate system for the clinical description of three-dimensional motions: application to the knee. *Transactions of the ASME* 105, 136-143.
- 20. Johnston. R.C. (1973) Mechanical considerations of the hip joint. *Archives of Surgery* 107, 411-417.

- 21. Kadaba, M.P., Ramakrishnan, H.K., Wooten, M.E., Burn, J., and Gorton, G. (1989) On the normalization of joint moments in gait analysis. *Proceedings of th 35th Annual Meeting of the Orthopaedic Research Society* p 245 Las Vegas, Nevada.
- 22. Marey, E.J. (1885) Le methode graphique dans les sciences experimentales. 2nd edition with supplement: le developpement de la methode graphique par l'emlploi de la photographic. Paris: G. Masson.
- 23. Muybridge, E, (1887) Animal locomotion, an electro-photographic investigation of consecutive phases of animal movements (11 volumes). Philadelphia, P.A.: J.B. Lippincott.
- 24. Ounpuu, S., Gage, J.R., and Davis, R.B. (1991) Three-dimensional lower extremity joint kinetics in normal pediatric gait. *Journal of Pediatric Orthopaedics* 11, 341-349.
- 25. Ramakrishnan, K.K., Kadaba, M.P., and Wooten, M.E. (1987) Lower extremity joint moments and ground reaction torque in adult gait. In *Biomechanics of Normal and Prosthetic Gait*, pp. 87-92, Am. Soc. Mech. Engng., New York.
- 26. Soutas-Little, R.W. (1987) Center of pressure plots for clinical uses. *Biomechanics of normal and pathological gait*, presented at the Winter Annual Meeting of the American Society of Mechanical Engineers, BED-Vol. 4, DSC-Vol. 7, 69-75.
- 27. Tylkowski, C.M., Simon, S.R. and Mansour, J.M. (1982) Internal rotation gait in spastic cerebral palsy in the hip. *Proceedings of the 10th Open Scientific Meeting of the Hip Society* (Edited by Nelson, J.P.), 89-125, Mosby, St. Louis.
- 28. Wells, R.P. (1981) The projection of the ground reaction force as a predictor of internal joint moments. *Bulletin of Prosthetics Research* BRP10-35, Vol. 18 #1, 15-19.
- 29. Winter, D.A. (1980) Overall principle of lower limb support during stance phase of gait. *Journal of Biomechanics* 13, 923-927.
- 30. Winter, D.A. (1984) Kinematic and Kinetic Patterns in Human Gait: Variability and Compensating Effects. *Human Movement Science* 3, 51-76.

- 31. Winter, D.A. Biomechanics and Motor Control of Human Movement, Second Edition New York: John Wileyt & Sons, Inc., 1990, 56-57.
- 32. Whittle, M.W. Gait Analysis: An introduction. Oxford, England: Butterworth-Heinemann Ltd., 1991.

